

## ABSTRACT

Title of Document: GIS-BASED ODOR IMPACT ASSESSMENT  
FROM BIOSOLIDS LAND APPLICATION  
SITES

Eakalak Intarakosit, Doctor of Philosophy, 2010

Directed By: Professor, Gregory B. Baecher, Civil &  
Environmental Engineering

Biosolids applied to agricultural land may upset neighboring communities due to the inherent malodorous smell of biosolids. The problem of the odor becomes a major concern in the wastewater treatment industry when community responses could vary from complaints to legal action to ban or reduce biosolids recycling through land.

Unlike odor at a wastewater treatment facility, which is produced from the characteristics of wastewater itself and from individual unit processes, land-applied biosolids odor depends not only on the quality of biosolids, but also on the biosolids emissions levels, unfavorable weather conditions and topographic characteristics, and variation of human perception. Those factors increase the complexity of nuisance odor at land application sites.

This dissertation aims to assess biosolids emission impacts on surrounding communities by estimating the level of biosolids odor emissions, simulating odor dispersion, and quantifying human perception to biosolids odor.

Odor emission rates at land-applied biosolids fields were estimated using three different approaches: assumed flow rate, statistical inference, and simulated-flux chamber. The estimated emission rates were used as an input to dispersion models. The U.S. Environmental Protection Agency Regulatory Models, both screening and refined models, were used to simulate dispersion of biosolids odor at land application sites. A Geographic Information System (GIS) was employed to support modeling steps and to create maps. Appraisal of odor perception by receptors was assessed by use of Steven's psychophysics power law.

The District of Columbia Water and Sewer Authority (DCWASA) land application fields in Virginia were used as case studies. More specifically, 45 fields in Albemarle and Orange Counties were focused on. Concentration prediction maps along with probability maps were created to support visualization and provide information on potential odor impacts to communities. Possible human perceptions were expressed in Intensity maps. The methods and results described in this dissertation can support decision makers in selecting appropriate land application sites prior distributing biosolids to reduce adverse effects from land-applied biosolids.

GIS-BASED ODOR IMPACT ASSESSMENT FROM BIOSOLIDS LAND  
APPLICATION SITES

By

Eakalak Intarakosit

Dissertation submitted to the Faculty of the Graduate School of the  
University of Maryland, College Park, in partial fulfillment  
of the requirements for the degree of  
Doctor of Philosophy  
2010

Advisory Committee:

Professor Gregory B. Baecher, Chair  
Professor Ashwani K. Gupta  
Associate Professor Eric A. Seagren  
Associate Professor Kaye L. Brubaker  
Associate Professor Steven A. Gabriel

© Copyright by  
Eakalak Intarakosit  
2010

## Acknowledgements

This dissertation would not have been possible without contributions from many people that I would like to mention here.

First and foremost, I would like to express my deepest gratitude to my advisor, Professor Gregory B. Baecher, for his guidance and support throughout my doctoral study. Especially, his suggestions and optimism shaped my vision and thinking.

It is my pleasure to thank Professor Ashwani K. Gupta, Associate Professor Eric A. Seagren, Associate Professor Kaye L. Brubaker, and Associate Professor Steven A. Gabriel for serving on my dissertation committee. Their comments improved the quality of the dissertation.

I am grateful to thank the District of Columbia Water and Sewer Authority (DCWASA) for an internship opportunity and research funding. My manager, Mr. Christopher Peot, and my supervisor, Mr. Mark Ramirez, at the Department of Wastewater Treatment, provided me with support and valuable comments. I also thank Mr. Al Razik from the Maryland Environmental Services (MES) for providing me the data used in this research.

Finally, I would like to thank my family and friends for their support throughout my graduate study in the United States.

# Table of Contents

Acknowledgements.....	ii
Table of Contents .....	iii
List of Tables .....	v
List of Figures .....	vii
Chapter 1: Introduction .....	1
1.1 Problem Definition and Significance.....	1
1.2 Goals and Objectives .....	2
1.3 Hypothesis.....	3
1.4 Overview of Research Approach and Outcomes .....	5
1.4.1 <i>Geographic Information System (GIS) – Based Biosolids Odor Impact Assessment for Planning Biosolids Distribution</i> .....	5
1.4.2 <i>Summary of Research Outcomes</i> .....	10
1.5 Contribution .....	11
1.6 Overview of Dissertation .....	12
Chapter 2: Background and Literature Review .....	14
Chapter 3: DCWASA Wastewater Treatment Processes and Related Data .....	21
3.1 DCWASA Background.....	21
3.2 DCWASA Reuse Sites Data .....	23
3.2.1 <i>Field Odor Measurement</i> .....	24
3.2.2 <i>Emission Testing</i> .....	29
3.3 Meteorological Data.....	30
3.4 Geographical Data .....	31
Chapter 4: Estimate of Biosolids Odor Emission .....	33
4.1 Biosolids Odor Emission and Measurement.....	33
4.2 Information about Emissions Rates and Current Estimation Method .....	37
4.3 Statistical Inference for Emission Estimates.....	39
4.3.1 <i>Model Estimation</i> .....	40
4.3.2 <i>Model Verification by Goodness-of-Fit Tests</i> .....	42
4.3.3 <i>Model Verification by Probability Paper</i> .....	46
4.4 Analysis of Variance (ANOVA).....	47
4.5 Case Studies: Development of Probability Distribution.....	50
4.5.1 <i>Odor Emissions at DCWASA’s Land Application Sites</i> .....	50
4.5.2 <i>Odor Emissions at DCWASA Wastewater Treatment Plant</i> .....	55
4.6 Case Study: ANOVA .....	59
4.6.1 <i>Design of Experiments</i> .....	59
4.6.2 <i>Analysis of Variance (ANOVA)</i> .....	60
4.7 Guideline for Emission Estimates.....	61
Chapter 5: Biosolids Odor Impact Assessment at Land Application Sites.....	64
5.1 Introduction to Dispersion Model.....	64
5.1.1 <i>Screening Model</i> .....	64
5.1.2 <i>Regulatory/Refined Model</i> .....	66
5.2 GIS-Based Odor Impact Assessment.....	83
5.2.1 <i>Introduction to Geographic Information System (GIS)</i> .....	83

5.2.2 GIS-Based Biosolids Odor Impact Assessment .....	86
5.2.3 Biosolids Odor Impact Assessment .....	96
5.2.4 Simple Linear Regression for Model Validation .....	100
5.3 Case Studies: Screening Model .....	103
5.3.1 Study Areas .....	103
5.3.2 Results .....	106
5.3.3 Validation with Data.....	110
5.4 Case Studies: GIS-Based Odor Impact Assessment .....	114
5.4.1 Study Areas .....	114
5.4.2 Results .....	115
5.4.3 Validation with Data.....	122
5.5 Comparing Screening and Refined Models .....	124
5.6 Implementation .....	127
Chapter 6: Conclusions and Future Works .....	131
6.1 Conclusions.....	131
6.2 Future Work .....	133
Appendices.....	136

## List of Tables

Table 1.1: Research Outcomes.....	11
Table 3.1: MES Data Description Used in Modeling Process.....	27
Table 4.1: Critical Values for Kolmogorov-Smirnov Goodness-of-Fit Test.....	45
Table 4.2: Critical Values for Anderson-Darling Statistic.....	46
Table 4.3: k Random Samples.....	48
Table 4.4: Analysis of Variance for One-Way ANOVA.....	50
Table 4.5: Summary Statistics of MES Odor Emission Data.....	52
Table 4.6: Summary of Distribution Fitting for MES Odor Emission Data.....	52
Table 4.7: Calculation for a Normal Probability Plot.....	54
Table 4.8: Summary Statistics of DCWASA Odor Concentration Data.....	56
Table 4.9: Summary of Distribution Fitting for DWT Odor Data.....	57
Table 4.10: Analysis of Variance (ANOVA) of Odor Emission Data.....	60
Table 4.11: Example Calculation of Odor Emission Rates.....	62
Table 5.1: SCREEN3 Modeling Inputs and Options.....	65
Table 5.2: Combinations of Wind Speed and Stability Class.....	66
Table 5.3: Data Description for Surface File.....	74
Table 5.4: Data Description for Profile File.....	75
Table 5.5: Example Calculation of Odor Impact to Population.....	100
Table 5.6: Summary of Site 05-A Characteristics.....	104
Table 5.7: Best Estimate Thresholds.....	105
Table 5.8: Summary of Site 06-A Characteristics.....	105
Table 5.9: Summary of Screen View Inputs or Site 05-A.....	106

Table 5.10: Summary of Screen View Inputs for Site 06-H.....	108
Table 5.11: Output of Regression Analysis for Screening (Emission Case 1).....	113
Table 5.12: Output of Regression Analysis for Screening (Emission Case 2).....	113
Table 5.13: Output of Regression Analysis for Screening (Emission Case 2).....	113
Table 5.14: Standard Error of Estimates for Screening Model Outputs.....	114
Table 5.15: ANOVA of Constant k.....	118
Table 5.16: ANOVA of Constant n.....	119
Table 5.17: Expected Number of Population Exposed to Odor.....	121,122
Table 5.18: Standard Error of Estimates for Refined Model.....	124
Table 5.19: Output of Regression Analysis for Comparing Models.....	126
Table 5.20: Frequency of D/T(s) for Jan 12-13.....	130

## List of Figures

Figure 1.1: Conceptual Model for Selection of Biosolids Land Application Sites...	6
Figure 1.2: Schematic of Biosolids Site Selection Procedure.....	7
Figure 1.3: Overview of Odor Impact Pathway.....	8
Figure 3.1: DCWASA Service Areas.....	21
Figure 3.2: DCWASA Solids Process.....	22
Figure 3.3: A Map of Biosolids Distribution in Virginia Counties, VA.....	23
Figure 3.4: MES Inspector with Nasal Field Olfactometer.....	24
Figure 3.5: Odor Sensitivity Test Kit Box.....	25
Figure 3.6: MES Inspection Site Visit Form.....	27
Figure 3.7: Amount of Tonnages Applied in Virginia Counties.....	28
Figure 3.8: Frequency Distribution of Field Dilution-to-Threshold.....	29
Figure 3.9: Available Hourly Surface Weather Stations in Virginia.....	31
Figure 4.1: Frequency Detection of Odor Description from MES Field Data.....	34
Figure 4.2: Statistical Inference Approach.....	40
Figure 4.3: Random Sampling from Three Reuse Fields.....	47
Figure 4.4: Normal Probability Plot for MES Odor Emission Data.....	55
Figure 4.5: Lognormal Distribution of Odor Concentration at Blue Plains.....	58
Figure 4.6: Lognormal Distribution of Odor Emission Rates at Blue Plains.....	59
Figure 5.1: Meteorological Data Input and Output in the AERMET.....	70
Figure 5.2: AERMET Processing.....	71
Figure 5.3: Example Runstream to Extract and QA Upper Air and Surface Data....	72
Figure 5.4: Example Runstream for Merging the Data.....	73

Figure 5.5: Example Runstream for Estimating Boundary Layer Parameters.....	73
Figure 5.6: First 52 Hours of the Boundary Layer Parameter File.....	75
Figure 5.7: First 52 Hours of the Profile File.....	76
Figure 5.8: Example Runstream for Control Pathway (CO).....	78
Figure 5.9: Example Runstream for Source Pathway (SO).....	79
Figure 5.10: Example Runstream for Receptor Pathway (RE).....	80
Figure 5.11: Example Runstream for Meteorology Pathway (ME).....	81
Figure 5.12: Example Runstream for Output Pathway (OU).....	81
Figure 5.13: Example Output from the AERMOD.....	82
Figure 5.14: Example of the geographic coordinate system.....	85
Figure 5.15: Defined Projection Model.....	87
Figure 5.16: The Clip Raster Model.....	88
Figure 5.17: Example Clipping of the Elevation Layer.....	89
Figure 5.18: Example GIS for the Supporting Modeling Setup Data Frame.....	90
Figure 5.19: Receptor Terrain Model.....	91
Figure 5.20: Semivariogram Modeling.....	94
Figure 5.21: Intensity Map Model.....	99
Figure 5.22: Impact Area Model.....	99
Figure 5.23: Screen View Output for Site 05-A Field 1.....	107
Figure 5.24: Screen View Output for Site 05-A Field 2.....	107
Figure 5.25: Screen View Output for Site 05-C Field 8 (Emission Case 1).....	109
Figure 5.26: Screen View Output for Site 05-C Field 8 (Emission Case 2).....	109
Figure 5.27: Screen View Output for Site 05-C Field 8 (Emission Case 3).....	110

Figure 5.28: Scatter Plot or Screening Analysis (Emission Case 1).....	111
Figure 5.29: Scatter Plot or Screening Analysis (Emission Case 2).....	111
Figure 5.30: Scatter Plot or Screening Analysis (Emission Case 3).....	112
Figure 5.31: Concentration Prediction Map of Field 3, Site 06-H.....	116
Figure 5.32: Concentration Prediction Map of Field 16, Site 06-G.....	116
Figure 5.33: Probability Map of Field 16, Site 06-G.....	118
Figure 5.34: Power Law Graph of Biosolids Odor.....	120
Figure 5.35: Intensity Map of Field 16, Site 06-G.....	120
Figure 5.36: Scatter Plot for Refined Analysis (Emission Case 1).....	123
Figure 5.37: Scatter Plot for Refined Analysis (Emission Case 2).....	123
Figure 5.38: Scatter Plot for Refined Analysis (Emission Case 3).....	124
Figure 5.39: Comparing Results from Screening and Refined Models.....	126
Figure 5.40: Relative Frequency of D/T Greater than 7 D/T.....	128

# Chapter 1: Introduction

## 1.1 Problem Definition and Significance

Air quality in the United States has become a national concern since the 1970s. Accordingly, the Clean Air Act (CAA) was established as a national law for setting and regulating national air quality standards. Pollutants that are potentially harmful to human health are stringently regulated. However, pollutants that might cause annoyances such as odorous gases from wastewater biosolids are not directly regulated.

Biosolids are treated sewage sludges resulting from wastewater treatment. They contain nutrient organic materials that can be used as a beneficial agricultural fertilization such as a supplement to improve soil condition (EPA, 2000b). Nevertheless, the associated malodorous smell of biosolids that are applied to agricultural land may upset neighboring communities even though those biosolids are processed to meet the *Standards for the Use or Disposal of Sewage Sludge* (EPA, 1994).

With substantial amount of biosolids produced in the United States, approximately 7,180,000 dry tons in 2004 (Guillot et al., 2007), nuisance odor from biosolids become a major concern in wastewater treatment industry especially when the responses from nearby communities to odor could vary from complaints to legal action in the form of legislation to ban or minimize biosolids recycling. In addition, the nuisance odor could have impacts on the society and the economy of the communities such as on quality of life and property value (Turk et al., 1974).

In California, for example, a grand jury recommended actions to the Orange County Sanitation District (OCSD) to enhance public acceptance and to phase out biosolids land application except in remote areas (Frank, 2005).

Odor on-site at a wastewater treatment facility is produced from the characteristics of wastewater itself and from individual unit processes. The inflowing wastewater is inherently unpleasant, and each treatment process can independently produce odorants. Off-site nuisance odors, on the other hand, depend not only on the quality of biosolids, but also on the elevated odor emission levels of the biosolids source, variation of atmospheric conditions, and sensitivity of human perception. Those factors increase complexity of nuisance odor at land application sites. For example, an inspector who goes to a site of complaint may or may not detect the odor. Even if he can detect the odor, he cannot determine that perceived by a complainer. In addition, the detection level is normally not the level of the odor complaint (Poostchi, 1985).

A key research need is to study factors associated with nuisance odor problems at land application sites. It is equally important to being able to identify sources of odorous gases generated during and after treatment processes. Moreover, it will also help practitioners to assess odor impacts from land-applied biosolids more effectively and support decisions on selecting suitable land application sites to reduce public resistance to biosolids.

### 1.2 Goals and Objectives

The goal of this research is to promote recycling of biosolids and to reduce public resistance by providing tools to select daily reuse sites that have less adverse effects

of biosolids nuisance odor. Aligned with this goal, this research will address the following objectives:

1. To draw conclusions about the characteristics of emission rates of biosolids odors and provide a guideline for emission estimates used in an odor dispersion model.
2. To predict biosolids odor concentrations at land application sites.
3. To determine the extent of potential odor impacts to a community near an application site and to quantify such impacts to the local population
4. To provide a supporting tool for decision makers to minimize biosolids odor impacts by selecting suitable sites.

### 1.3 Hypothesis

There are four hypothesizes to be tested in the study.

Hypothesis 1: Since pollutant concentration data often follow a skewed distribution (Singh et al., 1997), it is hypothesized that the odor emission rates at land application sites and at wastewater treatment facility can be described by the lognormal distribution. This hypothesis was confirmed by the results from developed probability distributions.

Hypothesis 2: Two types of variations of odor emissions exist in biosolids land application: variation within the field and among fields. This hypothesis was tested using the Analysis of Variance (ANOVA) described in Chapter 4. By assuming that biosolids samples taken from the hauling trucks before distribution represent biosolids samples taken at the reuse sites, the results from the ANOVA have the

implication that there exists variation within the field and among the fields on day-to-day operation.

The assumption used in this hypothesis implies that there are no dilutions of biosolids odor emissions during transporting biosolids from a wastewater treatment plant to land application sites. The assumption was set due to difficulty of collecting biosolids odor data at the land application sites. Even though the assumption was not hold, the ANOVA results can be used to explain variation of biosolids odor emissions at the wastewater treatment plant. Hypothesis 3: The biosolids odor generated from the wastewater treatment processes is not the only factor contributing to adverse effect at land application sites. This hypothesis was confirmed by use of the dispersion models to investigate biosolids odor concentration at land application sites. The basic factors include odor emission rates at the sites and atmospheric conditions.

Hypothesis 4: Regulatory dispersion models are typically used in the regulatory application such as contaminant pollutants. This hypothesis aimed to test that it is practical to use regulatory dispersion models for non-regulatory application, such as in the case of odor, to predict odor levels at land application sites with a degree of accuracy. By using the U.S. EPA's dispersion models, the validation results from Chapter 5 confirmed that it is feasible to use both screening and refined regulatory dispersion models with appropriate input data to predict the odor concentration at land application sites

## 1.4 Overview of Research Approach and Outcomes

### *1.4.1 Geographic Information System (GIS) – Based Biosolids Odor Impact Assessment for Planning Biosolids Distribution*

This research is a part of the ongoing research projects on biosolids management at the District of Columbia Water and Sewer Authority (DCWASA). It is an extension of a master thesis at the University of Maryland, College Park (Intarakosit, 2006).

The difference from the previous work has been emphasized on a more comprehensive approach for odor impact assessment: source, transport, and receptor.

In this study, we have developed the Geographic Information System (GIS) - Based Odor Impact Assessment to address potential odor impacts from biosolids at land application sites. The model is an integration of many subjects, which include environmental engineering, statistics, geographic information system (GIS), odor science, and atmospheric dispersion models, to solve a very complex odor problem. It serves as a supporting tool for selecting biosolids land application sites since that decision should always be subjected to the least possible negative response from communities. Potential odor complaints, for example, are good attribute to measure negative responses.

Figure 1.1 shows a developed conceptual model for selecting biosolids application sites. The decision making process for site selection includes a consideration of some other criteria such as potential odor impact to nearby communities, possible public responses, or transportation cost. Even though responses could greatly vary depending on biosolids site locations and public perception of biosolids, the conceptual model can still provide a systematic

framework for decision makers to achieve basic goals for possibly reducing public resistance to biosolids by being able to assess potential odor impacts to the communities.

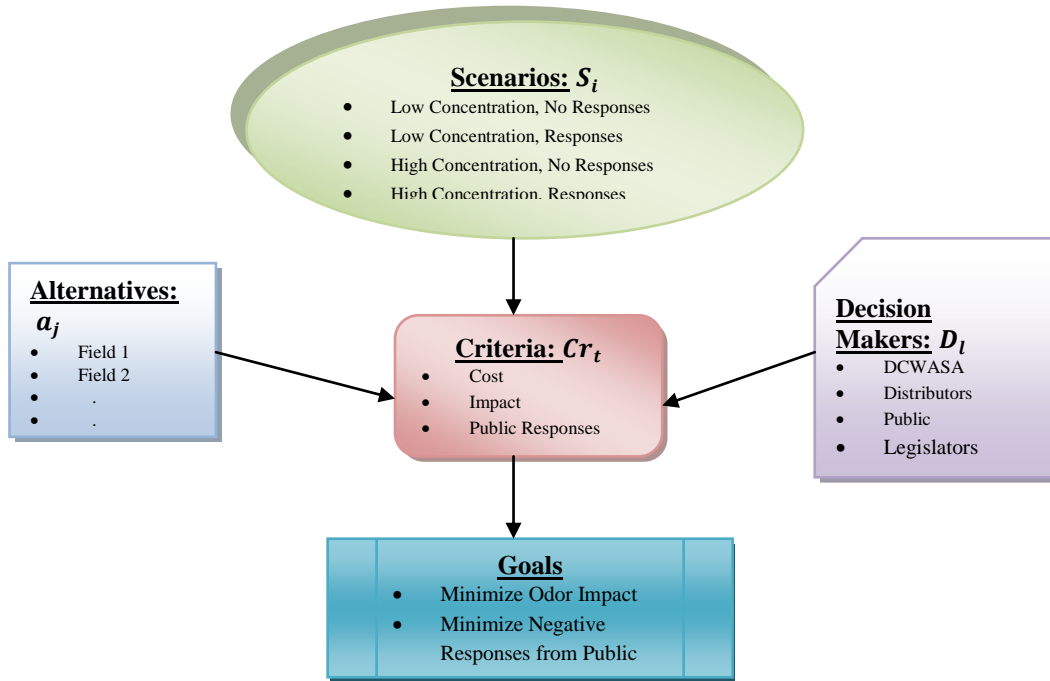


**Figure 1.1: Conceptual Model for Selection of Biosolids Land Application Sites**

Biosolids site selection consists of four principal steps: estimate of odor emission, prediction of odor concentration, assessment of odor impact, and selection of suitable distributional sites. These steps work in a sequential manner as shown in Figure 1.2. The output from the emissions estimation model, a field emissions rate, is used as an input when a dispersion model is employed. Similarly, predicted odor concentration in a study field is an attribute to estimate the consequences of odor impact in the study area. Eventually, a systematic selection of land application sites to distribute biosolids may be performed based on potential odor impacts.

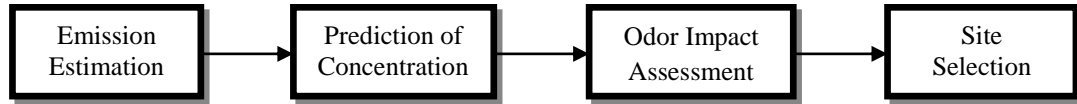


**Figure 1.2: Schematic of Biosolids Site Selection Procedure**

With this approach, the odor impact pathway is considered as a source-transport-reception pathway, which is a random process on spatial and temporal scales. The randomness comes from variation of biosolids odor emissions and atmospheric conditions. The site location or source coordinate is a user-defined origin in latitude ( $x$ ), longitude ( $y$ ), and elevation ( $z$ ). Using the concept of fields and states (Crawford-Brown, 2001), we can represent site location with field identification as  $field\_j(x, y, z), j = 1, 2, 3, \dots, n$ .

At the source, an odor emission for  $field\_j$  at time  $t, Q_{field\_j}(x, y, z, t)$ , is estimated and used as an input to a dispersion model. A United States Environmental Protection Agency (EPA) regulatory dispersion model called the AERMOD (Cimorelli et al., 2005) was employed to predict biosolids odor concentrations for  $field\_j$  at time  $t, C_{field\_j}(x, y, z, t)$ . Finally, an impact of biosolids odor can be performed as function of the predicted odor concentration at a receptor location,  $C_{receptor\_r}(x, y, z, t), r = 1, 2, 3, \dots, m$ , to determine population responses to biosolids odor, see Figure 1.3.

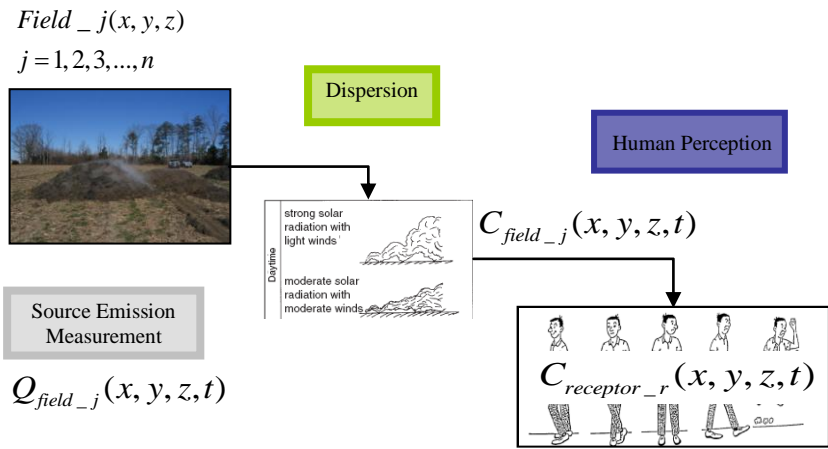


**Figure 1.3: Overview of Odor Impact Pathway**

A Geographic Information System (GIS) was used in mapping, visualizing, and modeling tasks. More specifically, the Environmental Systems Research Institute (ESRI)'s GIS software called ArcGIS was used to generate various maps in this study including predicted concentration map (C-Map), which expresses locations where people could potentially get effects from the biosolids odor, probability map (P-Map), which provides estimate of predicted concentration exceeding a certain threshold, and intensity map (I-Map), which expresses potential odor perception by human.

In summary, the principal advantage of the GIS-based odor impact assessment is to employ available tools including statistics, atmospheric science, and geography in an integrated approach to address the research problem. It is practical, and a wastewater biosolids generator could apply the model in the real world. In addition, the model addresses the odor problem by taking into account odor source emissions, variation of atmospheric conditions affecting dispersion of odor, and sensitivity of

odor perception by human, which is a significant parameter to quantify odor impact on surrounding communities.

Odor emissions at land application sites were investigated using the statistical inference. The probability distributions were developed to characterize the biosolids odor emissions at the land application fields and odor concentrations at the plant. The lognormal distribution was the proposed distribution to describe biosolids odor emissions. An analysis of variance (ANOVA) was employed to investigate the variation of odor emissions from day-to-day operations. The results from the ANOVA indicated that there were variations within the same field and from day-to-day operations. This implies that the estimate of odor emissions needs to be updated regularly in order to improve the prediction accuracy of biosolids odor concentrations.

The U.S. Environmental Protection Agency (EPA)'s dispersion models, screening and refined models, were applied to investigate odor dispersion in the land application sites. The three different approaches used for estimating biosolids odor emissions at the fields were input into the dispersion models. The first approach was to use the expert opinion on the air flow rate to calculate odor emission rates. The second approach was to use the best estimate from the probability distribution. The simulated-flux chamber method was the other approach to estimate biosolids odor emissions at the field.

Standard error of estimate ( $S_e$ ) indicated that the emission estimate using the assumed air flow rate provided the best modeling performance in the screening analysis compare to the MES data. While results from  $S_e$  showed that the predicted

concentration with odor emissions estimated by the probability distribution best described the modeling performance in case of refined models.

The geographic information system (GIS) was used to support visualizing, modeling, and mapping to the dispersion model. The predicted concentration maps (C-Map) were created to express the areas for odor strength. The probability maps (P-Map) for exceeding certain odor level, 7 dilution-to-thresholds in this case, were also generated. The 7 D/T was used as a criterion for potential odor complaints from neighborhoods. The study found that quality and quantity of input data such as odor emission rates, meteorological conditions, and measurement information affect the accuracy of the modeling predictions.

To assess the impact from biosolids odor, we proposed using two approaches to support the assessment. First, the intensity maps (I-Map), following Steven's power law, were created to estimate the human perception from the stimulus odor concentrations. The other approach was to estimate size of population potentially affected by the odor concentration levels. It was intended to assess the odor impact on the general population and not sensitive individuals. The impact areas for each odor strength categories were calculated for land application sites. The population density and the potential impact areas were used as a mean to assess the potential odor impact at land application sites.

#### *1.4.2 Summary of Research Outcomes*

Thirteen outcomes were developed in this research. Table 1.1 provides the outcomes with corresponding sections in the thesis.

**Table 1.1: Research Outcomes**

Items	Research Outcomes	Section (s)
1	Conceptual Model for Selection of Biosolids Application Sites	1.4.1
2	Biosolids Site Selection Procedure	1.4.1
3	Biosolids Odor Impact Pathway at Land Application Sites	1.4.1
4	Normal Probability Plot for the MES Odor Emission Data	4.5.1
5	Lognormal Distribution of Odor Concentration at Blue Plains	4.5.2
6	Lognormal Distribution of Odor Emission Rates at Blue Plains	4.5.2
7	Analysis of Variance (ANOVA) of Odor Emission Data	4.6.2
8	Guideline for Emission Estimates	4.7
9	Geoprocessing Models <ul style="list-style-type: none"> <li>• Defined Projection Model</li> <li>• The Clip Raster Model</li> <li>• Receptor Terrain Model</li> <li>• Intensity Map Model</li> <li>• Impact Area Model</li> </ul>	5.2.2    5.2.3
10	Results from Screening Analysis	5.3.2
11	Results from GIS-Based Odor Impact Assessment <ul style="list-style-type: none"> <li>• Prediction Map (C-Map),</li> <li>• Probability Map (P-Map),</li> <li>• Intensity Map (I-Map)</li> <li>• Odor Impact to Population</li> </ul>	5.4.2
12	Model Validation	5.3.3, 5.4.3
13	Comparing Screening VS Refined Analysis	5.5

1.5 Contribution

This research directly aids the District of Columbia Water and Sewer Authority (DCWASA) in providing a better understanding of factors associated with nuisance conditions in land application sites. It can serve as a supporting tool for decision makers to better manage and control malodorous conditions produced from land-applied biosolids. Concentration maps (C-Maps), probability maps (P-Maps), and intensity maps (I-Maps) provide a better visualization of potential impact areas; they can be used to support decision making for selecting suitable distributional sites. In

addition, it will benefit other wastewater facilities, which recycle biosolids through land application, by providing a procedure to estimate potential odor impacts.

The contribution of this study also expands to the field of environmental engineering to establish a framework for dealing with an inherent odor problem generated from wastewater treatment processes. Moreover, it is particularly useful for researchers in the area of environmental management and program management to develop planning and to improve decision-making processes. Ultimately, the conceptual approach of the research, by considering a problem as source-transport-receptor, can be used for other types of environmental pollutants, not just for odor control.

### 1.6 Overview of Dissertation

The rest of the dissertation is organized as followed:

Chapter two provides a background on biosolids and their characteristics. It also describes the generation of biosolids odor and potential impacts to community. Related research works are also presented in this chapter.

Chapter three presents the background on wastewater treatment processes at the Blue Plains wastewater treatment plant and related data used in this study such as biosolids reuse sites and biosolids odors data, meteorological data, and geographical data.

Chapter four deals with emissions estimates using three different approaches: expert opinion, statistical inference, and a simulated flux chamber method. This chapter provides a guideline for making a decision about emissions rates used in a

dispersion model when there is limited information, which is considered as the first step in the modeling procedure.

Chapter five demonstrates uses of dispersion models with developed framework in the Geographic Information System (GIS) to predict odor concentration and to assess odor impact at land application sites. Results and discussions follow.

The last chapter identifies important findings and possible future work.

## Chapter 2: Background and Literature Review

Biosolids are treated sewage sludges that result from treatment of domestic sewage at wastewater treatment facilities. They contain nutrient-rich organic materials used in recycling and agricultural fertilization. A national survey conducted in 2004 by the United States Environmental Protection Agency (EPA) found that 55% of the biosolids were beneficially used, of which 74% of all beneficial use went to agricultural application (Goldstein, 2007).

The biosolids are mainly produced through biological treatment. In addition, physical and chemical processes such as thickening, stabilization, and dewatering can produce biosolids (Evanylo, 2003). Several methods of distributing, utilizing, or disposing of biosolids are available including landfilling, incineration, and land application. Due to its beneficial use and inexpensive option, land application is widely used in the United States: 63 % in 1998, and 70 % are expected in 2010 (Oleszkiewicz, 2002).

Biosolids are characterized by wastewater constituents and treatment processes. There are, typically, two classes of biosolids regarding to pathogen reduction: class A and class B. The main difference of those classes is that pathogens of class A biosolids are reduced to below detectable levels; therefore, less restriction is needed when applied to land (Evanylo, 2003). Nevertheless, an inherent odor nuisance of biosolids could be present even though land applied biosolids meet pathogen reduction standards.

The most often detectable odorous compounds found in biosolids are ammonia, amines, and reduced sulfur-containing compounds that are generated during the wastewater treatment, storage, and use (EPA, 2000a). The decomposition of organic nutrients by heat, aeration, and digestion from individual unit processes are typical causes of released odorous compounds (EPA, 2000c). An ability to identify odorous compounds associated with biosolids will improve wastewater treatment process performance and enhance management of odor in wastewater facilities and application sites.

A number of studies have been conducted to identify odorants associated with individual unit processes. A study at the Blue Plains Advanced Wastewater Treatment Plant (AWTP) in Washington, DC, for example, found that volatile fatty acids were identified in the primary gravity thickeners, while Trimethylamine (TMA) released with ammonia, which has a fishy odor, could only be detected after lime addition resulting from polymer addition in the Dissolved Air Flotation (DAF) process (Kim et al., 2002; Kim et al., 2003).

The amount of lime addition, amount of polymer addition at dewatering and DAF, and the blanket depth affect change of the biosolids odor levels (Gabriel et al., 2006). For the secondary process, the sludge blanket level in secondary sedimentation basins had a relationship with Volatile Sulfur Compounds (VSC) (Sekyiamah, 2004). Moreover, the blanket level was a significant factor to dewatered solids odor, and a significant increase in odors could be observed if the blanket level is higher than 1.8 feet (Janpengpen et al., 2007). Recently, more process variables potentially promoted higher odor were identified by uses of various statistical models: percent solids and

temperature of biosolids, percentage of the gravity thickener solids (GT) in the blend tank, pH of the GT solids, concentration of the return activated sludge (RAS) at the secondary process, and number of centrifuges running (Vilalai, 2008).

Nevertheless, individual unit processes do not only create on-site odor problems but also resulting biosolids odor. Reduction in odors at the sources especially in solid-handling systems, such as thickening, drying, and lime stabilization, will reduce on-site air quality problems and also reduce odor emissions from the land applied biosolids (Kim et al., 2002). For instance, the addition of Bioxide, especially Bioxide-Anthraquinone (AQ), would help in reducing total reduced sulfurs from biosolids production (Kim et al., 2005). Yang and Hobson also stated that reduction of odor emissions at the source by 50 % would also reduce odor concentration at a receptor by 50 % if the distance from the source is considerable (Yang and Hobson, 2000).

At the land application sites, Volatile Solids (VS), which are readily decomposable organic matter usually expressed as percentage of total solids, are accounted for potential odor problems at land application sites (Evanylo, 2003). Those volatile solids often result from biosolids composting (Rosenfeld and Suffet, 2004). Ammonia level is expected to be high during the first few days and then drop off.

Measurement of ambient odor strength is recorded using a field olfactometer as dilution-to-thresholds (D/T), a dimensionless measure of odor concentration. Particularly, the principle of (D/T) is the widely used method for measuring odor concentration downwind from a source at land application sites (Nicell, 2003). The

D/T number recorded is the dilution ratio needed to make the sampling odorous ambient air non-detectable (McGinley and McGinley, 2005).

By using St.Croix's Nasal Ranger field olfactometer, the Western Lake Superior Sanitary District (WLSSD) in Minnesota conducted a study to gain a better understanding of biosolids odor impacts surrounding land application sites (Hamel et al., 2004). McGinley et al. (2004) also used the same field olfactometer to find a correlation between hydrogen sulfide ambient concentration and D/T (McGinley and McGinley, 2004).

The emitted odorous compounds are carried from one place to another place by wind (Turk et al., 1974). Typically, odorous emissions are not continuous but intermittent (Poostchi, 1985). A mixture of volatile compounds emitted to the air in varying quantities may have different odor detection thresholds, which is a level of odor concentration people can detect (Simms et al., 2000). The odor detection threshold represents the odorant perception in some specified percentage of the population, usually 50 % (Rafson, 1998).

Factors such as wind velocity and pollutant concentration in liquid phase influences emission rate and then odor concentration (Guillot et al., 2007). Given wind speed, wind direction, and the characteristics of the atmosphere turbulence, the downwind odor concentrations can vary greatly over space and time. For convective turbulence and strong winds, the maximum turbulences take place on hot summer days while with mechanical turbulence and cold mornings and low wind speeds, minimal levels of turbulence occur (Simms et al., 2000). Rough terrain and other

topographical features can also increase the complexity of atmospheric turbulence (Simms et al., 2000).

With its limitations, the determination of odor concentrations by D/T and established olfactometric methods alone (such as a field olfactometer at a single point downwind) can only represent the odor response by humans at a certain point in time and specific location. Alternative methods such as an electronic nose or a dispersion model are usually employed to deal with the lack of a continuous measurement by an olfactometer.

For the dispersion model, it can be used to predict the odor concentrations at particular receptors under given meteorological conditions, and topographical features. Using long-term meteorological conditions will also allow the determination of frequency of occurrence of concentrations exceeding a threshold level (Yang and Hobson, 2000). The significant components needed when using a dispersion model includes source emission rates and dispersion conditions.

Determination of the source emissions rates is essential for evaluating odor impacts. Many studies were conducted to estimate the emissions rates. For example, by using the concept of odor emission capacity (OEC), a German wastewater treatment facility determined an amount of odorants presented in the liquid phase in the area-related processes (Frechen, 2004). The dynamic flux chambers along with a wind tunnel were developed to measure odorant emissions from an area source and to calculate odor flow in its liquid phase. It is believed that known emissions rates could be used to follow the evolution of the source in terms of annoyance (Guillot et al., 2007).

By giving an emission flow rate of an odor, meteorological condition, and topographical features, an analysis of odor dispersion could be performed. There are an extensive number of studies that incorporate the techniques of dispersion models to study the odor impacts from a variety of sources including odor generated from wastewater treatment facilities and composting sites such as (Smith, 1995; Diosey, 1997; Alpert and Wu, 1997; Kaye and Jiang, 2000; McIntyre, 2000; Wu, 2000; Simms et al., 2000; Capodaglio et al., 2002; P. Gostelow et al., 2004; Todd Williams and Servo, 2005; Lisboa et al., 2006; Voelz et al., 2006; Diosey, 2008). However, from the best of our knowledge, there are few studies focusing on the odor impacts from biosolids land application sites (Rynk and Goldstein, 2003).

Human responses to odor are highly subjective. People detect and perceive odorous compounds very differently depending on their exposure to the environment, their odor detection thresholds, and individual human experience. A determination of odor impact by odor threshold alone is not sufficient, since the threshold fails to provide the information in terms of complaints potential (Henshaw et al., 2006).

Poostchi (1985) developed an odor impact model (OIM) for six different pure chemical compounds, with known thresholds, to assess the probability of complaint (PPC) and predicted degree of annoyance (PDA) from surrounding communities. Moreover, Nicell (2003) developed expressions to relate odor concentrations to probability of response and probability of annoyance from the population. A modified OIM could then be used in conjunction with a dispersion model to quantify population responses to odor (Nicell and Henshaw, 2007). However, the OIM might

not be, at this time, applicable to an odor with unknown odor threshold such as biosolids odor.

## Chapter 3: DCWASA Wastewater Treatment Processes and Related Data

### 3.1 DCWASA Background

The District of Columbia Water and Sewer Authority (DCWASA) operates an advanced wastewater treatment plant (AWTP) at Blue Plains that serves more than two million Washington metro area customers in the District of Columbia, portions of Montgomery and Prince George's Counties in Maryland, and portions of Fairfax and Loudoun Counties in Virginia, see Figure 3.1.

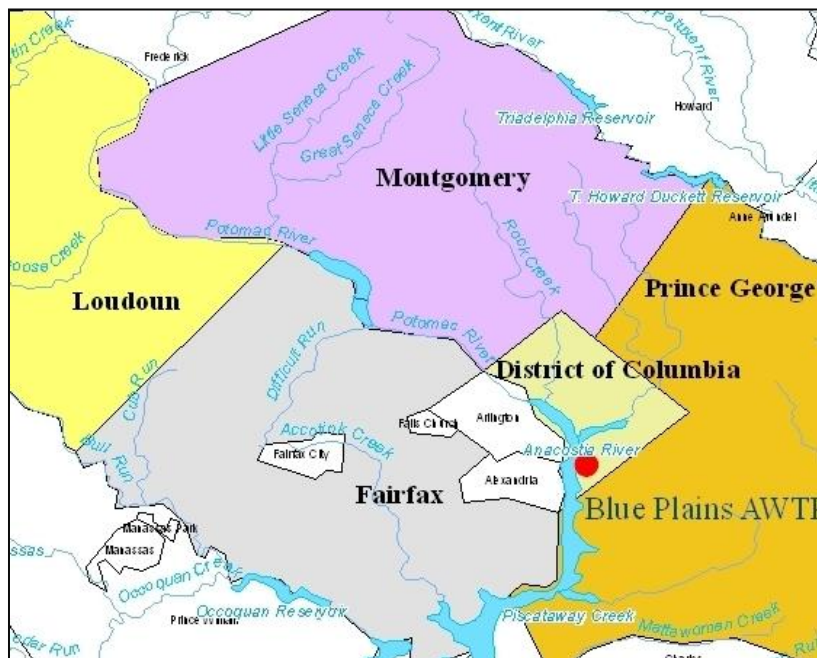


**Figure 3.1: DCWASA Service Areas**

As the largest facility of its kind, the plant has the capacity to treat 370 million gallons per day (MGD) of wastewater. The biosolids generation process begins with removing debris and grit from the sewage and trucking to a landfill. Resulting wastewater goes to the primary sedimentation tanks where the suspended solids are

separated from the liquids. The solids from the primary process then go to the tanks where the sludge solids settle to the bottom by gravity. The settled solids from the secondary process and nitrification reactors are thickened separately. The thickened solids are dewatered. Lime is added to reduce pathogens and diminish odors (Figure 3.2).

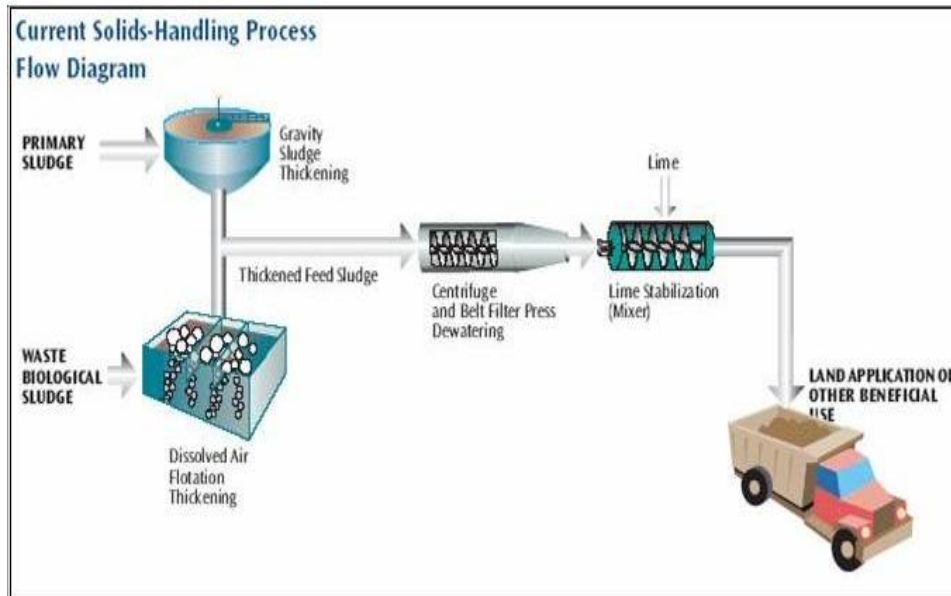


**Figure 3.2: DCWASA Solids Process (DCWASA, 2005b)**

More than 1,200 tons a day of the final biosolids product are then applied to farm application sites in Maryland and Virginia (DCWASA, 2005a;DCWASA, 2005b). Figure 3.3 shows a map of the number of times biosolids distributed in Virginia by counties from 2005 to 2008.

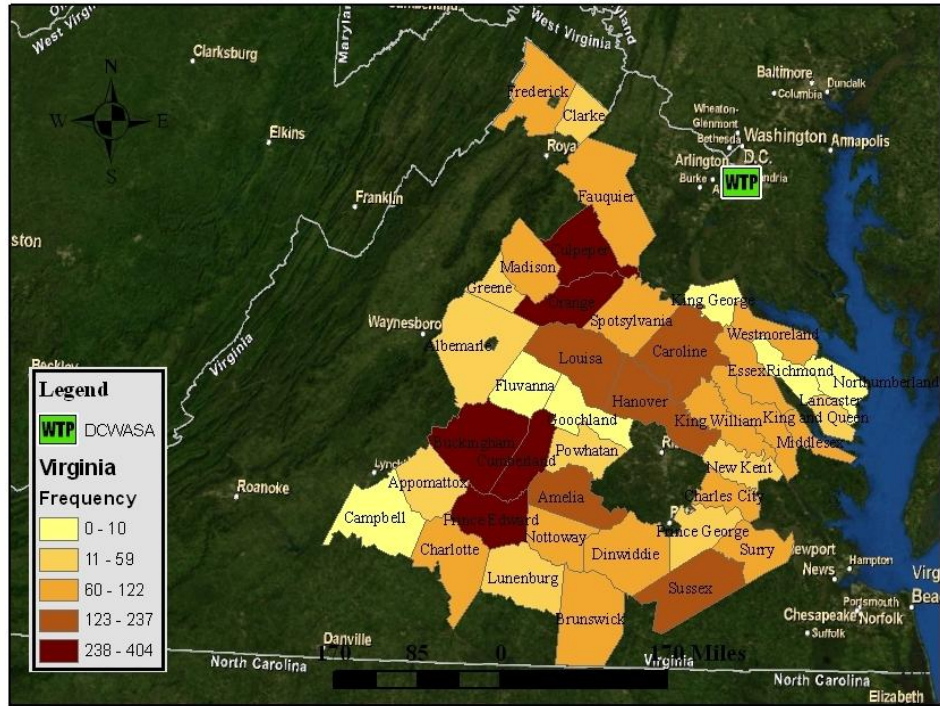


**Figure 3.3: A Map of Biosolids Distribution in Virginia Counties, Virginia (2005-2008)**

### 3.2 DCWASA Reuse Sites Data

Maryland Environmental Services (MES) collects DCWASA field data for biosolids odor monitoring purposes referred to as the odor monitoring land application inspection program (Razik, 2005). Odor monitoring is accomplished by inspectors using two different methods: a sniff test and a field olfactometer.

The sniff test is a measurement of biosolids odor by the human nose. There are no field instruments used with the sniff test. Following the test procedure, an inspector is asked to classify biosolids odors into one of four categories: none, slight, moderate, and strong. In contrast, an objective measurement of odor concentration expressed as dilution-to-threshold (D/T) is performed by use of the Nasal Ranger field olfactometer produced by St. Croix Sensory Inc. as shown in Figure 3.4.



**Figure 3.4: MES Inspector with Nasal Field Olfactometer**

### *3.2.1 Field Odor Measurement*

The odor sensitivity test assesses an individual's olfactory sensitivity. It is required before conducting odor strength assessments. The test combines two standard procedures. One is the ascending concentration procedure with fourteen n-butanol odor pens and two blank pens in a Test Kit box (see Figure 3.5). The n-butanol pens are numbered in discrete steps from 15 (lowest) to 2 (highest). The other standard procedure used is the Three-Alternative Forced Choice (3-AFC) or so called the Triangular Force-Choice (TFC).



The result of the test is an average value from rounds one and two, which is an individual detection threshold based on the standard odor, n-butanol. A detection threshold is the concentration of the odorant that has a 0.5 probability of being detected under test conditions. An individual detection threshold is not a fixed attribute but a value assuming the variation of olfactory sensitivity as a result of random factors such as health status.

After conducting the sensitivity test, an assessment of odor strength can be performed using the Nasal Ranger field olfactometer. The typical procedure of the field olfactometer is to have an inspector takes a reading of odor strength downwind at the location between the odor source and the nearest receptor location such as off-site residential or school areas. The inspector begins measurement with the highest dilution-to-threshold level 60 D/T. The reading is decreased in the following discrete steps: 60, 30, 15, 7, 4, and 2 D/T(s). The test is stopped when the inspector can detect the odor.

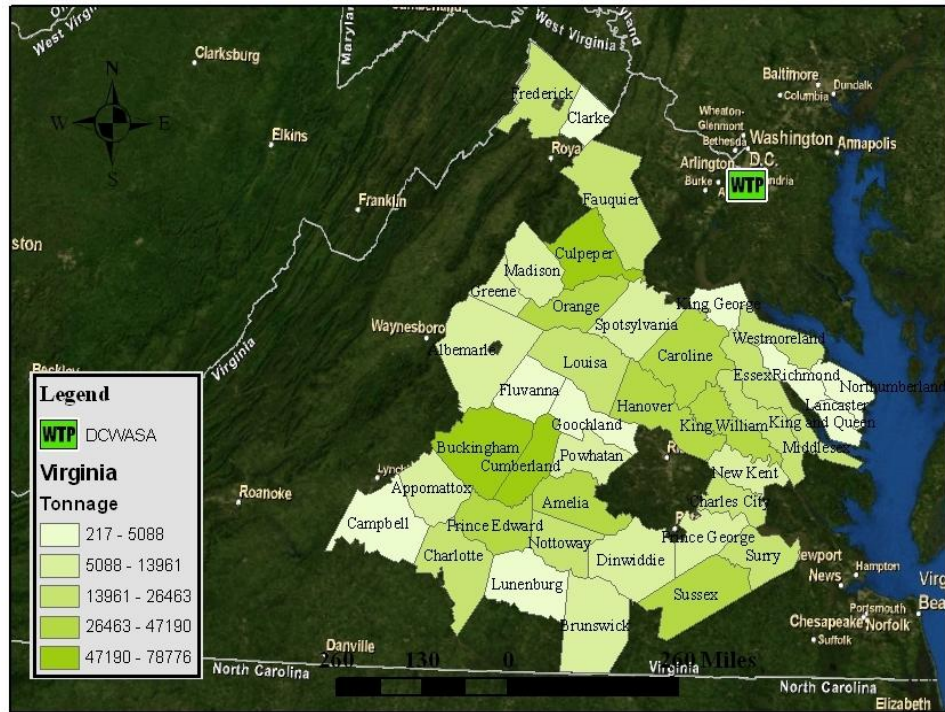
The inspector will also note odor character (what the odor smells like) and hedonic tone (a subjective assessment of pleasantness and unpleasantness of biosolids odor). Despite the information on odor measurement, the inspector is required to enter biosolids source information, type of application, and weather condition in the site visit form. Some of these entries are used in modeling process such as date unloaded, acres used, and source location. Figure 3.6 shows an example of the site visit form. Table 3.1 provides related data description used in the modeling processes.

Figure 3.6: MES Inspection Site Visit Form (Razik, 2005)

Table 3.1: MES Data Description Used in Modeling Process

<i>MES Data</i>	<i>Data Description</i>
Date Unloaded	The date that a particular load direct from the plant arrived to either a land application site or storage facility
Site Name	The site where the material was taken
Field Designation	The name of the particular field (or storage site) where the material was taken. A site can have more than one field assigned to it, i.e., there can be many fields on the site.
Latitude/Longitude	The location where the material was taken
Field Olfactometer Reading	The reading obtained from the inspectors' field olfactometer (Nasal Ranger), given in dilutions-to-threshold (D/T). The Nasal Ranger provides discrete readings as follows: 2, 4, 7, 15, 30, and 60 D/T(s)
Odor Measurement Time	The time that the odor measurements were taken
Odor Measurement Location	The approximate location at that land application field where the odor measurements were taken
Acres Used	The acreage used for land spreading on particular day

The MES data were preprocessed for data cleaning and data exploration. The data cleaning was performed to investigate missing data or outliers. The exploration of data aimed to provide a summary of data statistics. Figures 3.7 and 3.8 provide some examples of the MES data .



**Figure 3.7: Amount of Tonnages Applied in Virginia Counties from 2005-2008**

Figure 3.7 shows the amount of biosolids that were applied to land application fields in Virginia from 2005 to 2008. in wet tons of and varies in different counties. Figure 3.8 shows a frequency distribution of biosolids odor strength in dilution-to-threshold (D/T). The D/T values are categorized into five major ranges: 2, 4, 7, 15, and 30 following a dial in the Nasal Ranger field olfactometer.

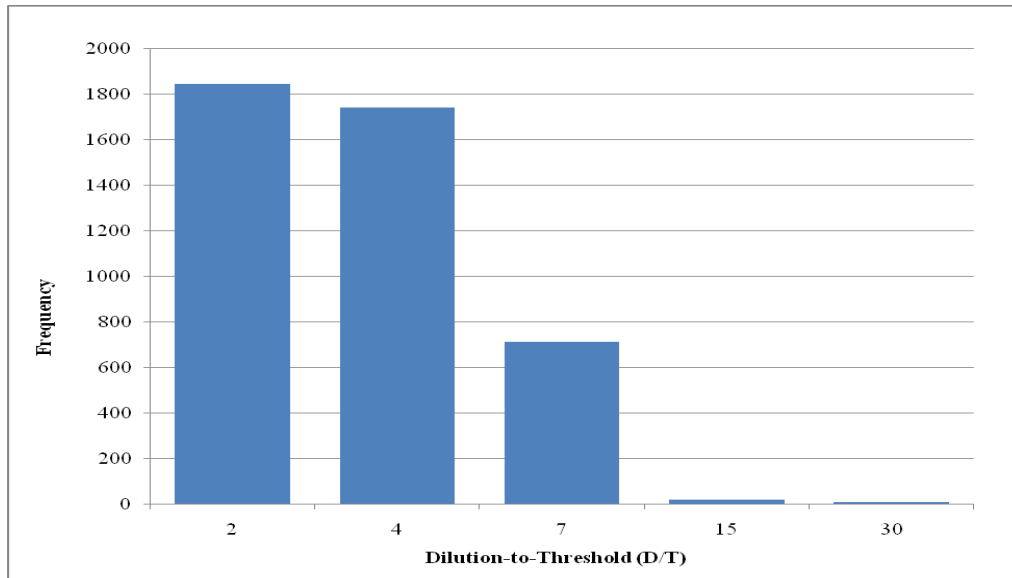


**Figure 3.8: Frequency Distribution of Field Dilution-to-Threshold (2005-2008)**

### *3.2.2 Emission Testing*

Odor emission is a combination of physical and chemical processes. Measurement of gas emission rates can be divided into three approaches: indirect measurements, direct measurements, and laboratory simulations. Indirect techniques require measurements of ambient concentration at or near a site. Source characteristics and meteorological conditions are included in a model such as a dispersion model to determine an emission rate. The second approach directly measures emission rates using the flux chamber while the third approach creates an emission source in the laboratory to determine an emission rate.

The isolation flux chamber technique, which is a direct measurement technique, was selected to test emission rates in this study. The isolation flux chamber is the most promising technique for measuring gas emission rates with a high degree of accuracy and precision. It is economical relative to other techniques and simple to

use. This approach uses a flux chamber to sample gaseous emissions from a defined source area with a known flow rate. The flow rate is taken as the sweep air for the flux chamber. The samples are sent out to a laboratory for an analysis of odor parameters such as odor concentration. The odorous emission rate is calculated by multiplying the odor concentration by the sweep air flow rate of the flux chamber used to collect the sample

### 3.3 Meteorological Data

The two types of meteorological data, National Weather Service (NWS) Integrated Surface Hourly Data (ISH), DS-3505, and NWS twice-daily upper air soundings, TD-6201, are required in meteorological preprocessing in the modeling process. The ISH is meteorological data measured at the earth's surface. The data includes physical parameters directly measured by an instrument, such as station number (ID), year, month, date, and hour, ceiling height in hundreds of feet, wind direction in tens of degrees, wind speed in knots, dry bulb temperature in degree Fahrenheit, cloud cover in tens of percent, opaque cloud cover in tens of percent.

The surface data can be obtained from the National Climatic Data Center (NCDC), in Asheville, North Carolina. The data are mostly available from weather stations located near or at airports. Figure 3.9 shows the locations of available weather stations in Virginia, all of them are located at airports.

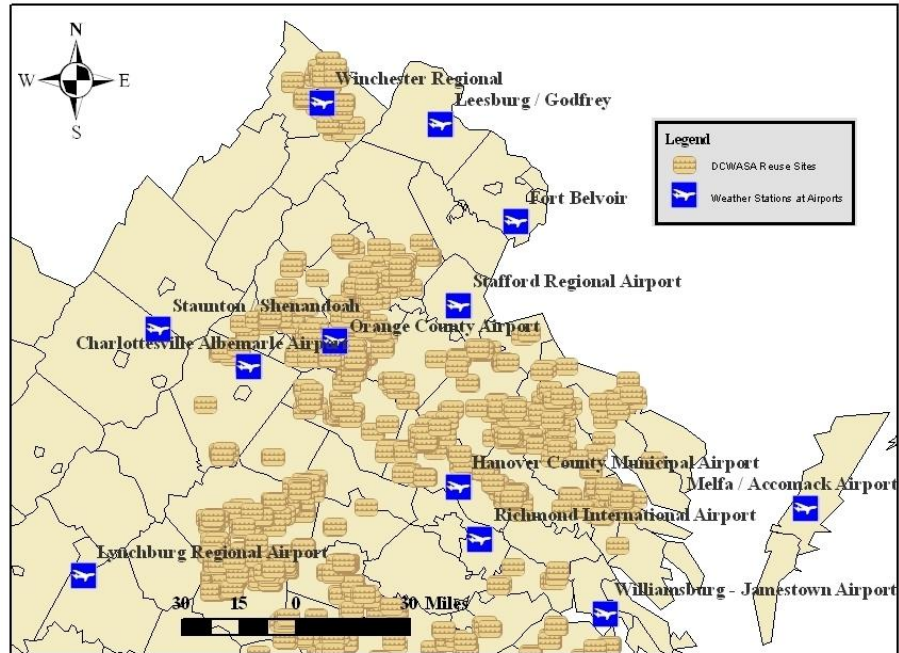


**Figure 3.9: Available Hourly Surface Weather Stations in Virginia**

The upper air data can also be obtained from the National Climatic Data Center in Asheville, North Carolina. The upper air data is a meteorological data measured in the vertical layers of the atmosphere such as atmospheric pressure, free air temperature, relative humidity, wind direction, and wind speed.

### 3.4 Geographical Data

The study used geographical data obtained from the Environmental Systems Research Institute, Inc. (ESRI)'s Data & Map 2007 that includes StreetMap<sup>TM</sup> USA, Elevation, and Image Data World. The geographical data were used in the Geographic Information System (GIS) to visualize, mapping, and modeling.

There are two type of geographical data used in the GIS: vector data and raster data. The vector data are in discrete forms of point, line, and polygon such as source

coordinate and counties shapfile. The raster data, on the other hand, are continuous stored z-values such as height of the features. Examples of the raster data used in this study are elevation, temperature, or pollution concentration. Vector data, raster data, or the combination of both form a layer. In this study, all GIS tasks are dealt with in layers.

## Chapter 4: Estimate of Biosolids Odor Emission

### 4.1 Biosolids Odor Emission and Measurement

Biosolids odor emission consists of a complex mixture of odorous compounds, as odorants, which are produced from wastewater characteristics and treatment processes. The most common odorants found in biosolids emissions are sulfur (S)-containing and nitrogen (N)-containing compounds. Specific odorants are generally associated with aerobic or anaerobic conditions. There are a number of studies conducted to identify main odorants from wastewater treatment processes.

For S-containing compounds, the most widely measured compound in wastewater facilities is hydrogen sulfide. The reason is that because of its presence in liquid wastewater and its numerous availability of measured devices (Hentz, 1998). Hydrogen sulfide is normally produced under anaerobic conditions. It has a rotten egg odor, and its emission depends on pH levels of the biosolids.

Another S-containing compound frequently found during the heat of hydration is the Dimethyl disulfide (DMDS). The DMDS has rotten cabbage odor and accounts for 55-98% of the total reduced sulfur found in biosolids applications to soil such as a land application (Rosenfeld and Suffet, 2004). Methyl mercaptan, the other main sulfur compound with smell like rotten cabbage, has similar origins as DMDS and a low odor detection threshold and can potentially lead to odor complaints (Hentz, 1998).

N-containing compounds such as Ammonia and Trimethylamine are released from lime stabilization process (Bremner and Banwart, 1976). Ammonia has a pungent medicinal odor, while Trimethylamine has a fishy odor (Suffet et al., 2004).

Ammonia odor is frequently reported to be found during the first few days after a land application. Evidence from MES's field data can confirm this claim. Figure 4.1 shows the frequency of biosolids odor descriptions from 2005 to 2008. MES collected those data by asking its inspectors to perform a subjective assessment of how the odors smelled. Apparently, ammonia is the most detected compound on the first day of land application.

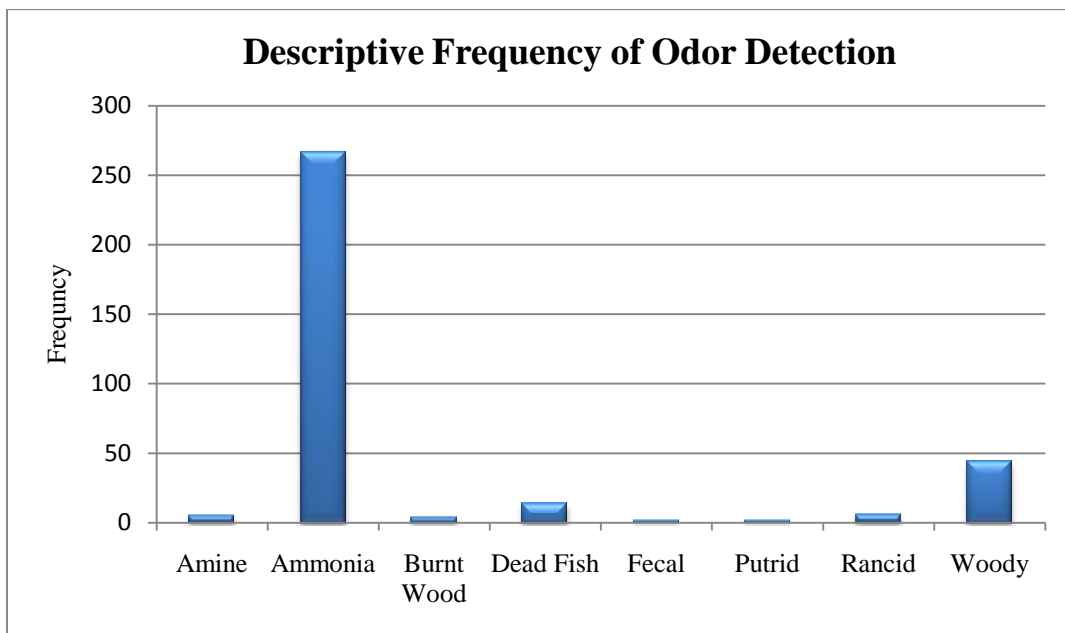


**Figure 4.1: Frequency Detection of Odor Description from MES Field Data (2005-2008)**

The decomposition of organic nutrients is generally accounted for volatile emissions of biosolids odorants (EPA, 2000a). In addition, there are other factors driving biosolids emissions. At wastewater treatment facilities, a certain process, such as the case for sedimentation tanks, and meteorological conditions are also important factors (P.Gostelow et al., 2004). For biosolids applied to land, on the other hand, there are two general types of emission processes which are either controlled by the

diffusion rate of the chemical compounds through the air-filled spaces of the soil or controlled by the rate of evaporation (EPA, 1986).

The first case occurs particularly in underground facilities such as landfills while the latter is most often found when biosolids are surface-applied. In the case of surface application, the emission rate is dependent on time and the evaporation process. Some of the important parameters affecting the evaporation process are the volatility or vapor pressure of the biosolids and ambient meteorological conditions, i.e., solar radiation, wind, and surface roughness. The vaporization rate reaches its maximum immediately after biosolids are applied to land since it is easy for biosolids nearest the surface to vaporize and diffuse through a thin layer of soil. However, it is more difficult for biosolids in deeper soil levels to diffuse through a thicker soil layer, so the rate of emission decreases with time (EPA, 1986). Determination of odor emission rate at the biosolids source is essential in assessing the impact of the emission.

The measurement of biosolids emission typically falls into two categories: analytical measurement and sensory measurement. Analytical measurement focuses on a specific odorants or odorous compounds such as total reduced sulfur compounds. Sensory measurement, on the other hand, tends to a sense of smell or odor perception by human. There is no preferred method for measuring biosolids odor emission. It depends on the purpose of the study.

Typically, biosolids odor emissions at land application sites are considered a passive source, for which mass flow rate data are not available or difficult to measure especially for an area source. However, it is practical and desirable to measure the

emissions rate with a standard measurement device that has a known flow rate. Such measurement devices are designed for both analytical measurement and sensory measurement. At biosolids land application sites where low-level or ground level releases are usually expected, the biosolids odor emission is a combination of varying quantities of biosolids odorous compounds. This study, therefore, focused on sensory measurements since they would better represent human perception of biosolids odors. However, it is important to distinguish between odorant and odor.

Odorants are any chemical in the air, and the term “odor” refers to perception experience of one or more chemicals by human olfactory nerves (McGinley and McGinley, 2002). Measurement of odor perception or sensory measurement of odors can be expressed as odor evaluation parameters. The United States Environmental Protection Agency (U.S. EPA) recommends using five typical parameters:

- 1) Odor Concentration ( $C_{odor}$ ) measured as dilution ratios and reported as detection Threshold (DT) and recognition Threshold (RT) or as dilution-to-thresholds (D/T)
- 2) Odor Intensity (I),
- 3) Odor Character,
- 4) Odor Persistency, and
- 5) Odor Hedonic Tone.

Each of those parameters serves as criteria for measuring an odor in different aspects. The first four parameters are objective because they are measured without personal sensation. Threshold values provide an indication of odor strength or levels of dilution needed to bring odor strength to its threshold. The detection threshold

(DT) is a level where people just notice the odor, but the recognition threshold (RT) is a level where people can recognize what it smells like. Odor intensity is the relative strength of the odor comparing with the reference odorant n-butanol. The character of an odor is referred to as “odor quality.” There are eight standard odor descriptors used as a referencing vocabulary, including vegetable, fruity, floral, medicinal, chemical, fishy, offensive, and earthy. Odor persistency refers to the rate at which perception of odor intensity decreases as the odor is diluted also referred to as the Steven’s power law (Stevens, 1960). The last parameter, Hedonic tones, is a subjective measurement of pleasantness or unpleasantness of an odor sample. An arbitrary scale for ranking odors is ranged from -10 (unpleasant) to +10 (pleasant). An assessor assigns a hedonic tone for an odor using her/his personal experience and memories.

#### 4.2 Information about Emissions Rates and Current Estimation Method

Information on biosolids odor emissions in land application sites is often not available. Even though there are devices available for measurement of odor emissions, it is not practical or economical to sample all sensitive locations of different times. Thus, the current practice for sampling of odor emissions on the day of application is only for monitoring purposes.

Traditionally, as shown below, the odor emissions rate (odor unit per second,  $OU/s$ ) is estimated by the product of flux rate (liters per minute ,lpm), which is assumed constant over time, and odor concentration (odor unit per cubic meter,  $OU/m^3$ ). In addition, the flux rate is a product of air velocity (meter per

second,  $m/s$ ) and area source (square meters,  $m^2$ ).

$$Q = (V)(C_{Odor}) \quad (4.1)$$

$Q$  = Odor Emission Rate (odor unit per second,  $OU/s$ )

$V$  = Flux rate (liters per minute,  $m^3/s$ )

$C_{Odor}$  = Odor Concentration (odor unit per cubic meters,  $OU/m^3$ )

In general, the odor concentration can be obtained by measurement, in this case nearby the biosolids site. Information of the air velocity, however, is often not available and considered an unknown variable. Estimate of emission rates at a source with an unknown air velocity or a passive source is a difficult task. However, one can assume a flow rate based on results from a laboratory. For example, Rafson (1998) suggested using 0.1 foot per second (ft/s) or 0.03048 meter per second ( $m/s$ ) to represent air velocity (Rafson, 1998).

In a similar manner, a source emission rate per unit area at a land application field with a specified time,  $Q_{field\_j}(x, y, z, t)$ , can be deterministically calculated by multiplying a constant air velocity in meters per second with odor concentration in odor units recorded by inspectors from the Maryland Environmental Services using the Nasal Ranger field olfactometer.

Even though a deterministic estimate of the emissions rate is widely used in practice, it does not capture the uncertainties and answer the question about the characteristic of emission rates. As previously mentioned, information on emissions rates is not often available, and there are a number of sources of variability and uncertainty.

Odor emissions inherently vary both in spatial and temporal scales. The degree of variability is influenced by averaging time, atmospheric conditions, and geographic areas. Additional study or measurement cannot reduce its variability. Variability is also referred to as Type A uncertainty or stochastic/aleatory uncertainty. In contrast, Type B uncertainty or epistemic uncertainty in odor emission comes from incompleteness of knowledge or information about an unknown quantity of the true level of emissions. The uncertainty arises when there is a limited availability of site-specific data and/or imperfections of emission measurement (Cullen and Frey, 1999)

#### 4.3 Statistical Inference for Emission Estimates

The use of the statistical inference is considerably helpful to develop representations from available information of emission rates in the form of sample (s) and to draw conclusions or making predictions. Inferences about model parameters can be made with confidence intervals for the selected distribution. An interpretation of probability can be made using two general approaches:

1. Frequency or empirical interpretation of probability and
2. Subjective interpretation of probability.

One consideration between the two major interpretations of probability is the availability of data. Subjective interpretation is preferred when there are few data or when the data are not representative. Often, both frequency interpretation and subjective interpretation are employed when there is a concern with data quality and data quantity. The typical statistical inference approach can be summarized as shown in Figure 4.2

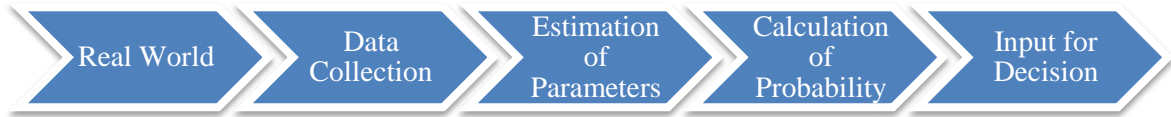


**Figure 4.2 Statistical Inference Approach**

In this research, we used the frequentist approach to develop probability distributions for biosolids odor emission rates that can be used to quantify variability and uncertainty in the emission rates. More specifically, it can be done in two sequential steps: 1. Estimation of model parameters, and 2. Model verification through goodness-of-fit methods and probability plots.

The frequentist approach assumes availability of emissions data. Conceptually, this approach is used to relate a theoretical probabilistic model to sets of observed data. The first step is estimation of model parameters such as sample mean and standard deviation. This process is simply a selection of an appropriate distribution to the data and to summarize variability of information about the distribution of sampled emission rates. Depending on sample sizes summary statistics provide three keys of characteristics of the distribution that are its central tendency, dispersion, and shape. The second step is verification of the model prediction with the observations.

#### *4.3.1 Model Estimation*

The first step in model estimation is to decide what kind of distribution is appropriate. Generally, biosolids odor emissions ( $Q$ ) can be considered as a continuous random variable due to physical, chemical, and biological characteristics of the biosolids itself and atmospheric conditions. In addition, the emission rates cannot be negative and its upper bound is not known for certain. After selecting the appropriate distribution, the

next step is to choose values of the distribution parameters such as mean ( $\mu$ ) and standard deviation( $\sigma$ ).

This study used the Palisade<sup>TM</sup> risk analysis software called @Risk<sup>TM</sup> to fit a distribution to the emissions data by using a parameter estimation method called maximum likelihood (MML). MML is based on the concept that only relevant information from an experiment is contained in the likelihood function. The distribution parameters in the MML are called the maximum likelihood estimators (MLEs). The MLEs of a distribution are the parameters of that function that maximize the probability of obtaining the given data set. The likelihood function of any distribution  $f(x)$  with its parameters  $(\theta_1, \theta_2, \dots, \theta_m)$  can be defined as:

$$L(\theta_1, \theta_2, \dots, \theta_m) = \prod_{i=1}^n f(x_i | \theta_1, \theta_2, \dots, \theta_m)$$

(4.2)

where the  $f(x_n | \theta_m)$  is a probability density function (pdf). The concept of the maximum likelihood method (MML) is to find an estimator ( $\theta_m$ ) that maximizes the value of likelihood function. To maximize the likelihood, we set the first derivative of the likelihood function with respect to  $\theta_m$  to zero and then solve to obtain the values of the distribution parameters. For lognormal distribution, the uniqueness of maximum likelihood estimators exists (Box and Tiao, 1973). Appendix 2 shows actual optimum of the likelihood function of the lognormal distribution.

#### 4.3.2 Model Verification by Goodness-of-Fit Tests

Model verification is the second step in determining a probability distribution by comparing model predictions with observed data. The simplest way to verify the model is to compare an observed histogram with the proposed probability density function. Another method for model verification is the use of statistical techniques called goodness-of-fit tests. A goodness-of-fit test is based on the concept of statistical techniques that compare statistical tests with critical values of the test statistics. There are three widely used methods of statistical tests: Chi-squared goodness of fit, Kolmogorov-Smirnov Statistics (K-S), and Anderson-Darling Statistics (A-D) (Benjamin and Cornell, 1970; Cullen and Frey, 1999).

@Risk<sup>TM</sup> employs all three methods to fit the theoretical distribution to the data. Before conducting the statistical tests, there is one issue that needs to be considered, data availability. The Chi-squared test is suitable for a data set that has at least twenty five observations. The A-D test is valid for a smaller data set but no less than eight data points while K-S could take as few as five data points.

The calculation of the Chi-squared statistic, which is generally known as the goodness-of-fit statistic, begins with grouping the data into several classes or so called binned data. The probabilities of sampling data within any given bins need to be determined. In this particular analysis, the equal probabilities were selected to reduce the arbitrariness of the bin selection that potential by result in the different conclusions of the same data. The test statistic  $\chi^2$  is then defined as:

$$X^2 = \sum_{i=1}^b \frac{(M_i - E_i)^2}{E_i} \quad (4.3)$$

where

$b$  = the numbers of bins

$M_i$  = the observed number of samples in the  $i^{\text{th}}$  bin

$E_i$  = the expected number of samples in the  $i^{\text{th}}$  bin.

The calculated test statistics  $X^2$  will be compared with the critical values of the chi-squared distribution with  $b - r - 1$  degrees of freedom, where  $r$  is the number of parameters in the hypothesized distribution. For example, in the case of a normal distribution, there are two parameters, which are its mean and standard deviation. The critical values for the chi-squared distribution can usually be found in a typical statistics textbook (Walpole et al., 2002).

The advantage of the Chi-squared statistic is its flexibility. It can be used with either discrete or continuous data. However, the weakness of the Chi-squared statistic is that there are no clear guidelines for selecting the number and location of bins. We can reach different conclusions from the same data depending on how we specified the bins.

Another fit statistic that can be used for continuous sample data is the Kolmogorov-Smirnov statistic. The K-S method compares stepwise empirical

cumulative distribution function with the CDF of hypothesized distribution. The goal of this method is to find the maximum vertical distance between the empirical stepwise CDF and fitted CDF. The first step is to calculate the maximum discrepancy or maximum difference between  $F(x)$  and  $S_n(x)$  defined as:

$$D_n = \max_x |F(x) - S_n(x)| \quad (4.4)$$

where

$n$  = total number of data points

$F(x)$  = the fitted cumulative distribution function

$S_n(x)$  = the empirical stepwise cumulative distribution function

The next step is the comparison of the maximum discrepancy to a critical value of the test statistic. If the maximum discrepancy value is greater than the critical value, then we reject the hypothesized distribution. Even though the K-S statistic does not require binning, which makes it less arbitrary than the Chi-squared tests, it does not fit well with the hypothesized distribution tails. . Table 4.1 provides information on critical values with respect to their significance levels ( $\alpha$ ).

**Table 4.1: Critical Values for Kolmogorov-Smirnov Goodness-of-Fit Test (Benjamin and Cornell, 1970)**

<i>Sample Size</i>	$\alpha = 0.10$	$\alpha = 0.05$	$\alpha = 0.01$
5	0.51	0.56	0.67
10	0.37	0.41	0.49
15	0.30	0.34	0.40
20	0.26	0.29	0.35
25	0.24	0.26	0.32
30	0.22	0.24	0.29
40	0.19	0.21	0.25
Large $n$	$1.22/\sqrt{n}$	$1.36/\sqrt{n}$	$1.63/\sqrt{n}$

The final fit statistic that can be used with continuous sample data is the Anderson-Darling Statistic. The A-D method is an improvement on K-S for fitting the hypothesized distribution tails.. The method compares a stepwise empirical CDF and the CDF of the hypothesized distribution based on a weighted square of the vertical distance and calculates critical values from the specific distribution. The first step is to calculate the A-D statistic from the equation below:

$$A^2 = - \sum_{i=1}^n \frac{(2i-1)[\ln(p_i) + \ln(1-p_{n+1-i})]}{n} - n \quad (4.5)$$

where

$i$  = ranked data in ascending order

$p_i$  = the cumulative probability calculated using the standard normal distribution

The next step is to compute a modified statistic from the A-D statistic and then compare it to a critical value, see Table 4.2 for the critical values for the A-D test. The modification of the A-D statistics is based on the sample size for comparison

with the critical value. Note that the critical values in Table 4.2 are valid for sample sizes greater than or equal to eight. The formula for the modified value is defined as:

$$A^* = A^2 \left( 1 + \frac{0.75}{n} + \frac{2.25}{n^2} \right) \quad (4.6)$$

**Table 4.2: Critical Values for Anderson-Darling Statistic (Cullen and Frey, 1999)**

<i>Significance Levels</i>	<i>Critical Values</i>
0.10	0.631
0.05	0.752
0.025	0.873
0.01	1.035
0.005	1.159

For each fit, @Risk reports one or more fit statistics. The fit statistics provide information on how well the selected distribution describes the data. As often is the case, there might be more than one distribution that fits the data well; the decision to select the appropriate distribution depends solely on subjective judgment and current practices. For example, it is known that concentration of pollutants resemble a lognormal distribution (Walpole et al., 2002; Clemen and Reilly, 2001; Singh et al., 1997)

#### *4.3.3 Model Verification by Probability Paper*

The probability paper plot is a graphical technique for comparing distributional assumptions with data. The method is considered subjective and good for small data sets. The typical procedure of the probability paper is to: 1) rank the data from smallest to largest observations, 2) estimate the fractiles of the data, 3) plot the value

of each data point versus its fractiles on the probability paper, 4) inspect the result, and 5) if appropriate, perform a regression analysis.

#### 4.4 Analysis of Variance (ANOVA)

Analysis of Variance (ANOVA) is the proposed method to investigate variations of emissions rates in land application fields. Two types of variations were considered: 1. variation of emission rates within the field, and 2. variation of emission rates among fields applied. Figure 4.3 shows a situation when the ANOVA might be needed to investigate the variations of odor emissions rates.

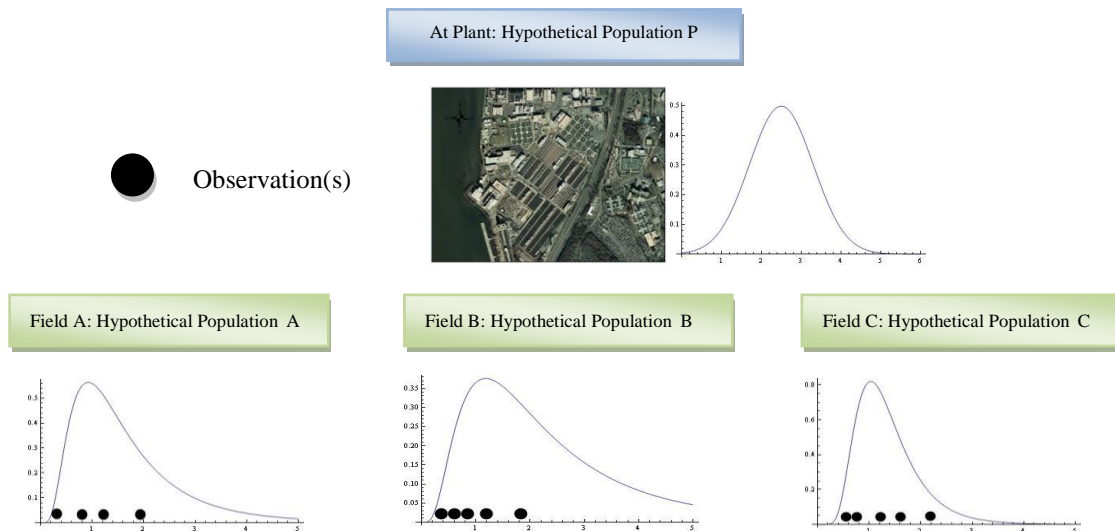


**Figure 4.3: Random Sampling from Three Reuse Fields**

In Figure 4.3, it was assumed that there is a hypothetical population distribution of odor emission rates at a wastewater treatment plant before being applied to fields A, B, and C. When biosolids were applied to those fields, random samples of biosolids odor emissions rates size  $n$  can be selected from each of  $k$  hypothetical populations at fields A, B, and C, respectively. The three different

populations are classified on the basis of different field locations for the day biosolids were applied. ANOVA is an appropriate tool to investigate variations of biosolids odor emissions rates within the field and among fields.

Generally, in ANOVA,  $k$  populations are assumed independent and normally distributed with means  $\mu_1, \mu_2, \dots, \mu_k$  and common variance  $\sigma^2$ . The hypothesis to be tested for the situation in Figure 4.3 is:

$$H_0: \mu_1 = \mu_2 = \dots = \mu_k$$

$H_1$ : At least two of the means are not equal.

Let  $y_{ij}$  denote the  $j$ th observation from the  $i$ th treatment. The treatment refers to various classification such as different biosolids land application sites. Table 4.3 provides an example of  $k$  random samples.

**Table 4.3:  $k$  Random Samples**

Treatment:	1	2	...	$i$	...	$k$	
	$y_{11}$	$y_{21}$	...	$y_{i1}$	...	$y_{k1}$	
	$y_{12}$	$y_{22}$	...	$y_{i2}$	...	$y_{k2}$	
	.	.		.		.	
	.	.		.		.	
	$y_{1n}$	$y_{2n}$	...	$y_{in}$	...	$y_{kn}$	
Total	$Y_1$	$Y_2$	...	$Y_i$	...	$Y_k$	$Y_{..}$
Mean	$\bar{y}_1$	$\bar{y}_2$	...	$\bar{y}_i$	...	$\bar{y}_k$	$\bar{y}_{..}$

For One-Way ANOVA model, each observation may be written in the form (Walpole et al., 2002)

$$y_{ij} = \mu + \alpha_i + \varepsilon_{ij}$$

(4.7)

where

$\mu$  = the grand mean; that is  $\mu = \frac{\sum_{i=1}^k \mu_i}{k}$

$\varepsilon_{ij}$  = random error and measures the deviation of the  $j$ th observation of the  $i$ th sample from the corresponding treatment mean.

$\alpha_i$  = the effect of the  $i$ th treatment.

The null hypothesis for  $k$  treatments is  $H_0 = \alpha_1 = \alpha_2 = \dots = \alpha_k = 0$ , and  $H_1$ : At least one of the  $\alpha_i$ 's is not equal to zero. The total variability for the One-Way ANOVA is expressed as a total sum of squares (SST), which is a combination of the treatment sum of squares (SSA) and the error sum of squares (SSE), or  $SST = SSA + SSE$  where:

$$SST = \sum_{i=1}^k \sum_{j=1}^n (y_{ij} - \bar{y}_{..})^2$$

(4.8)

$$SSA = n \sum_{i=1}^k (\bar{y}_{i.} - \bar{y}_{..})^2$$

(4.9)

$$SSE = \sum_{i=1}^k \sum_{j=1}^n (y_{ij} - \bar{y}_{i.})^2$$

(4.10)

For testing of equality of means ( $H_0: \mu_1 = \mu_2 = \mu_3$ ), the F-ratio,  $f = \frac{s_1^2}{s_2^2}$ , is used to test the null hypothesis at the  $\alpha$ -level of significance when

$$f > f_{\alpha}[k - 1, k(n - 1)]$$

The computations for the One-Way ANOVA are summarized in Table 4.4.

**Table 4.4: Analysis of Variance for One-Way ANOVA**

Source of variation	Sum of squares	Degrees of freedom	Mean square	Computed $f$
Treatments	SSA	$k - 1$	$s_1^2 = \frac{SSA}{k - 1}$	$\frac{s_1^2}{s^2}$
Error	SSE	$k(n - 1)$	$s_2^2 = \frac{SSE}{k(n - 1)}$	
Total	SST	$nk - 1$		

For unequal sample sizes, the sums of squares are revised as shown below:

$$SST = \sum_{i=1}^k \sum_{j=1}^{n_i} (y_{ij} - \bar{y}_{i.})^2$$

(4.11)

$$SSA = \sum_{i=1}^k n_i (\bar{y}_{i.} - \bar{y}_{..})^2$$

(4.12)

$$SSE = SST - SSA.$$

(4.13)

The degree of freedom are  $N-1$  for SST,  $k-1$  for SSA, and  $N-k$  for SSE, where

$$N = \sum_{i=1}^k n_i.$$

#### 4.5 Case Studies: Development of Probability Distribution

##### *4.5.1 Odor Emissions at DCWASA's Land Application Sites*

In 2003, DCWASA, by the Maryland Environmental Services, conducted experiments for measuring odor emission levels at land-applied biosolids sites using the flux chamber method. The MES collected ambient odor concentration data in the

dilution-to-threshold (D/T) and sent them to St.Croix Sensory, Inc for odor evaluation.

With a known flow rate, the results obtained in the dilution-to-threshold method were back calculated for determination of odor emission rates. For example, if a result obtained from the laboratory was 214 D/T and the volumetric flow rate from the flux chamber was three liters per minute ( $5 \times 10^5$  cubic meters per second), using the flux hood with an area of 0.13 square meters, the emission rate can be calculated from a product of concentration and mass flow rate (volumetric flow rate per area).

$$\text{Emission rate } (q) = 214 \times (5 \times 10^5 / 0.13) = 0.0822 \frac{OU}{m^2-s}$$

Table 4.5 provides summary statistics for the MES odor emission data collected from nine reuse fields. The mean of the data set is 0.2769 odor units per square meters-second ( $OU/m^2 - s$ ). The standard deviation is 0.1378.

By using the @Risk “Distribution Fitting” function, distribution parameters were estimated by the Maximum Likelihood Method. The three goodness-of-fit tests were applied to the emission data. Table 4.6 summarizes the output.

**Table 4.5: Summary Statistics of MES Odor Emission Data**

<i>One Variable Summary</i>	<i>Emission Rate (OU/s – m<sup>2</sup>)</i>
Mean	0.2769
Variance	0.0190
Std. Dev.	0.1378
Skewness	-0.2517
Kurtosis	1.0311
Median	0.3310
Mean Abs. Dev.	0.1233
Minimum	0.0822
Maximum	0.4279
Range	0.3457
Count	9
Sum	2.4922
1st Quartile	0.1581
3rd Quartile	0.3922
Interquartile Range	0.2341
1.00%	0.0822
2.50%	0.0822
5.00%	0.0822
10.00%	0.0822
20.00%	0.1256
80.00%	0.4279
90.00%	0.4279
95.00%	0.4279
97.50%	0.4279
99.00%	0.4279

**Table 4.6: Summary of Distribution Fitting for MES Odor Emission Data**

<i>Fit Method</i>	<i>Fit Ranking Distribution</i>	<i>Test Statistics</i>	<i>Mean</i>	<i>Standard Deviation</i>
Chi-Square	Lognormal	0.1111	0.2829	0.1774
	Gamma	0.1111	0.2769	0.1455
	Weibull	0.1111	0.2777	0.1267
A-D	Gamma	0.5657	0.2769	0.1455
	Lognormal	0.5809	0.2829	0.1774
	Weibull	0.5953	0.2777	0.1267
K-S	Beta general	0.2222	0.3008	0.1318
	Weibull	0.2343	0.2777	0.1267
	Lognormal (7)	0.268	0.2829	0.1774

The results in Table 4.6 show the three best fit distributions and their test statistics. Since there were only nine data points in this analysis, the results from the chi-squared test were not considered.

For the Anderson-Darling test, the Gamma distribution was ranked first given its test statistic of 0.5657. The lognormal distribution was ranked second, and its test statistic was close to the Gamma. However, since the test statistics of the proposed distributions are below all critical values of any significance levels considered (0.1, 0.05, 0.025, 0.01, and 0.005), see Table 4.2, so we can describe the data with those proposed distributions.

For the Komolgorov-Smirnov test, the Beta general distribution gives the maximum was best. The Lognormal distribution was ranked seventh, but its test statistic is still below the critical values of any significance levels for sample size 10. Therefore, the null hypothesis to characterize the data with the lognormal distribution was accepted.

The decision to select an appropriate distribution to represent the odor emission data in biosolids reuse fields is subject to judgment if there is more than one distribution that provides a good description of the data. In environmental applications, however, it is appropriate and practical to assume that the probability distribution is lognormally distributed. Then, in this study, we focused on the lognormal distribution.

Since there are only nine data points, it is difficult to verify the proposed distribution with a histogram. As a result, the subjective probability plot was employed to investigate the goodness-of-fit of the lognormal distribution to the data.

Following the procedure mentioned in 4.3.3, we first took a natural logarithm for the data. The nine data were then ranked so that  $\ln q_1 < \ln q_2 < \dots < \ln q_9$ . The plotting positions were calculated from  $(\text{rank}-0.5)/n$  and the Z-Score from the inverse CDF and were estimated.

**Table 4.7: Calculation for a Normal Probability Plot of the MES Odor Emission Data**

<i><b>ln(Emission)</b></i>	<i><b>Rank</b></i>	<i><b>Plotting Position</b></i>	<i><b>Z-Scores</b></i>
-2.4986	1	0.056	-1.59
-2.0747	2	0.167	-0.97
-1.8445	3	0.278	-0.59
-1.6777	4	0.389	-0.28
-1.1056	5	0.500	0.00
-1.0203	6	0.611	0.28
-0.9360	7	0.722	0.59
-0.8489	8	0.833	0.97
-0.8489	9	0.944	1.59

Table 4.7 provides calculations for a normal probability plot of the MES odor emission data in 2003. The calculations of the Z-scores were done by use of the Excel function, NORMSINV (plotting position). Figure 4.4 shows a graphical plot of the normal probability plot from the calculations in Table 4.7. The straight line appears to fit the data with  $R^2=0.884$ . Using the probability plot it was confirmed that the MES odor emission data could be described by the lognormal distribution.

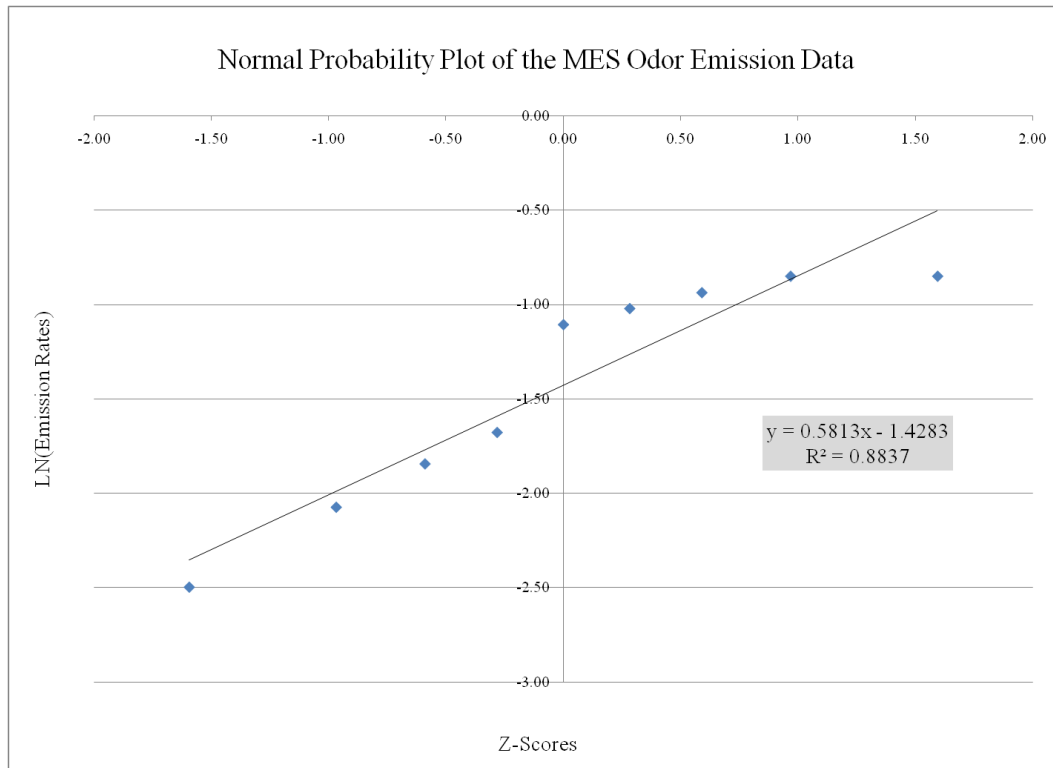


**Figure 4.4: Normal Probability Plot for the MES Odor Emission Data**

#### *4.5.2 Odor Emissions at DCWASA Wastewater Treatment Plant*

In 2005, DCWASA, the Department of Wastewater Treatment (DWT) started experiments for measuring odor levels of biosolids before they were trucked for land application. The DWT collected odor concentration data and sent them to St.Croix Sensory, Inc. for odor evaluation. The data collection detail is available from a PhD dissertation at the University of Maryland, College Park (Vilalai, 2008).

**Table 4.8: Summary Statistics of DCWASA Odor Concentration Data**

<i>One Variable Summary</i>	<i>Plant Concentration Data 05-06</i>
Mean	1581.90
Variance	2878185.62
Std. Dev.	1696.52
Skewness	1.9638
Kurtosis	6.9929
Median	825.00
Mean Abs. Dev.	1245.71
Minimum	240.00
Maximum	8694.00
Range	8454.00
Count	77
Sum	121806.00
1st Quartile	480.00
3rd Quartile	1800.00
Interquartile Range	1320.00
1.00%	240.00
2.50%	280.00
5.00%	330.00
10.00%	340.00
20.00%	440.00
80.00%	2756.00
90.00%	4100.00
95.00%	5486.00
97.50%	6426.00
99.00%	8694.00

Table 4.8 provides summary statistics for the odor concentration data. There were 77 data points collected. The mean of the data set is 1581.9 dilution-to-thresholds (D/T), the standard deviation is 1696.52

By using the @Risk “Distribution Fitting” function, distribution parameters were estimated by Maximum Likelihood Method. The three goodness-of-fit tests were applied to the odor concentration data. The summary of distribution fitting that contains fit ranking, test statistics for each fit, distribution parameters, and the three best distributions are provided in Table 4.9.

**Table 4.9: Summary of Distribution Fitting for DWT Odor Concentration Data**

<i>Fit Method</i>	<i>Fit Ranking Distribution</i>	<i>Test Statistics</i>	<i>Mean</i>	<i>Standard Deviation</i>
Chi-Square	Pearson 5	9.8831	1884.85	N/A
	InvGauss	14.8182	1581.9	1731.73
	Lognormal	21.3117	1533.3	1748.8
A-D	Pearson 5	0.9383	1884.86	N/A
	InvGauss	1.2816	1581.9	1731.73
	Lognormal (4)	1.5786	1533.3	1748.8
K-S	Pearson 5	0.1068	1884.85	N/A
	LogLogistic	0.1127	1618.28	N/A
	Lognormal (5)	0.1317	1533.3	1748.8

For the Chi-square test, at the significance level 0.05, the test statistics of the first and second ranks, Pearson 5 and InvGauss, are below the critical values 16.92. However, at the same significance level, the test statistic of the Lognormal distribution is greater than the critical value (Test statistic = 21.3117 > Cr. Value = 16.92).

For the Anderson-Darling test, at the significance level 0.050, the critical value is 0.752. The test statistics for the third best fits are greater than the critical value; we cannot describe the data with the proposed distributions. However, at the significance level 0.01, the Pearson 5 distribution is the only one that can be used to describe the odor concentration data (test statistic = 0.9383 < Cr. value = 1.035).

For the Komolgorov-Smirnov test, the critical statistics for a large sample size can be computed from the Table 4.1. For the significance level 0.05, the test statistic is 0.155,  $1.36/\sqrt{77}$ . All the proposed distributions in Table 4.9 have the test statistics that are below the critical value 0.155.

As previously mentioned, the decision to select the distribution is based on subjective judgment and current practices. Accordingly, the lognormal distribution by the chi-square test was chosen to represent the odor concentration at the Blue Plains Wastewater Plant as shown in Figure 4.5.

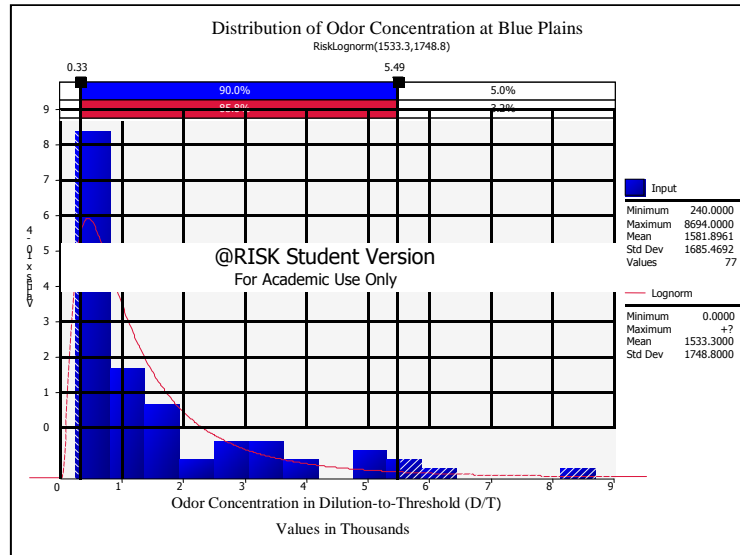


**Figure 4.5: Lognormal Distribution of Odor Concentration at Blue Plains**

With the known flow rate and measured area, the odor emission rates can be calculated. Since the emission rates are proportional to the concentrations, the distribution of emission rates can also be described by the lognormal distribution as shown in Figure 4.6. The results of test statistics for odor emission rates are similar to Table 4.9.

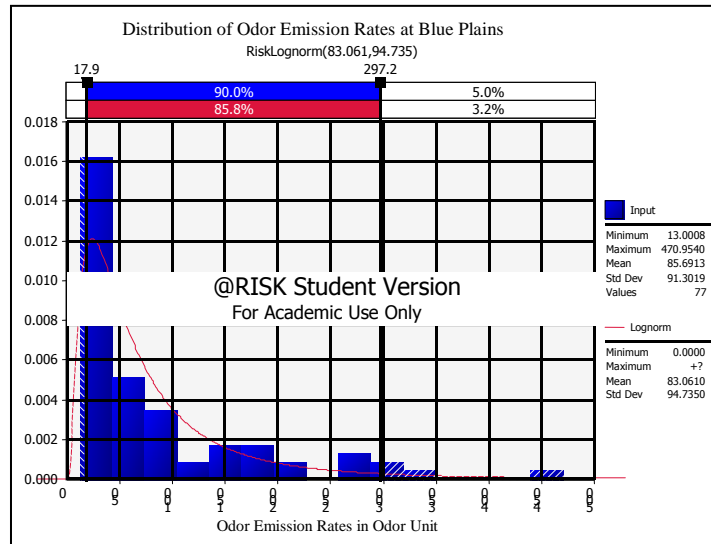


**Figure 4.6: Lognormal Distribution of Odor Emission Rates at Blue Plains**

#### 4.6 Case Study: ANOVA

##### *4.6.1 Design of Experiments*

This case study was conducted to investigate the variations of odor emission rates as previously stated in Section 4.4. Since it is not practical to sample odor emission rates at biosolids land application sites, the data collection of odor concentration was done after treatment processes before distribution.

The main focus is on a sensory measurement of biosolids odor concentration in dilution-to-threshold (D/T), recognition-to-threshold (R/T), and hedonic tone. The data obtained from the experiments were used for determination of biosolids odor emission and evaluation of biosolids odor concentration in the fields.

The seven samples of biosolids from seven operational days were taken from trucks while loading biosolids for the distribution. Each sample was duplicated in two Teflon jars with 400 grams per jar. Then, the biosolids odors were measured using an

Isolation Flux Chamber with a known flow rate of 2.9 liters per minute and sent out to the St. Croix’s laboratory for the determination of D/T. The D/T values obtained from the laboratory were used to calculate an odor emission rate similar to those previously demonstrated in Section 4.5.1.

4.6.2 Analysis of Variance (ANOVA)

Table 4.10 provides the results of the one-way ANOVA. The null hypothesis ( $H_0$ ) to be tested was whether at least two means of odor concentrations in D/T are equal at the 0.05 level of significance.

**Table 4.10: Analysis of Variance (ANOVA) of Odor Emission Data**

<i>OneWay ANOVA Table</i>	Sum of Squares	Degrees of Freedom	Mean Squares	F-Ratio	p-Value
Between Variation	14637142.86	6	2439523.81	13.34	0.0016
Within Variation	1280000.00	7	182857.14		
Total Variation	15917142.86	13			

There were seven samples with a 14 sample size. The grand mean of the data is 3314.29 dilution-to-thresholds (D/T). The sum of square computations gave SSA = 14,637,142.86, SSE = 1,280,000.00, and SST = 15,917,142.86

From the critical values of the F-Distribution (Walpole et al., 2002), the critical region with  $v_1 = k - 1 = 6$  and  $v_2 = k(n - 1) = 7$  at the significance level = 0.05 gave  $f_{0.05} = 3.87$ .

The result is to reject the null hypothesis and conclude that the emissions of biosolids odors at the Blue Plains day-to-day operations do not have the same mean ( $F - Ratio > f_{0.05}$ ).

#### 4.7 Guideline for Emission Estimates

In this section, we propose a guideline for emission estimates that can be used as an input for a dispersion model. As previously mentioned, the emissions rate is a product of the air or volumetric flow rate (cubic meters per second,  $m^3/s$ ) with odor concentration (odor units per cubic meter,  $OU/m^3$ ). Since it is rare in practice that the air velocity is known, the emissions estimate is usually done with a measurement. An advantage of using a device to measure odor emission rates is to know the air flow rate (i.e., three liters per minutes). Without such a device, the flow rate has to be assumed.

One approach is to use the air velocity from available sources. As previously mentioned in Section 4.2, Rafson (1998) suggested using 0.1 foot per second (ft/s) for typical air velocity. emissions rates per unit area can be back-calculated by multiplying the air flow rate with measured odor concentration. This approach can be referred to as an estimate from expert opinion and can be expressed in Equation 4.14

$$\text{Emission rate per unit area} = \text{assumed air velocity} \times \text{odor concentration measured in the field as Dilution-to-Threshold} \quad (4.14)$$

Alternatively, by using a statistical inference, probability distributions for odor emission rates can be developed. For example, a mean emission rate of the lognormal distribution in Table 4.6 can be used as input into a dispersion model. This approach can be expressed in Equation 4.15.

$$\text{Emission rate per unit area} = \text{best estimate from probability distribution (mean emission rate)} \quad (4.15)$$

Another estimation involves using a simulated-flux chamber. This method assumes use of the flux chamber method in the field with known odor concentration at the plant. An important assumption is that there is no loss of odor concentration during transportation. With a known air velocity and measured area, which is an area of the flux hood, the measured odor concentration at land application site is substituted by the odor concentration data at the plant. An estimated odor emission rate can be calculated. Table 4.11 shows calculation of odor emissions rates for odor concentration data at Blue Plains in 2005 and 2006 using the simulated-flux chamber method with three liters per minute flow rate and a flux hood area of 0.13 square meters.

**Table 4.11: Sample Calculation of Odor Emission Rates Using the Simulated-Flux Chamber**

<i>Date</i>	<i>D/T</i>	<i>Volumetric Flow Rate (m<sup>3</sup>/s)</i>	<i>Area (m<sup>2</sup>)</i>	<i>Air Velocity (<math>\frac{m}{s}</math>)</i>	<i>Odor Emission (<math>\frac{OU}{m^2 - s}</math>)</i>
10/17/05	570	5× 10 <sup>5</sup> 0.00005417	0.13	4× 10 <sup>4</sup> 0.000416692	0.238
11/07/05	350	5× 10 <sup>5</sup> 0.00005417	0.13	4× 10 <sup>4</sup> 0.000416692	0.146
11/08/05	410	5× 10 <sup>5</sup> 0.00005417	0.13	4× 10 <sup>4</sup> 0.000416692	0.171
11/15/05	500	5× 10 <sup>5</sup> 0.00005417	0.13	4× 10 <sup>4</sup> 0.000416692	0.208
04/26/06	3874	5× 10 <sup>5</sup> 0.00005417	0.13	4× 10 <sup>4</sup> 0.000416692	1.614
06/06/06	979	5× 10 <sup>5</sup> 0.00005417	0.13	4× 10 <sup>4</sup> 0.000416692	0.408
06/07/06	495	5× 10 <sup>5</sup> 0.00005417	0.13	4× 10 <sup>4</sup> 0.000416692	0.206
06/13/06	638	5× 10 <sup>5</sup> 0.00005417	0.13	4× 10 <sup>4</sup> 0.000416692	0.266
07/05/06	1274	5× 10 <sup>5</sup> 0.00005417	0.13	4× 10 <sup>4</sup> 0.000416692	0.531
07/10/06	867	5× 10 <sup>5</sup> 0.00005417	0.13	4× 10 <sup>4</sup> 0.000416692	0.361
07/11/06	5018	5× 10 <sup>5</sup> 0.00005417	0.13	4× 10 <sup>4</sup> 0.000416692	2.091

<b>Date</b>	<b>D/T</b>	<b>Volumetric Flow Rate (m<sup>3</sup>/s)</b>	<b>Area (m<sup>2</sup>)</b>	<b>Air Velocity (<math>\frac{m}{s}</math>)</b>	<b>Odor Emission (<math>\frac{OU}{m^2 - s}</math>)</b>
07/18/06	825	5× 10 <sup>5</sup> 0.00005417	0.13	4× 10 <sup>4</sup> 0.000416692	0.344
07/19/06	2990	5× 10 <sup>5</sup> 0.00005417	0.13	4× 10 <sup>4</sup> 0.000416692	1.246
07/25/06	8694	5× 10 <sup>5</sup> 0.00005417	0.13	4× 10 <sup>4</sup> 0.000416692	3.623

## Chapter 5: Biosolids Odor Impact Assessment at Land

### Application Sites

#### *5.1 Introduction to Dispersion Model*

This section describes dispersion models used in this study to simulate biosolids odor concentration at land application sites. Typically, there are two levels of model sophistication: screening and refined models. The screening model assumes worst case meteorological conditions to simulate pollutant concentration while the refined model requires more extensive inputs of meteorological and geographical data.

##### *5.1.1 Screening Model*

Screening model is a dispersion model usually applied to determine if a refined model is needed for further analysis. In this study, the United States Environmental Protection Agency screening model called SCREEN3, (EPA, 1995a), was used for initial air quality assessment. SCREEN3 is a single source Gaussian plume model, which provides maximum ground-level concentrations for point, area, and volume sources. By default, the SCREEN3 model calculates one-hour averaging concentrations with relative distances from the source. The worst case meteorological conditions are assumed and used for model simulation. Table 5.1 provides modeling inputs and options required in the SCREEN3 modeling procedure.

**Table 5.1: SCREEN3 Modeling Inputs and Options**

<i>Model Inputs</i>	<i>Model Options</i>
Source type	Point, area, and volume sources
Dispersion coefficient	Urban or rural studied area
Receptor height	Defined receptor height above the ground in meters
Emission rate	Rates of pollutant emitted as an emission rate per area ( $g/s - m^2$ )
Source release height	Height of released pollutant in meter
Wind direction	Possible wind direction for studied area
Terrain	Simple or complex
Meteorological conditions	Stability classes and wind speeds

In this study, the area source was selected to represent the biosolids land-applied area after spreading to a farm. Similar to the Industrial Source Complex (ISC) Model, the SCREEN3 model uses a numerical integration algorithm to model impacts from the area source. The algorithm detail is available in the ISC user's guide (EPA, 1995b). The receptor height was assumed 1.7 meters to represent population heights.

As previously mentioned, the SCREEN3 model simulates concentrations by assuming worst-case meteorological conditions. This means that the screen model will examine all stability classes and wind speeds to identify the worst-case meteorological conditions and generate results as maximum ground level concentrations for all wind directions. Table 5.2 shows combinations of wind speed and stability classes used in the SCREEN3 model. The stability class shown in Table 5.2 was developed by Pasquill in 1961 to categorizing atmospheric turbulence.

**Table 5.2: Combinations of Wind Speed and Stability Class (Haug, 1993)**

<i>Wind Speed (m/s)</i>	<i>Pasquill Stability Class*</i>					
	<i>A</i>	<i>B</i>	<i>C</i>	<i>D</i>	<i>E</i>	<i>F</i>
0.5	×	×				
0.8	×	×		×		
1.0	×	×		×		
1.5	×	×		×		
2.0	×	×	×	×	×	×
2.5	×	×	×	×	×	×
3.0	×	×	×	×	×	×
4.0		×	×	×		
5.0		×	×	×		
7.0			×	×		
10.0			×	×		
12.0			×	×		
15.0			×	×		
20.0				×		

\* A: Extremely unstable; B: Moderately unstable; C: Slightly unstable; D: Neutral; E: Slightly stable; and F: Moderately stable

With all required model inputs defined, the SCREEN3 model searches through all stability classes and wind speeds for defined wind direction and generates one-hour averaging concentrations for the defined receptor array. In this study, however, a more user friendly version of the SCREEN3 called Screen View was used in the screening analysis. The Screen View is available from Lake Environmental <sup>TM</sup>, <http://www.weblakes.com/index.html>.

### *5.1.2 Regulatory/Refined Model*

Regulatory or refined model is a more sophisticated dispersion model comparing to a screening model. It requires more extensive inputs of atmospheric conditions and terrain elevations. This study employed AERMOD for simulating biosolids odor concentrations. AERMOD, (Cimorelli et al., 2005), is a refined dispersion model

developed by the U.S. EPA and the American Meteorological Society (AMS), hence **AMS/EPA Regulatory MODel (AERMOD)**. The AERMOD is a steady-state dispersion model for estimation of pollutant concentrations from a variety of sources in the planetary boundary layer (PBL). The steady-state approach assumes a constant of meteorological parameters over time (i.e., one hour). The model is suitable for a short-range (up to 50 kilometers) dispersion from stationary sources and comparable to the EPA's Industrial Source Complex Short-term Model (ISCST3) (Perry et al., 2005).

The AERMOD estimates concentration distributions by including the effects of vertical variations in the PBL (Cimorelli et al., 2005). The PBL is the closest part of the atmosphere to the ground where ground friction exists. The thickness of the PBL varies between 100 meters at night to three kilometers during the daytime.

Typically, there are two types of layers in the PBL: stable and unstable (convective). In the stable boundary layer (SBL) vertical and horizontal concentration distributions assumed by the AERMOD are both Gaussian as well as the horizontal concentration distribution in the convective boundary layer (CBL). However, the vertical concentration distribution in the CBL is described with a bi-Gaussian probability density function. The AERMOD calculates total concentration with a weighted sum of concentrations in terrain-impacting (horizontal plume), and terrain-following plume (Cimorelli et al., 2005) as shown below.

$$C_T\{x_r, y_r, z_r\} = fC_{c,s}\{x_r, y_r, z_r\} + (1 - f)C_{c,s}\{x_r, y_r, z_p\} \quad (5.1)$$

where

$C_T\{x_r, y_r, z_r\}$ : The total concentration at a receptor coordinate  $\{x_r, y_r, z_r\}$

$C_{c,s}\{x_r, y_r, z_r\}$ : The contribution from horizontal plume (subscripts  $c$  and  $s$  refer to convective and stable boundary layers, respectively) at a receptor coordinate  $\{x_r, y_r, z_r\}$

$C_{c,s}\{x_r, y_r, z_p\}$ : The contribution from the terrain-following plume

$f$ : is the weighting factor

$z_p$ : The receptor height above ground

AERMOD model formulations are provided in the Appendix A-2.

The AERMOD modeling system consists of a dispersion model and two preprocessing models: 1) an air dispersion model (AERMOD), 2) a meteorological data preprocessor called AERMOD METEOROLOGICAL PREPROCESSOR (AERMET), and 3) a terrain data preprocessor called AERMAP.

The odor is carried from one place to another by wind. It is then dispersed by atmospheric turbulence. The meteorological conditions and topographical features influence the atmospheric turbulence and consequently dispersion of odor. AERMOD simulates dispersion process through meteorological and topographical preprocessors. The results are estimated concentrations over a defined receptor network.

### ***Meteorological Preprocessor (AERMET)***

AERMET, (EPA, 2004), is a meteorological preprocessor for organizing available meteorological data into a format suitable for use by the AERMOD dispersion model. It is also used to characterize the structure of the planetary boundary layer (PBL) and to estimate its parameters.

The minimum two types of data, which are National Weather Service (NWS) hourly surface observations and NWS twice daily upper air soundings, are needed as inputs for AERMET, which provide information on surface characteristics, cloud cover, one near-surface measurement of wind speed, wind direction, and temperature. The surface characteristics influence the depth and the dispersion of pollutants in the PBL. Some important surface characteristics are 1) surface roughness (height at which mean horizontal wind is zero), 2) albedo (the fraction of solar radiation reflected by the surface back to space without absorption), and 3) surface moisture in the PBL.

With the information from surface characteristics and standard meteorological observations, the AERMET calculates the PBL parameters for use by the AERMOD. The parameters are 1) friction velocity( $u_*$ ), 2) Monin-Obukhov length( $L$ ), 3) convective velocity scale( $w_*$ ), 4) temperature scale( $\theta_*$ ), 5) mixing height( $z_i$ ), 6) surface heat flux( $H$ ), and 7) surface roughness length ( $z_0$ ). Those scaling parameters as a result from the AERMET are used with the AERMOD modeling system to construct vertical profiles of wind speed( $u$ ), lateral and vertical turbulent fluctuations( $\sigma_v, \sigma_w$ ), and potential temperature gradient( $d\theta/dz$ ). AERMET model formulations are provided in the Appendix A-2. Figure 5.1 shows a schematic of the input data required by the AERMET to generate the PBL parameters that are further used with the AERMOD.

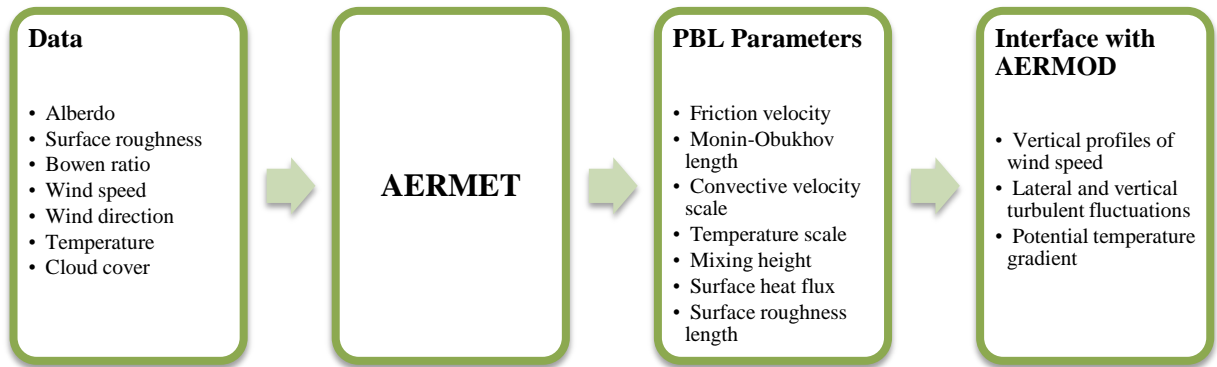


**Figure 5.1: Meteorological Data Input and Output in the AERMET**

In the AERMET modeling setup and process, there are three stages for processing meteorological data and generating the PBL parameters. The first stage extracts meteorological data, which are raw hourly surface observations and raw upper air soundings, from archive data files and processes the data through quality assessment (QA) checks. The second stage merges all available data for 24-hour periods and stores these data together in a single file. The third stage reads the merged meteorological data and estimates the necessary boundary layer parameters for dispersion calculations by AERMOD.

Two meteorological files are written for use in the AERMOD: a file of hourly boundary layer scaling parameter estimates (surface file) that contains surface friction velocity and mixing height, and a file of multiple-level observations (profile file) of wind speed and direction, temperature, and standard deviation of the fluctuating components of the wind.

AERMET requires an input runstream file to work as a command language with different functional groups or pathways to run the program. The runstream files

for each stage can be written in any ASCII format. The statements in a runstream are divided into six different pathways:

1. **JOB** pathway for specifying information for the entire run;
2. **SURFACE** pathway for extracting and QA the NWS hourly surface observation data;
3. **UPPERAIR** pathway for extracting and QA the NWS upper air sounding data;
4. **ONSITE** pathway for QAing user-supplied, on-site meteorological data;
5. **MERGE** pathway for combining the meteorological data;
6. **METPREP** pathway for estimating boundary layer parameters for AERMOD.

Figure 5.2 show an example of the running stream files for all three stages.



**Figure 5.2: AERMET Processing**

Figure 5.3 shows a runstream file in stage 1 for extracting and assessing the quality of upper air and surface data from a weather station in Orange County, Virginia from January 01, 2005 to December 31, 2008.

The upper air data file, UPPERAIR.OP in Figure 5.3, is in the TD-6201 fixed-length blocks format. The weather station for the data is located at the coordinate (77.28W, 38.58N). The AUDIT keyword was used to QA the data for missing values and range violations. In this example, the temperature (UATT), wind speed (UAWS), and lapse rate (UALR) were checked.

The surface data file, 722167.OP in Figure 5.3, is in TD-3505 format, which is known as the Integrated Surface Hourly Data (ISHD). The weather station is located at the coordinate (78.05W, 38.25N) and at the elevation 142 meters above sea level. With the runstream shown below, stage 1 performed extraction and QA for the upper air and the surface data, respectively. The output files from stage 1 were written in the file STAGE\_1\_UA.QQA for the upper-air data and in the file STAGE\_1\_SF.QQA for the surface data. All the errors and summary of the run were written in the JOB pathway. The STAGE\_1.RPT specifies all the errors and warning generated by the AERMET, while the STAGE\_1.MSG reports the summary of the run.

```

JOB
  REPORT   STAGE_1.RPT
  MESSAGES STAGE_1.MSG

UPPERAIR
  DATA    UPPERAIR.OP 6201FB 1
  EXTRACT  STAGE_1_UA.IQA
  QAOUT    STAGE_1_UA.QQA

  XDATES    05/01/01 TO 08/12/31

  LOCATION 00093734 77.28W 38.58N 5
  AUDIT    UATT UAWS UALR

SURFACE
  DATA    722167.OP ISHD 1
  EXTRACT  STAGE_1_SF.IQA
  QAOUT    STAGE_1_SF.QQA

  XDATES    05/01/01 TO 08/12/31

  LOCATION 722167 38.250N 78.050W 5 142

```

**Figure 5.3: Example Runstream to Extract and QA Upper Air and Surface Data**

Stage 2 merged the extracted meteorological files generated from stage 1 to a file in 24-hour format. Figure 5.4 shows the runstream file for stage 2, merging the upper-air data, STAGE\_1\_UA.QQA, with the surface data, STAGE\_1\_SF.QQA. The output file was written in the MERGE keyword, STAGE\_2\_MR.MET.

```

JOB
  REPORT      STAGE_2.RPT
  MESSAGES    STAGE_2.MSG

UPPERAIR
  QAOUT       STAGE_1_UA.OQA

SURFACE
  QAOUT       STAGE_1_SF.OQA

MERGE
  OUTPUT      STAGE_2_MR.MET

  XDATES      05/01/01 08/12/31

```

**Figure 5.4: Example Runstream for Merging the Data**

Figure 5.5 shows stage 3, data processing, from stage 2, STAGE\_2\_MR.MET in DATA keyword, that contain the PBL parameters for the AERMOD. The surface file, MET\_INPUT.SFC, in the OUTPUT keyword contains boundary layer parameters including surface friction velocity, mixing height, and near surface winds and temperature. On the other hand, the profile file, MET\_INPUT.PFL, in the PROFILE keyword produces the multi-level observations of temperature, winds, and fluctuating components of the wind.

```

JOB
  REPORT      STAGE_3.RPT
  MESSAGES    STAGE_3.MSG

METPREP
  DATA       STAGE_2_MR.MET
  OUTPUT      MET_INPUT.SFC
  PROFILE     MET_INPUT.PFL
  LOCATION    MYSITE 77.862W 38.321N 5
  METHOD       REFLEVEL SUBNWS
  METHOD       WIND_DIR  RANDOM
  NWS_HGT     WIND      6.1
  FREQ_SECT   ANNUAL  1
  SECTOR      1      0      360
  SITE_CHAR   1 1 0.20 1.5 0.20

```

**Figure 5.5: Example Runstream for Estimating Boundary Layer Parameters**

Stage 3 includes determination of parameters to characterize surface characteristics in the SITE\_CHAR keyword. In the AERMET's user guide, the EPA provides guidance to specify those parameters based on land use (EPA, 2004).

In this example, land use was in rural areas. Figure 5.5 shows values of the albedo (0.2), bowen ratio (1.5), and surface roughness length (0.2) in the SITE\_CHAR keyword. Selection of those parameters could affect the surface characteristics and model accuracy (Diosey, 2008).

Ultimately, two meteorological files, surface and profile data, are generated from stage 3 which would then be used in the AERMOD dispersion model. The data description and examples of the surface file and the upper-air file are shown in Tables 5.3-5.4 and Figures 5.6-5.7

**Table 5.3: Data Description for Surface File (EPA, 2004)**

<i>Field(s)</i>	<i>Data Description</i>
1-5	Year (2-digit), month, day, Julian day, and hour
6	Sensible heat flux, watts per square meters ( $W/m^2$ )
7	Surface friction velocity, meters per second( $m/s$ )
8	Convective velocity scale (set to -9.0 for stable atmosphere), meters per second( $m/s$ )
9	Potential temperature gradient above the mixing height in Kelvin per meter ( $K/meter$ )
10	Convectively-driven mixing height (-999 for stable atmosphere), meters( $m$ )
11	Mechanically-driven mixing height (computed for all hours), meters( $m$ )
12	Monin-Obukhov length, meters( $m$ )
13	Surface roughness length, meters( $m$ )
14	Bowen ratio (non-dimensional)
15	Albedo (non-dimensional)
16-18	Wind speed, wind direction, and anemometer height that were used in the computations in Stage 3, meters per second( $m/s$ ), degrees, meters( $m$ )
19-20	Temperature and measurement height that were used in the computations in Stage 3 ( $K$ and meters)

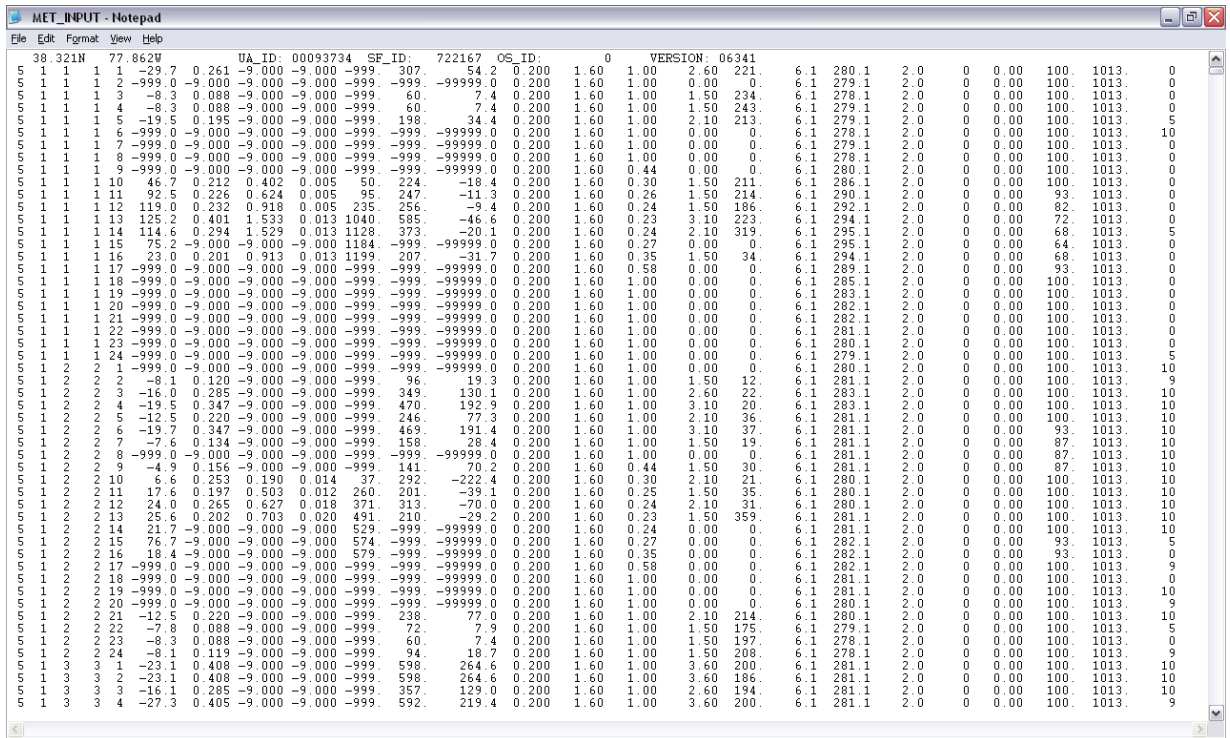


Figure 5.6: First 52 Hours of the Boundary Layer Parameter File

Table 5.4: Data Description for Profile File (EPA, 2004)

<i>Field(s)</i>	<i>Data Description</i>
1-4	Year (2-digit), month, day, and hour
5	Measurement height, meters ( <i>m</i> )
6	Indicator flag: 1 = last level in profile for the hour, 0 = not the last level
7-8	Wind direction and speed, meters per second ( <i>m/s</i> ), meters ( <i>m</i> )
9	Temperature, Celsius
10	Standard deviation of the lateral wind direction, degrees ( $\sigma_A$ )
11	Standard deviation of the vertical wind speed, meters per second ( <i>m/s</i> ), ( $\sigma_w$ )

File	Edit	Format	View	Help
5	1	1	1	6.1 1 221. 2.60 7.0 99.0 99.00
5	1	1	2	6.1 1 0. 0.00 6.0 99.0 99.00
5	1	1	3	6.1 1 234. 1.50 5.0 99.0 99.00
5	1	1	4	6.1 1 243. 1.50 6.0 99.0 99.00
5	1	1	5	6.1 1 213. 2.10 6.0 99.0 99.00
5	1	1	6	6.1 1 0. 0.00 5.0 99.0 99.00
5	1	1	7	6.1 1 0. 0.00 6.0 99.0 99.00
5	1	1	8	6.1 1 0. 0.00 5.0 99.0 99.00
5	1	1	9	6.1 1 0. 0.00 7.0 99.0 99.00
5	1	1	10	6.1 1 211. 1.50 13.0 99.0 99.00
5	1	1	11	6.1 1 214. 1.50 17.0 99.0 99.00
5	1	1	12	6.1 1 186. 1.50 19.0 99.0 99.00
5	1	1	13	6.1 1 223. 3.10 21.0 99.0 99.00
5	1	1	14	6.1 1 319. 2.10 22.0 99.0 99.00
5	1	1	15	6.1 1 0. 0.00 22.0 99.0 99.00
5	1	1	16	6.1 1 34. 1.50 21.0 99.0 99.00
5	1	1	17	6.1 1 0. 0.00 16.0 99.0 99.00
5	1	1	18	6.1 1 0. 0.00 12.0 99.0 99.00
5	1	1	19	6.1 1 0. 0.00 10.0 99.0 99.00
5	1	1	20	6.1 1 0. 0.00 9.0 99.0 99.00
5	1	1	21	6.1 1 0. 0.00 9.0 99.0 99.00
5	1	1	22	6.1 1 0. 0.00 8.0 99.0 99.00
5	1	1	23	6.1 1 0. 0.00 7.0 99.0 99.00
5	1	1	24	6.1 1 0. 0.00 6.0 99.0 99.00
5	1	2	1	6.1 1 0. 0.00 7.0 99.0 99.00
5	1	2	2	6.1 1 12. 1.50 8.0 99.0 99.00
5	1	2	3	6.1 1 22. 2.60 10.0 99.0 99.00
5	1	2	4	6.1 1 20. 3.10 10.0 99.0 99.00
5	1	2	5	6.1 1 36. 2.10 8.0 99.0 99.00
5	1	2	6	6.1 1 37. 3.10 8.0 99.0 99.00
5	1	2	7	6.1 1 19. 1.50 8.0 99.0 99.00
5	1	2	8	6.1 1 0. 0.00 8.0 99.0 99.00
5	1	2	9	6.1 1 30. 1.50 8.0 99.0 99.00
5	1	2	10	6.1 1 21. 2.10 7.0 99.0 99.00
5	1	2	11	6.1 1 35. 1.50 7.0 99.0 99.00
5	1	2	12	6.1 1 31. 2.10 7.0 99.0 99.00
5	1	2	13	6.1 1 359. 1.50 8.0 99.0 99.00
5	1	2	14	6.1 1 0. 0.00 8.0 99.0 99.00
5	1	2	15	6.1 1 0. 0.00 9.0 99.0 99.00
5	1	2	16	6.1 1 0. 0.00 9.0 99.0 99.00
5	1	2	17	6.1 1 0. 0.00 9.0 99.0 99.00
5	1	2	18	6.1 1 0. 0.00 8.0 99.0 99.00
5	1	2	19	6.1 1 0. 0.00 8.0 99.0 99.00
5	1	2	20	6.1 1 0. 0.00 7.0 99.0 99.00
5	1	2	21	6.1 1 214. 2.10 7.0 99.0 99.00
5	1	2	22	6.1 1 175. 1.50 6.0 99.0 99.00
5	1	2	23	6.1 1 197. 1.50 5.0 99.0 99.00
5	1	2	24	6.1 1 208. 1.50 5.0 99.0 99.00
5	1	3	1	6.1 1 200. 3.60 8.0 99.0 99.00
5	1	3	2	6.1 1 186. 3.60 8.0 99.0 99.00
5	1	3	3	6.1 1 194. 2.60 8.0 99.0 99.00
5	1	3	4	6.1 1 200. 3.60 8.0 99.0 99.00
5	1	3	5	6.1 1 197. 2.10 8.0 99.0 99.00

**Figure 5.7: First 52 Hours of the Profile File**

### ***AERMOD Dispersion Model with Terrain***

The AERMOD simulates pollutant plume based on available meteorological data provided by the AERMET and topographical features of a site under investigation provided by the AERMAP. The total concentration is a weighted sum of concentrations from both the horizontal plume and the terrain-following plume.

The AERMOD dispersion model in the AERMOD modeling system contains all algorithms necessary to combine source information, meteorological data, and

topography to produce an output file of concentrations at the specified receptor locations.

AERMOD requires two input files: a runstream setup file and a meteorological file. The runstream setup controls selected modeling options, as well as source location, receptor locations, meteorological data, and output options. The two types of meteorological data files, single and profile files, are provided by the AERMET meteorological preprocessor program.

The input runstream file works as a command language that can be divided into 5 functional pathways: 1) Control Pathway (**CO**), 2) Source Pathway (**SO**), 3) Receptor Pathway (**RE**), 4) Meteorology Pathway (**ME**), and 5) Output pathway (**OU**). The explanation of the five pathways is provided through an example in Figure 5.8-5.12.

The control pathway (**CO**) controls dispersion options in the AERMOD dispersion model such as name of studied field and averaging time concentration. In Figure 5.8, for example, the field under investigation is DF3, and averaging time concentration for the model output is one hour as defined in the TITLEONE and AVERTIME keywords, respectively. The AERMOD gives an option to define the averaging time from one hour to twenty-four hours. In this study, a one-hour averaging time was selected because the shorter averaging time would allow the AERMOD to simulate a predicted concentration distribution closer to an instantaneous characteristic of odor concentration.

```

CO STARTING
  TITLEONE DF 3
  MODELOPT CONC NOSTD
  AVERTIME 1
  POLLUTID ODOR
  RUNORNOT RUN
  ERRORFIL ERRORS .OUT
CO FINISHED

```

**Figure 5.8: Example Runstream for Control Pathway (CO)**

The source pathway (**SO**) contains information of a source such as source geometry and characteristics. The source geometry includes type of the source and source coordinates. In this study, it is practical to consider biosolids land application as an area source. The source coordinates contains a user-defined origin that could be in the standard coordinate system. For example, it could be defined in the Universal Transverse Mercator (UTM) coordinate system containing easting and northing coordinate pairs. The elevation of the source is also taken into account.

In Figure 5.9, for example, the source geometry is defined in the **LOCATION** keyword including an area source, UTM coordinate pairs (752638, 4230281), and elevation 147 meters above sea level. The size of the area source, however, is defined in the source parameters (**SRCPARAM**) keyword, in this runstream 114.51 square meters. The size of the area source is the length of the X and Y sides of the field after the biosolids are applied, expressed in square meters. Because the tonnage of biosolids applied is in wet tons and the field area is limited by the number of acres permitted, there is a need to convert the daily biosolids applied area in to square meters.

```

SO STARTING
ELEVUNIT METERS
LOCATION FARM3 AREA 752638 4230281 147
SRCPARAM FARM3 0.152 0.00 114.51
EMISUNIT 1 OU/S OU/M**3
SRCGROUP ALL
SO FINISHED

```

**Figure 5.9: Example Runstream for Source Pathway (SO)**

The significant component when using a dispersion model includes a source emission rate. Emission rate is one of the most important factors to assess an odor impact. In addition, it could be used to follow the evolution of the source in terms of annoyance. Typically, odor emission levels are expressed as rate of release per time in odor unit per second ( $ou/s$ ) or rate of release per time per unit area ( $ou/m^2 - s$ ). The detail of emission estimate is provided in Chapter 4. The estimated emission levels were then used as an input in the AERMOD dispersion model through the source pathway, SRCPARAM keyword. For this example, the estimated emission rate of  $0.152\ ou/m^2 - s$  was used.

In addition, the other data needed as input to the source pathway involves the release height above ground. The release height is the vertical distance that a pollutant could be released to the air. There is no certain method to determine the release height value used in the model. Thus, the release height could be subjectively determined and, in this study, was assumed to release from the ground.

Another important pathway designed to investigate the effects of terrain to the dispersion process is receptor pathway (RE). The receptor pathway contains keywords that define the receptor information for a particular run. Defining a receptor grid is usually the first step.

There are two types of receptor grids: Cartesian grid and Polar grid. The difference between these two grid systems is mainly the grid spacing which could be evenly spaced (Cartesian grid) or unevenly spaced (Polar grid). The Cartesian grid was selected to represent hypothetical receptor locations at specified time  $R(x, y, z, t)$  when running the model because of its uniformity.

To facilitate the generation of elevated terrain and hill height, the terrain preprocessor called AERMAP, which uses the U.S. Geological Survey (USGS) Digital Elevation Model (DEM) data, may be used to generate terrain elevation for each receptor. This study, however, applied the Geographic Information System (GIS) to determine receptor terrain.

Figure 5.10 provides an example runstream for the receptor pathway (RE) with a defined Cartesian grid receptor network in the UTM coordinate system. The receptor's terrain was determined by the GIS as shown in the GRIDCART CAR1 ELEV, HILL keywords.

```

RE STARTING
RE GRIDCART CAR1 STA
RE GRIDCART CAR1 XPNTS 752138 752238 752338 752438 752538 752638 752738 752838 752938 753038 753138
RE GRIDCART CAR1 YPNTS 4229781 4229881 4229981 4230081 4230181 4230281 4230381 4230481 4230581 4230681 4230781

RE GRIDCART CAR1 ELEV 1 147. 147. 147. 147. 147. 147. 147. 147. 147. 147.
RE GRIDCART CAR1 ELEV 2 147. 147. 147. 147. 147. 147. 147. 147. 147. 147.
RE GRIDCART CAR1 ELEV 3 147. 147. 147. 147. 147. 147. 147. 147. 147. 147.
RE GRIDCART CAR1 ELEV 4 147. 147. 147. 147. 147. 147. 147. 147. 147. 147.
RE GRIDCART CAR1 ELEV 5 147. 147. 147. 147. 147. 147. 147. 147. 147. 147.
RE GRIDCART CAR1 ELEV 6 147. 147. 147. 147. 147. 147. 147. 147. 147. 147.
RE GRIDCART CAR1 ELEV 7 147. 147. 147. 147. 147. 147. 147. 147. 147. 147.
RE GRIDCART CAR1 ELEV 8 147. 147. 147. 147. 147. 147. 147. 147. 147. 147.
RE GRIDCART CAR1 ELEV 9 147. 147. 147. 147. 147. 147. 147. 147. 147. 147.
RE GRIDCART CAR1 ELEV 10 147. 147. 147. 147. 147. 147. 147. 147. 147. 147.
RE GRIDCART CAR1 ELEV 11 147. 147. 147. 147. 147. 147. 147. 147. 147. 147.
RE GRIDCART CAR1 HILL 1 178. 178. 178. 178. 178. 178. 178. 178. 178. 178.
RE GRIDCART CAR1 HILL 2 178. 178. 178. 178. 178. 178. 178. 178. 178. 178.
RE GRIDCART CAR1 HILL 3 178. 178. 178. 178. 178. 178. 178. 178. 178. 178.
RE GRIDCART CAR1 HILL 4 178. 178. 178. 178. 178. 178. 178. 178. 178. 178.
RE GRIDCART CAR1 HILL 5 178. 178. 178. 178. 178. 178. 178. 178. 178. 178.
RE GRIDCART CAR1 HILL 6 178. 178. 178. 178. 178. 178. 178. 178. 178. 178.
RE GRIDCART CAR1 HILL 7 178. 178. 178. 178. 178. 178. 178. 178. 178. 178.
RE GRIDCART CAR1 HILL 8 178. 178. 178. 178. 178. 178. 178. 178. 178. 178.
RE GRIDCART CAR1 HILL 9 178. 178. 178. 178. 178. 178. 178. 178. 178. 178.
RE GRIDCART CAR1 HILL 10 178. 178. 178. 178. 178. 178. 178. 178. 178. 178.
RE GRIDCART CAR1 HILL 11 178. 178. 178. 178. 178. 178. 178. 178. 178. 178.

RE GRIDCART CAR1 END
RE FINISHED

```

**Figure 5.10: Example Runstream for Receptor Pathway (RE)**

The meteorology pathway (ME), in Figure 5.11, processes the meteorological data obtained from the AERMET output, MET\_INPUT.SFC for the surface file and MET\_INPUT.PFL for the profile file. The SURFDATA and UAIRDATA keywords provide information of weather station identification and year data was processed.

```
ME STARTING
SURFFILE MET_INPUT.SFC
PROFFILE MET_INPUT.PFL
SURFDATA 722167 2006
UAIRDATA 93734 2006
PROFBASE 0.0 METERS
ME FINISHED
```

**Figure 5.11: Example Runstream for Meteorology Pathway (ME)**

The output pathway (OU) controls output options: the option for determining model outputs for different maximum concentrations and the option for plotting the results in a form that can be easily imported to another programs such as Excel spreadsheet. Figure 5.12 shows an example runstream file for the output pathway (OU). The AERMOD, with this OU runstream file, generated four levels of maximum concentration for defined receptors in four different files that can be exported to the spreadsheet.

```
OU STARTING
RECTABLE 1 FIRST SECOND THIRD FOURTH
PLOTFILE 1 ALL FIRST MAX_FIRST.OUT
PLOTFILE 1 ALL SECOND MAX_SECOND.OUT
PLOTFILE 1 ALL THIRD MAX_THIRD.OUT
PLOTFILE 1 ALL FOURTH MAX_FOURTH.OUT
OU FINISHED
```

**Figure 5.12: Example Runstream for Output Pathway (OU)**

After all runstream files created, the AERMOD written in FORTRAN will run on the MS-DOS by default. To run the AERMOD, both input file and output file need

to be created in the same directory with the AERMOD program. An input file is basically a file that contains all input data and pathway code manually created by users and preprocessor AERMET. An output file is simply a blank file that the result is created.

The result generated from AERMOD is the average concentration values with relative date of concentration for selected receptor network, Cartesian grid (CAR), and selected average concentration time. In addition, if the model accounts for elevated terrain situation, the result would show relative elevation values for each grid location. Figure 5.13 shows an example of result in produced file of design values that can be imported into graphics software like the GIS for plotting contours.

```

* AERMOD (07026) : DF 3
* MODELING OPTIONS USED:
* CONC
* ELEV NOSTD
* PLOT FILE OF HIGH 1ST HIGH 1-HR VALUES FOR SOURCE GROUP: ALL
* FOR A TOTAL OF 121 RECEPTORS.
* FORMAT: (3(1X,F13.5),3(1X,F8.2),3X,A5,2X,A8,2X,A4,6X,A8,2X,I8)
* X Y AVERAGE CONC ZELEV ZHILL ZFLAG AVE GRP HIVAL NET ID DATE(CONC)
*
752338 00000 4230281 00000 0.04297 127.00 0.00 0.00 1-HR ALL 1ST CAR1 6071816
752438 00000 4230281 00000 0.07870 127.00 0.00 0.00 1-HR ALL 1ST CAR1 6071816
752538 00000 4230281 00000 0.18044 136.00 0.00 0.00 1-HR ALL 1ST CAR1 6071816
752638 00000 4230281 00000 1.64365 136.00 0.00 0.00 1-HR ALL 1ST CAR1 6071816
752738 00000 4230281 00000 0.98390 136.00 0.00 0.00 1-HR ALL 1ST CAR1 6071816
752838 00000 4230281 00000 0.00000 136.00 0.00 0.00 1-HR ALL 1ST CAR1 0
752938 00000 4230281 00000 0.00000 136.00 0.00 0.00 1-HR ALL 1ST CAR1 0
753038 00000 4230281 00000 0.00000 136.00 0.00 0.00 1-HR ALL 1ST CAR1 0
753138 00000 4230281 00000 0.00000 136.00 0.00 0.00 1-HR ALL 1ST CAR1 0
752138 00000 4230381 00000 0.02218 127.00 0.00 0.00 1-HR ALL 1ST CAR1 6071816
752238 00000 4230381 00000 0.03200 127.00 0.00 0.00 1-HR ALL 1ST CAR1 6071816
752338 00000 4230381 00000 0.05149 127.00 0.00 0.00 1-HR ALL 1ST CAR1 6071816
752438 00000 4230381 00000 0.09823 127.00 0.00 0.00 1-HR ALL 1ST CAR1 6071816
752538 00000 4230381 00000 0.24641 136.00 0.00 0.00 1-HR ALL 1ST CAR1 6071816
752638 00000 4230381 00000 3.28516 136.00 0.00 0.00 1-HR ALL 1ST CAR1 6071816
752738 00000 4230381 00000 2.12704 136.00 0.00 0.00 1-HR ALL 1ST CAR1 6071816
752838 00000 4230381 00000 0.00000 136.00 0.00 0.00 1-HR ALL 1ST CAR1 0
752938 00000 4230381 00000 0.00000 136.00 0.00 0.00 1-HR ALL 1ST CAR1 0
753038 00000 4230381 00000 0.00000 136.00 0.00 0.00 1-HR ALL 1ST CAR1 0
753138 00000 4230381 00000 0.00000 136.00 0.00 0.00 1-HR ALL 1ST CAR1 0
752138 00000 4230481 00000 0.01561 145.00 0.00 0.00 1-HR ALL 1ST CAR1 6071816
752238 00000 4230481 00000 0.01997 145.00 0.00 0.00 1-HR ALL 1ST CAR1 6071816
752338 00000 4230481 00000 0.02608 145.00 0.00 0.00 1-HR ALL 1ST CAR1 6071816
752438 00000 4230481 00000 0.03303 145.00 0.00 0.00 1-HR ALL 1ST CAR1 6071816
752538 00000 4230481 00000 0.02983 147.00 0.00 0.00 1-HR ALL 1ST CAR1 6071816
752638 00000 4230481 00000 0.00555 147.00 0.00 0.00 1-HR ALL 1ST CAR1 6071816
752738 00000 4230481 00000 0.00000 147.00 0.00 0.00 1-HR ALL 1ST CAR1 0
752838 00000 4230481 00000 0.00000 147.00 0.00 0.00 1-HR ALL 1ST CAR1 0
752938 00000 4230481 00000 0.00000 147.00 0.00 0.00 1-HR ALL 1ST CAR1 0
753038 00000 4230481 00000 0.00000 147.00 0.00 0.00 1-HR ALL 1ST CAR1 0
753138 00000 4230481 00000 0.00000 147.00 0.00 0.00 1-HR ALL 1ST CAR1 0
752138 00000 4230581 00000 0.00767 145.00 0.00 0.00 1-HR ALL 1ST CAR1 6071816
752238 00000 4230581 00000 0.00772 145.00 0.00 0.00 1-HR ALL 1ST CAR1 6071816
752338 00000 4230581 00000 0.00678 145.00 0.00 0.00 1-HR ALL 1ST CAR1 6071816
752438 00000 4230581 00000 0.00413 145.00 0.00 0.00 1-HR ALL 1ST CAR1 6071816
752538 00000 4230581 00000 0.00085 147.00 0.00 0.00 1-HR ALL 1ST CAR1 6071816
752638 00000 4230581 00000 0.00000 147.00 0.00 0.00 1-HR ALL 1ST CAR1 6071816
752738 00000 4230581 00000 0.00000 147.00 0.00 0.00 1-HR ALL 1ST CAR1 0
752838 00000 4230581 00000 0.00000 147.00 0.00 0.00 1-HR ALL 1ST CAR1 0
752938 00000 4230581 00000 0.00000 147.00 0.00 0.00 1-HR ALL 1ST CAR1 0
753038 00000 4230581 00000 0.00000 147.00 0.00 0.00 1-HR ALL 1ST CAR1 0
753138 00000 4230581 00000 0.00000 147.00 0.00 0.00 1-HR ALL 1ST CAR1 0
752138 00000 4230681 00000 0.00253 145.00 0.00 0.00 1-HR ALL 1ST CAR1 6071816

```

Figure 5.13: Example Output from the AERMOD

Since the human nose can detect odors very quickly, odor problems usually occur in shorter periods of time, less than an hour. For that reason, we might need to convert average hourly concentrations to shorter averaging times such as 3-Minute concentration. Theoretically, the concentration value of the same location over different period of times follows a power law. A power law as a result is suggested as a possible conversion for use with single source and averaging times of 24 hours or less (Schnelle and Dey, 2000). Thus;

$$C_s = C_k \left[ \frac{t_k}{t_s} \right]^p \quad (5.1)$$

where  $C_s$  = concentration for time  $t_s$        $C_k$  = concentration for time  $t_k$   
 $t_s$  = longer averaging time       $t_k$  = shorter averaging time  
 $p$  = power (values of  $p$  have ranged from 0.17 to 0.75; the suggested value is 0.2 for odor problem (Porter and Elenter, 2008))

## 5.2 GIS-Based Odor Impact Assessment

### *5.2.1 Introduction to Geographic Information System (GIS)*

The Geographic Information System (GIS) is an integration of computer software and geographical data designed for use to integrate, analyze, and visualize the data, to identify relationships, patterns, and trends and to find solutions to problems (GIS Dictionary, ArcGIS 9.2).

The first application of the GIS was developed by Roger Tomlinson for the national natural resource inventory in Canada. For the United States, GIS was first used in the military and intelligence imagery programs of the 1960s. In this study, GIS was employed as a base tool for supporting modeling and analysis. Particularly,

ArcGIS developed by the Environmental Systems Research Institute (ESRI) was used for data management, mapping, and spatial modeling and analysis.

ArcGIS consists of three functionality levels, ArcView, ArcEditor, and ArcInfo. ArcView makes the maps and data that ArcReader can view and print. ArcEditor gives ArcView functionality and has additional data creation and editing tools. ArcInfo gives complete ArcEditor functionality plus a full set of spatial analysis tools. This study employed ArcInfo that plays a significant role for mapping, and data management through ArcMap and ArcCatalog.

#### *Mapping and Visualization with ArcMap*

A GIS map contains a collection of layers called a data frame. The data frame has properties such as coordinate system. The coordinate system is a reference system used to represent information for a defined geographic location such as features, imagery, and observations (GIS Dictionary, ArcGIS 9.2). In addition, it is used to integrate data sets for mapping and analysis.

There are two common coordinate systems: a geographic coordinate system and a projected coordinate system. The geographic coordinate system measures a spherical location from the earth's center (in degree) to the earth surface, and it is represented as a latitude-longitude. The latitude angles are measured in the north-south direction. For the northern hemisphere, the latitude is recorded as north (N), and south (S) in the southern hemisphere. The longitude measured angles in the east-west direction based on the prime meridian, an imaginary line from the North Pole through Greenwich to the South Pole. West of the prime meridian has a negative longitude

value. For example, in Figure 5.14 the geographic location has a latitude-longitude (40 degrees north, 50 degrees east).

The geographic coordinates in this study are all in the Northern Hemisphere and West of the prime meridian. As a result, a location can be expressed in a positive value of latitude and in a negative value of longitude.

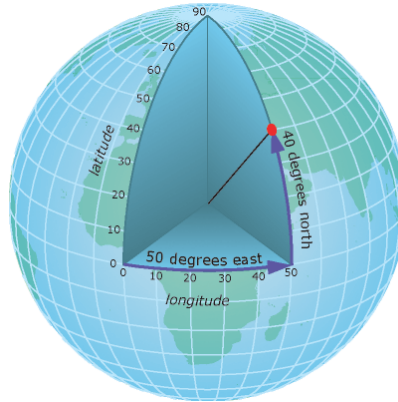


**Figure 5.14: Example of the geographic coordinate system (GIS Dictionary, ArcGIS 9.2)**

The projected coordinate system, on the other hand, measures an earth location by projecting it into Cartesian plane( $x, y$ ). The one horizontal ( $x$ ) represents east-west direction, and the one vertical ( $y$ ) represents north-south direction. The projected coordinate system is usually employed when preserving a shape or an area.

With well-defined coordinate systems, mapping in the GIS can be performed more accurately. In the GIS-Based Biosolids Odor Impact Assessment Models, the two coordinate systems were used for different purposes. The geographic coordinate system was specifically used for spatial analysis when the projected coordinate system was purposely used for area calculations.

As previously mentioned, a map contains layers, and adding layers is considered the first task when mapping. However, deciding on what layers or information we need is a crucial step.

#### *Data Management with ArcCatalog*

ArcCatalog is a tool to provide an integrated and unified view of geographic information, which connects GIS to data source location and manages data properties. Data used in GIS may exist in many forms including files and databases. Some common tasks performed by the ArcCatalog include browsing and finding geographic information and defining, exporting, and importing data models and data sets.

#### *ArcGIS Extensions and Geoprocessing*

ArcGIS has Extensions that can be used for specific tasks. For example, the Geostatistical Analyst in the Extension was used to statistically analyze the values of concentration data and to create maps.

#### *5.2.2 GIS-Based Biosolids Odor Impact Assessment*

GIS-Based Odor Impact Assessment was developed to provide decision makers a systematic tool for assessing possible impacts from biosolids odor at land application sites. Basically, it can be used for supporting the AERMOD modeling setup and visualizing odor impact areas. Those tasks often include visualization and data management, mapping, and modeling to provide a better way to visualize odor impact areas. More specially, it generates information on terrains for use in the meteorological preprocessor (AERMET) and the dispersion modeling (AERMOD)

for model prediction. The assessment of odor impact was focused on making prediction concentration maps (C-Maps), probability maps (P-Maps) and intensity maps (I-Maps). The GIS-Based Odor Impact Assessment works in sequential steps and the procedure can be summarized below.

The first step is to create a map that contains a data frame for adding layers necessary to support the modeling setup. The accuracy of the map depends on the coordinate system. The geographic coordinate system North American Datum 1983 (NAD 1983) was assigned to the data frame. Transformation of the coordinate system might be needed if the added layers are not in the same coordinate system as the data frame.

A model called the “Defined Projection Model” was created by the Geoprocessing for transformation of coordinate system. Basically, the model will convert an input layer coordinate system to the defined coordinate system. It could be used for both the feature and the raster data. Figure 5.15 shows the schematic of the Define Projection Model.

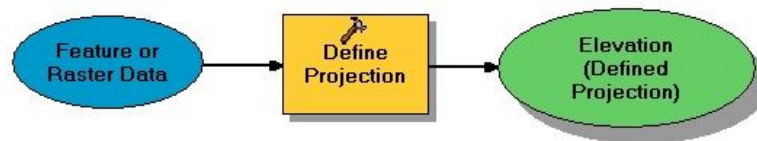


**Figure 5.15: Defined Projection Model**

After defining coordinate systems, all the layers were added to the data frame.

Layers added for supporting modeling setup were:

1. Maryland Environmental Service’s Reuse Fields Data (MES Data) layer
2. Virginia Counties layer

3. Weather stations for Hourly Surface Observations and Upper Air Data layer
4. Elevation layer

For some layers, there is a need for preprocessing the data before adding them to the GIS. For example, the MES data had to be preprocessed for cleaning and compiling the data using a spreadsheet. The data with its geographic coordinates were then imported to the GIS as a feature data containing information of land application sites. Similarly, the weather stations data had to be preprocessed before adding them to the data frame.

For those others, it may come as a ready-to-use geographical data. The ESRI provides geographic information data in many dimensions including census and elevation. The elevation data are raster data created by the U.S. Geological Survey (USGS). Typically, their values are stored as unit meters above sea level in the elevation layer. The elevation layer is derived from the global digital elevation model (DEM). However, the size of the layer might be too big, and it could slow down model running time.

A model called “Clip Raster Model” shown in Figure 5.16 was used to create a spatial subset of a raster data. To be clipped, the model needs four coordinates to define the clipped area. Figure 5.17 shows an example of clipping the elevation layer in Virginia (on the right) from the world elevation layer (on the left).



**Figure 5.16: The Clip Raster Model**

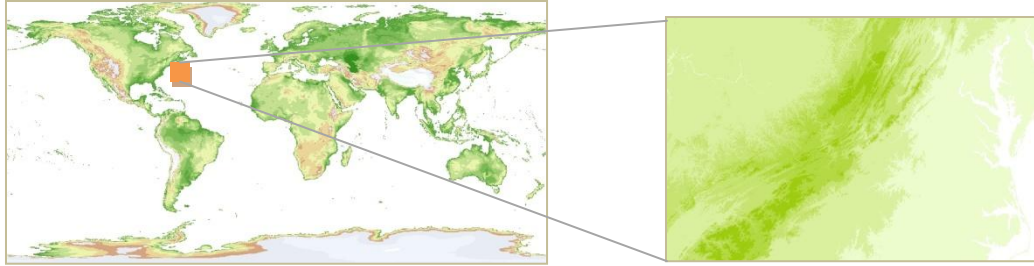


**Figure 5.17: Example Clipping of the Elevation Layer**

The next step is to select the studied area. Since the accuracy of prediction is the main priority, selecting the studied area, in this case, was bounded by the distance of studied fields to the locations of weather stations. The closest weather stations will provide a more representative sample of weather condition in the field. Using the “Selection by Location” analysis tool in the GIS, the average distance of fields approximately closest to the weather stations were in Orange and Albemarle counties.

Orange County is a county located in the northern part of Virginia. As of the 2007 census, the population was 32,276, and its population density was 94 people per square mile (PP\_SQMI). The weather station in Orange County is located in Orange county airport with a coordinate (38.2472N, 78.0456W). Its elevation is 142 meters above sea level.

Albemarle County is a Virginia county located on the southwest side of the Orange County. The population in 2007 was 95,543. Its population density was 131.5 PP\_SQMI. The weather station is located in Charlottesville - Albemarle Airport. The airport is located at a coordinate (38.1383N, 78.4558W) and 192 meters above sea level.

Figure 5.18 shows an example of GIS screenshot for the data frame “Supporting Modeling Setup” that contains MES field data layers, weather stations layer, Virginia counties layer, and elevation layer.

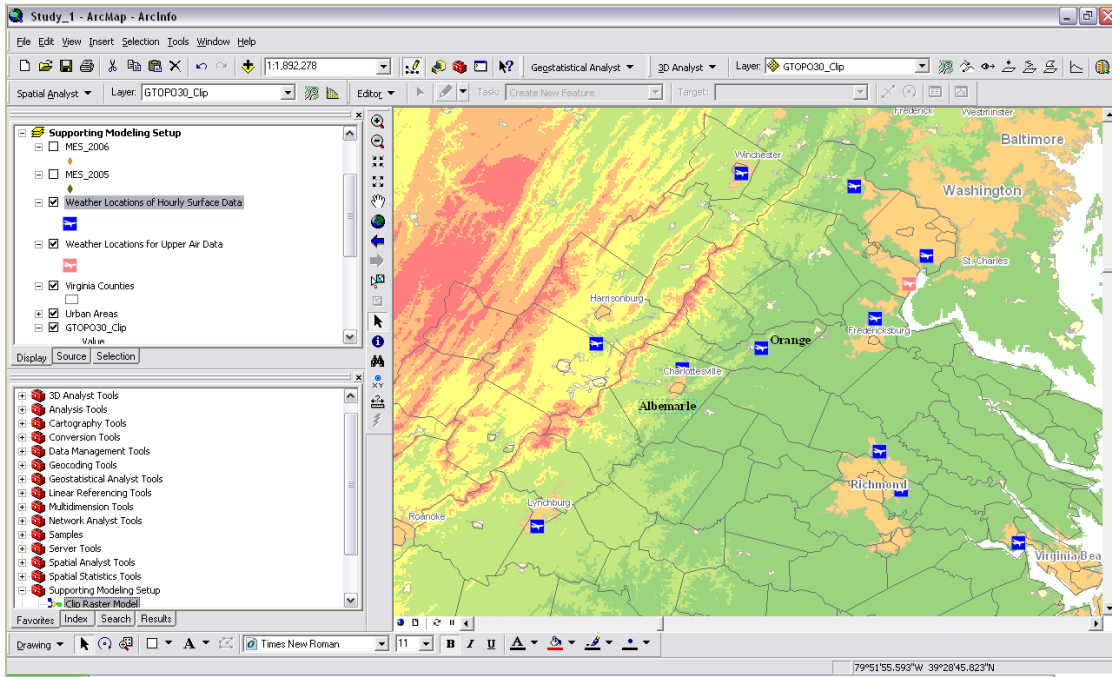


**Figure 5.18: Example GIS Screenshot for the Supporting Modeling Setup Data Frame**

In addition to elevation layer, the hillshade values are needed in the AERMOD, through the receptor pathway (RE), to characterizing the terrain. The hillshade layer was created from the elevation data in ESRI Data & Map. An ArcGIS Extension tool called “Spatial Analyst” was used to create the hillshade layer with 315 degrees of Azimuth angle of the light source and 45 degrees of Altitude angle of the light source above the horizon.

The next step is characterizing receptor terrain. Determining receptor terrain is the required step for the receptor pathway (RE) in the AERMOD, and it can be done by use of “Supporting Modeling Setup” in the GIS. With all the layers added, a model developed called “Receptor Terrain Model” can be used to define receptor terrain and hillshade values. Figure 5.19 shows a schematic for the Receptor Terrain Model.

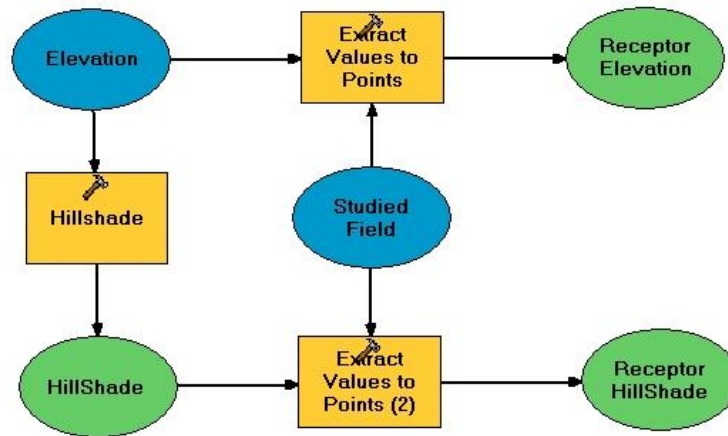


**Figure 5.19: Receptor Terrain Model**

With all the required inputs the AERMOD simulated odor concentration in micrograms per cubic meters. The output of concentration values was stored with their coordinates in a specified receptor grid network. The odor concentrations were converted to grams per cubic meters or odor units per cubic meters ( $OU/m^2$ ) for comparing with the measured odor concentration obtained by the Nasal Ranger field olfactometry, in Dilution-to-Threshold. Due to impossibility of measuring concentration values at every location, the Geostatistical Analyst was used for generating continuous concentration data.

### *Geostatistical Analyst*

Geostatistical Analyst is an integration of Geostatistics and GIS. It is the advanced surface modeling that provides the tool for exploratory spatial data analysis (ESDA) and for creating statistical surface. The goal of the Geostatistics is to predict values at locations where measurement can be made but often available in a limited number of sampled points.

Typically, there are two groups of interpolation techniques: deterministic and Geostatistical interpolation or Kriging models. Deterministic interpolation relies on mathematical function, but the geostatistical interpolation depends on both mathematical and statistical methods with information of uncertainty. Despite differences in model algorithm the geostatistical interpolation provides information on prediction error.

Deterministic models are based on either the distance between points (e.g., Inverse Distance Weighted) or the degree of smoothing (e.g., Radial Basis Functions and Local Polynomials). Geostatistical models or Kriging are based on the statistical properties of the observations and provide some measure of the certainty or accuracy of the predictions while deterministic models do not. It also tells us how good the predictions are.

Geostatistics requires two main steps: spatial data analysis and modeling. The spatial data analysis serves as a tool to verify assumptions on spatial data: distribution, dependency, and stationarity. If those assumptions were satisfied, the modeling steps for spatial data are performed.

Theoretically, Geostatistics works best when input data are Gaussian. If not, data have to be made close to Gaussian distribution. The tools available in Geostatistical Analyst used to explore data include a histogram and normal quantile-quantile (Q-Q) plot. The histogram plots frequency histograms for the attributes in the data set. The important features of the distribution are its central value, its spread, and its symmetry. As a quick check, if the mean and the median are approximately the same value, we have one piece of evidence that the data may be normally distributed. The normal Q-Q Plot, on the other hand, compares the distribution of the data to a standard normal distribution providing another measurement of normality. The closer the points are to creating a straight line, the closer the distribution is to being normally distributed.

Another important feature of the data is the dependency. The dependency is referred to so that data from neighboring values are close to each other. The Semivariogram/Covariance cloud allows us to roughly examine that relationship. Moreover, the Semivariogram/Covariance modeling provides more details on investigating the dependency of the data. Figure 5.20 shows a semivariogram of concentration data with an evident of spatial dependence.

The other important feature, stationarity, also needs to be investigated when analyzing statistical data. Stationarity means that statistical properties do not depend on location. Therefore, the mean (expected value) of a variable at one location is equal to the mean at any other location.

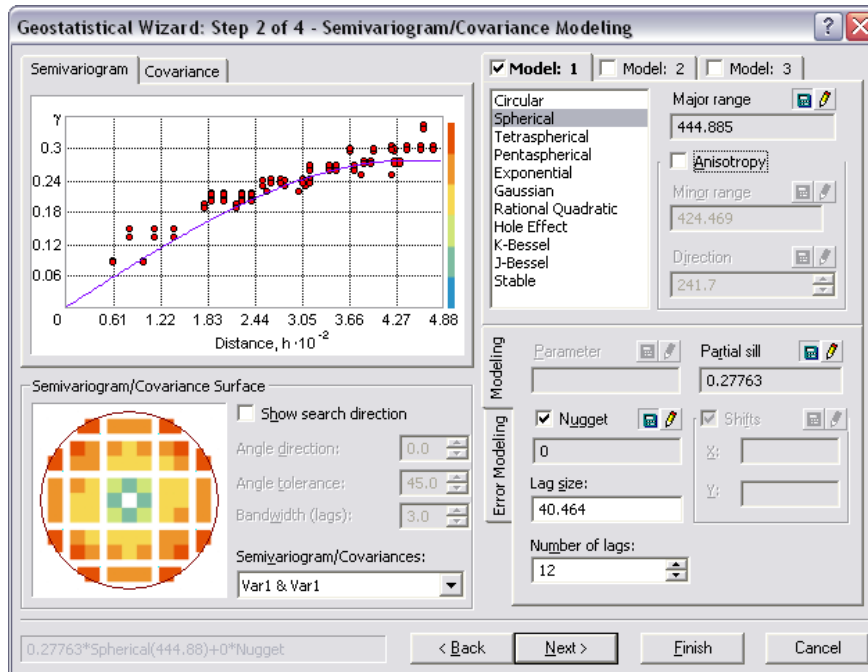


**Figure 5.20: Semivariogram Modeling**

After exploring the data, the interpolation technique could then be employed to generate a continuous surface, concentration plot in this case. Normally, Kriging, (Webster and Oliver, 2007), is divided into two distinct tasks: quantifying the structure of the spatial data and producing a prediction. Quantifying the structure, known as variography, is fitting a spatial-dependence model to data. Then, Kriging will use the fitted model from variography, the spatial data configuration, and the values of the measured sample points around the prediction location to make a prediction for an unknown value.

Basically, each Kriging method relies on the notion of autocorrelation. The typical Kriging equation could be expressed in a simple mathematical formula,

$$z(s) = \mu(s) + \varepsilon(s) \quad (5.2)$$

where  $z(s)$  is the variable of interest at any location in space ( $s$ ), decomposed into a deterministic trend  $\mu(s)$ , and random, autocorrelated errors form  $\varepsilon(s)$ . It is that formula that forms the basis for all of the different Kriging models. The summary of the different Kriging methods based on the variation of the formula is briefly described below.

1. Ordinary Kriging assumes that trend  $\mu(s)$  is constant and unknown.
2. Universal Kriging, on the other hand, assumes variation of trends  $\mu(s)$  and regression coefficients are unknown.
3. Simple Kriging would be used when trend  $\mu(s)$  is completely known whether constant or not.
4. Indicator Kriging is used when you perform transformation on  $z(s)$ . For example, you can change it to indicator variable, where it is 0 if  $z(s)$  is below some value (e.g., 1 for odor concentration).
5. Probability Kriging may be used when you wish to predict the probability that  $z(s)$  is above the threshold value or not.
6. Last, disjunctive Kriging is used when you want to make unspecific transformation of the  $z(s)$ , which is not used in this research.

The Geostatistical analyst was used in this study to create predicted odor concentration maps (C-Map) and probability maps (P-Map). The C-Map provides potential impact areas to neighborhoods. The predicted odor concentrations associated with the impact areas are comparable with discrete dilution scales of the Nasal Ranger field olfactometer, which is used to measure ambient odor strength.

Probability map (P-Map) is defined as a map containing probabilities of exceeding the defined threshold at receptor locations. It can be expressed as:

$$P(C \geq C_T) \quad (5.3)$$

where  $P$  is the probability of the predicted concentration exceeding the defined threshold concentration,  $C$  is the predicted concentration, and  $C_T$  is the threshold concentration. The P-Map can support decisions on biosolids distribution by providing a chance of human perception to particular odor levels.

### *5.2.3 Biosolids Odor Impact Assessment*

Assessment of land-applied biosolids odor impact to nearby communities is a difficult task because of individual variation in odor perception. Generally, the human perception to odor is based on many factors including, for example, gender, age, and health condition. The first theory of sensation measurement as part of the psychophysics stated that the sensory responses to stimuli follows the power law (Stevens, 1960). In case of odor perception, the relationship of the relative odor strength and the stimulus odor can be defined as:

$$I = kC^n \quad (5.4)$$

where  $I$  is the relative odor strength or intensity,  $C$  is the mass concentration of odorant, and  $k$  and  $n$  are constants that differ from one odorant to another.

To assess impacts from odors, it usually begins with an assessment of odor parameters. As previously mentioned in Section 4.1.2, U.S. Environmental Protection Agency (EPA) recommends using five independent parameters for the complete assessment: detectability, intensity, character, hedonics, and persistency.

Furthermore, a conceptual model for citizen complaints was developed consisting of

odor character, odor intensity, duration, and frequency; the cumulative effect of these parameters may contribute to nuisance experience and possibly lead to complaints (McGinley et al., 2000).

The odor character is basically what the odor smells like. The odor intensity refers to overall strength of the perceived odor in referencing n-butanol scales that is the relative magnitude of the odor above the recognition threshold, as defined in ASTM E544-99, “Standard Practice for Referencing Suprathreshold Odor Intensity.” Duration is the period of time in which odorants are transported downwind to citizens and are perceived as odor. Longer period of perception can cause more nuisances to community. The frequency refers to how often the citizen experience odor episodes of any type.

The odor parameters proposed to assess impacts from biosolids odor usually requires field and laboratory odor testing. The laboratory odor testing requires collecting samples on the application date shipped overnight to an odor-testing laboratory. It is considered a test of the actual emission. On the other hand, the Nasal Ranger field olfactometer is used to measure odor concentration in ambient conditions. As previously described in Section 3.2.1, the Nasal Ranger field olfactometer is the current practice for Maryland Environmental Services (MES) to measure odor concentration in land application fields, and it can only be performed after biosolids being applied. For those reasons, it seems difficult to assess biosolids odor impact at land application sites beforehand.

In biosolids land application sites, a receptor usually sniffs the diluted odor. Depending on the individual variation of odor perception and the four parameters

described above, a receptor may or may not detect the odor. If the receptor detects the odor, then the odor in the atmosphere is above the detection threshold level that is equivalent to odor concentration value of 1 gram per cubic meter ( $g/m^3$ ) calculated by the odor dispersion model (McGinley and McGinley, 2002). A value less than 1 represents no odor or sub-threshold, and a value greater than 1 represents odor at supra-threshold level. The results from the screening and refined analysis are, by default, in mass concentration units (i.e., micrograms per cubic meter,  $\mu g/m^3$ ). A conversion factor needs to be applied to the results obtained from the EPA dispersion models.

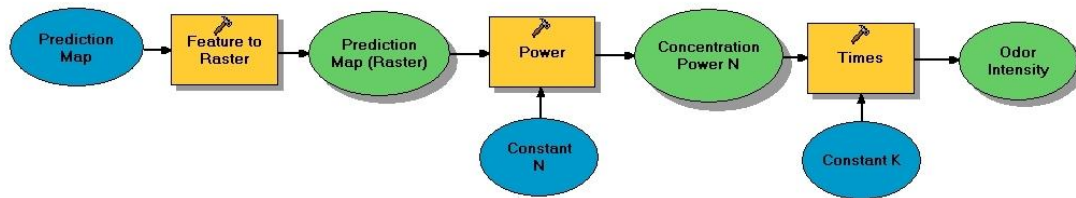
In reality, assessment of odor impact to humans is very difficult. Human perception is subjective. Variations within individuals, among individuals, and among populations play significant roles. However, it is essential for biosolids generators to estimate potential impact. In this study, two approaches were presented as possible ways to support assessment of biosolids odor impact at land application sites.

1. Intensity map (I-Map): the intensity map was developed from the Stevens' power law that relates odor concentration with odor intensity as n-butanol referencing scale so called odor persistency. The greater value indicates higher intensity and then perception. Comparing the odor intensities of two candidate application fields for biosolids distribution could be helpful for selection of reduce nuisance conditions in nearby communities.

Similar to the P-Map, the concentration values are obtained from the predicted concentration map (C-Map). The constants  $k$  and  $n$  can be obtained from historical laboratory results. Typically, the values of the constants vary from one sample to

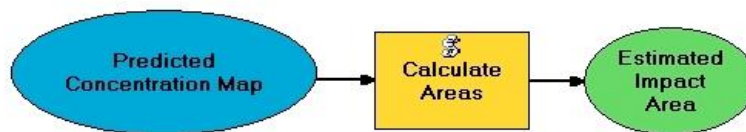
another. Deciding on method to estimate the values of  $k$  and  $n$  when creating I-Map requires careful consideration. However, it is appropriate to use the average values for the same odor source (i.e., biosolids odor from DCWASA).

Figure 5.21 shows the Intensity Map Model developed in the GIS to support creation of intensity maps. Basically, the prediction map in vector form has to be converted to raster. The power law was applied to generate the intensity map.



**Figure 5.21: Intensity Map Model**

2. Estimated impact to population: this approach simply relates estimated impact area for each dilution scales with population density in that area. The impact area is estimated from a predicted concentration map (C-Map) using the Geoprocessing Spatial Statistics, See Figure 5.22.



**Figure 5.22: Impact Area Model**

Table 5.5 provides an example of calculating the expected number of population affected by odor. The impact areas for each dilution levels were calculated from the Impact Area Model in Figure 5.21. The population density obtained from the

ESRI Data & Map is 94 per square mile. The expected number of population is a product of impact area in square meters and population density in square meters.

This approach, however, is intended to quantify general population potentially affected by different odor concentration categories not sensitive population. The estimation is respected to the fact that population density is varied depending on the area. For example, more populated areas will have higher population density. With the best census data available, nevertheless, the assessment of odor impact to population using population density is considered appropriate.

**Table 5.5: Example Calculation of Odor Impact to Population**

<i>D/T</i>	<i>Impact Area (square meters)</i>	<i>Population Density (per square mile)</i>	<i>Expected Population</i>
0-1	936128.186	94	34
2-3	32445.533	94	1
4-7	30693.859	94	1

#### *5.2.4 Simple Linear Regression for Model Validation*

Regression analysis is a tool to identify inherent relationships among variables. It is basically the relationships between dependent and independent variables. In case that there exists a linear relationship between them, linear regression analysis is widely used to deal with finding that relationship.

In this study, to validate the results from the models with measurement, simple linear analysis, (Walpole et al., 2002), was employed to investigate if a linear relationship exists. The linear relationship approach was the first attempt used to validate the model predictions with the measurement from Nasal Ranger

olfactometer. More complicated models can be employed in a future work. Equation 5.5 shows the typical linear model:

$$Y = \beta_0 + \beta_1 x + \varepsilon \quad (5.5)$$

where  $\beta_0$  = intercept,  $\beta_1$  = slope, and  $\varepsilon$  = random error assumed to be normally distributed with  $E(\varepsilon) = 0$ ,  $Var(\varepsilon) = \sigma^2$ .

The regression coefficients ( $\beta_0, \beta_1$ ) are estimated to find the smallest sum of squares. Then, the true regression line can be replaced with the least squares regression line:

$$\hat{y} = \hat{\beta}_0 + \hat{\beta}_1 x + e \quad (5.6)$$

where

$$\hat{\beta}_1 = \frac{\sum(x_i - \bar{x})(y_i - \bar{y})}{\sum(x_i - \bar{x})^2} \quad (5.7)$$

$$\hat{\beta}_0 = \bar{y} - \hat{\beta}_1 \bar{x} \quad (5.8)$$

$$e_i = y_i - \hat{y}_i \quad (5.9)$$

For the purpose of this study, the coefficient of determination ( $R^2$ ) is used to explain the percentage of variation in dependent variable. It can be defined as

$$R^2 = \frac{SSR}{SST} \quad (5.10)$$

where sum of squares total (SST) =  $\sum(y_i - \bar{y})^2$ , sum of squares error (SSE) =  $\sum(y_i - \hat{y}_i)^2 = \sum e_i^2$ , and sum of squares regression (SSR) = SST-SSE. Since the  $R^2$  will always increase as the number of independent variables in the model increase, the adjusted  $R^2$  can be used to adjust this error. The adjusted  $R^2$  is defined as:

$$1 - \left(\frac{n-1}{n-p}\right) \left(\frac{SSE}{SST}\right) \quad (5.11)$$

where n = number of the observations used for estimation and p = number of the variables to be estimated

In addition, a measure of the prediction accuracy is derived from the standard error of estimate ( $S_e$ ) where

$$S_e = \sqrt{\frac{SSE}{n-2}} \quad (5.12)$$

The t-test is used to test the significance of a linear relationship. The null hypothesis  $H_0: \beta_1 = 0$  (no significant linear relationship between dependent and independent variables) against  $H_a: \beta_1 \neq 0$  (significant linear relationship exists). The t-statistic is given by

$$t = \frac{\hat{\beta}_1}{\text{stdErr}(\hat{\beta}_1)} \quad (5.13)$$

For the simple linear regression, there are assumptions required to follow.

1. The variance of the error term does not depend on independent variables.

This assumption can be checked by plotting the independent variable with the residual.

2. Errors are normally distributed, which can be checked by performing the normality test such as normal quantile – quantile (Q-Q) test.

3. The errors should be independent. To see whether this assumption holds, we can plot the errors in time-series sequence. If there is no pattern presented, the assumption appears to be satisfied.

### 5.3 Case Studies: Screening Model

#### *5.3.1 Study Areas*

The Screen view was applied to predict biosolids odor concentration in 14 land application sites (45 fields) in Virginia. More specifically, the study focused on the application of biosolids to the fields in Albemarle and Orange counties for the periods of 2005 and 2006.

Albemarle County is located in Central Virginia about 110 miles southwest of Washington, D.C. As of the census of 2007, there were 95,543 people, 31,876 households, and 21,069 families in the county. The population in 2000 was spread out with 28.53% under age 21, 42.78% from 22 to 49, and 28.69% from 50 or older. The county has a total area of 726.3 square miles, which 16% are crop area.

In 2005, for example, a site 05-A located in Albemarle county contained two fields: field 1 and field 2. The biosolids were applied to both fields on the same day. Emission rates used in this case study were estimated by using an expert judgment on the mass flow rate as stated in Section 4.2. The mass flow rate was assumed to be 0.03048 meters per second( $m/s$ ). The emission rates for the site 05-A can be calculated from the known flow rate and the measured odor strength. Table 5.6 provides a summary of the site characteristics.

**Table 5.6: Summary of Site 05-A Characteristics**

<i>Field Characteristics</i>	<i>Field Designation</i>	
	<i>1</i>	<i>2</i>
Date Applied	10/17/05	10/17/05
Coordinate (Latitude, Longitude)	(38.18N, 78.58W)	(38.29N, 78.59W)
Area Used (square meters)	240.73×240.73	351.21×351.21
Measured Odor Strength (Dilution-to-threshold, D/T)	4	4
Estimated Emission Rate ( $OU/s - m^2$ )	0.156	0.156
Wind Direction (Degrees)	67.5	67.5

Since the field odor concentrations were measured in discrete categories (0, 2, 4, 7, 15, 30, and 60 D/T(s)); it is necessary to convert the measured odor concentrations to the best estimate thresholds using the geometric mean. The geometric mean is used when there is a lack of equal variance along the dilution ration scale (Stevens, 1962). An example below shows a calculation of the geometric mean between 4 and 7. The first step is to find an average of the sum of logarithms for lower D/T (4 D/T) and higher D/T (7 D/T). The result was transformed using a logarithm base 10 to make an equal variance along the logarithm scale. With the best estimate thresholds, the emission rates can be back-calculated using the same concept described in Section 4.2. The estimated emission rates in Table 5.5 were obtained by use of the best estimate thresholds. Table 5.7 provides the best estimate threshold values for Nasal Ranger field olfactometer scales.

$$(\text{Log } 4 + \text{Log } 7)/2 = (0.602+0.845) /2 = 0.7235 \quad \{10^{0.7235} = 5\}$$

**Table 5.7: Best Estimate Thresholds**

<i>Lower D/T</i>	<i>Higher D/T</i>	<i>Best Estimate Threshold</i>
0	1	1
2	3	2
4	6	5
7	14	10
15	29	21
30	59	42

Orange County located in Northern Virginia had 32,276 people in 2007. There were 10,150 households and 7,441 families. As of the census of 2000, the population was spread out with 26.85% under age 21, 37.53% from 22 to 49, and 35.62% from 50 or older. The total area in the county is 343.5 square miles, which about 26% are crop area.

Site 06-H is located in Orange County, VA. The site had three fields that were land-applied on July 19, 2005. Table 5.8 provides a summary of the site characteristics.

**Table 5.8: Summary of Site 06-A Characteristics**

<i>Field Characteristics</i>	<i>Field Designation</i>		
	<i>2</i>	<i>3</i>	<i>5</i>
Date Applied	07/19/06	07/19/06	07/19/06
Coordinate (Latitude, Longitude)	(38.188N, 78.123W)	(38.185N, 78.117W)	(38.196N, 78.121W)
Area Used (square meters)	83.19×83.19	140.53×140.53	143.24×143.24
Measured Odor Strength (Dilution-to-threshold, D/T)	2	7	7
Estimated Emission Rate ( $OU/s - m^2$ )	0.061	0.305	0.305
Wind Direction (Degrees)	157.5	157.5	157.5

### 5.3.2 Results

Using the Screen View with input data from the 45 fields, the results were generated. For the site 05-A, the summary of inputs was provided in Table 5.9. The selected source type was an area source in rural area. The receptor height above ground was considered as a height of average person, in this study, 1.7 meters. An estimated area source for field 1 was 240.73 square meters and 351.21 square meters for field 2. The meteorology input was assumed for full stability classes.

**Table 5.9: Summary of Screen View Inputs for Site 05-A**

<b>Required Inputs</b>	<b>Field Designations</b>	
	<b>1</b>	<b>2</b>
Dispersion Coefficient	Rural	Rural
Receptor Height (meters)	1.7	1.7
Emission Rate <i>OU/s – m<sup>2</sup></i>	0.156	0.156
Source Release Height(meters)	0.1	0.1
Area (square meters)	240.73	351.21
Wind Direction	67.5	67.5
Terrain Option	Simple	Simple
Meteorology	Full Stability	Full Stability
Automated Distance	Yes	Yes

The Screen View simulated one-hour averaging concentration for ambient biosolids odor with 67.5 degrees wind direction for 130 meters to 1,500 meters from the center of the source. The output from the model, by default, was in micrograms per cubic meter ( $\mu\text{g}/\text{m}^3$ ). Figures 5.23 and 5.24 show example outputs of concentrations from field 1 and field 2 with their relative distances.

However, it is practical to use the pseudo-dimensions of odor unit per cubic meter taking place of grams per cubic meter for modeling odor dispersion purpose

(McGinley and McGinley, 2002). Moreover, the dimensioned values of odor concentration can be compared with the dimensionless dilution ratio in Dilution-to-Threshold (D/T). In this study, results in micrograms per cubic meter were converted to grams per cubic meter and then were expressed in D/T for use in comparison with field measurement. In this case study, the maximum one-hour concentration for field 1 was found at 160 meters from the center of the source, 8 D/T. The maximum one-hour concentration for field 2 was found at 216 meters from the source, 10 D/T.

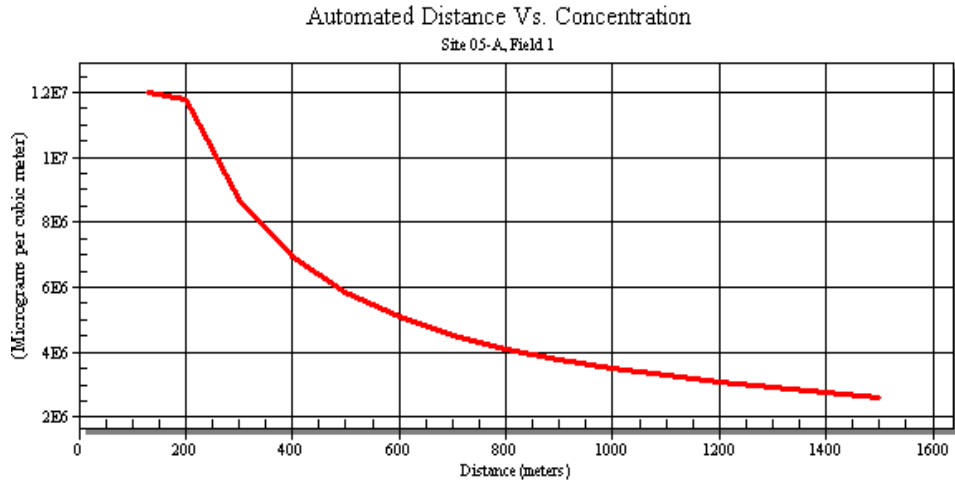


Figure 5.23: Screen View Output for Site 05-A, Field 1

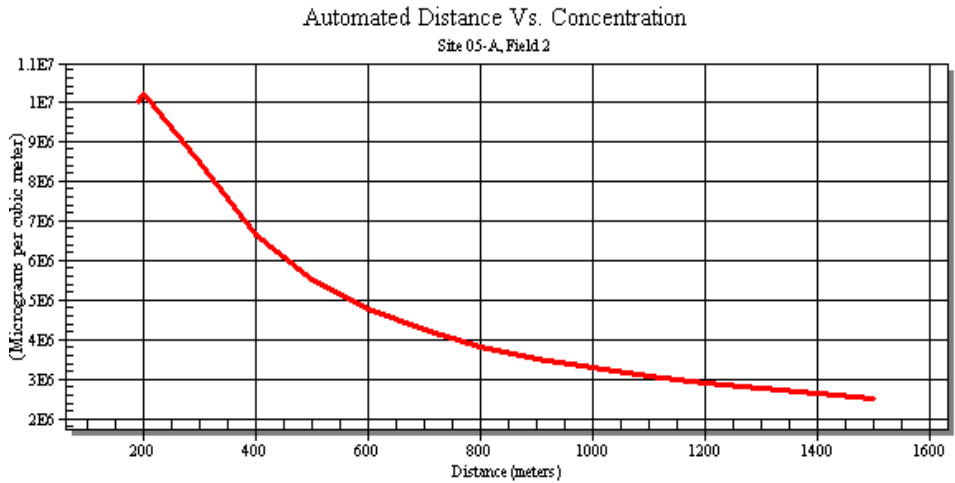


Figure 5.24: Screen View Output for Site 05-A, Field 2

For site 06-H, the summary of inputs for field 2, 3, and 5 was provided in Table 5.10. The selected source type for the three fields was also an area source. The rural area was selected to calculate the dispersion coefficient. The receptor height above ground was considered as a height of average person, in this case, 1.7 meters. Estimated areas for field 2, 3, and 5 were 83.19, 140.53, and 143.24 meters, respectively. The meteorology input was assumed for full stability classes.

**Table 5.10: Summary of Screen View Inputs for Site 06-H**

<i>Required Inputs</i>	<i>Field Designations</i>		
	<i>2</i>	<i>3</i>	<i>5</i>
Dispersion Coefficient	Rural	Rural	Rural
Receptor Height (meters)	1.7	1.7	1.7
Emission Rate $OU/s - m^2$	0.061	0.305	0.305
Source Release Height(meters)	0.1	0.1	0.1
Area (square meters)	83.19	140.53	143.24
Wind Direction	157.5	157.5	157.5
Terrain Option	Simple	Simple	Simple
Meteorology	Full Stability	Full Stability	Full Stability
Automated Distance	Yes	Yes	Yes

Using the same concept described previously, the maximum one-hour concentrations for those fields were expressed in D/T and found at 87 meters (1 D/T) for field 2, 111 meters (11 D/T) for field 3, and 112 meters (11 D/T) for field 5.

To investigate the variation of model outputs by using a different emission estimate approach, the emission rates estimated by three approaches described in Section 4.7 were applied to 47 land application fields. Figures 5.25 – 5.27 show the results of predicted concentration for Site 05-C field 8 using three different emission rates: 0.153, 0.283, and 0.146 odor units per cubic meter-second,  $\frac{OU}{m^2-s}$ . The maximum

one-hour concentrations generated from those emission rates were found at the same distance, about 175 meters from the source, but different odor concentrations.

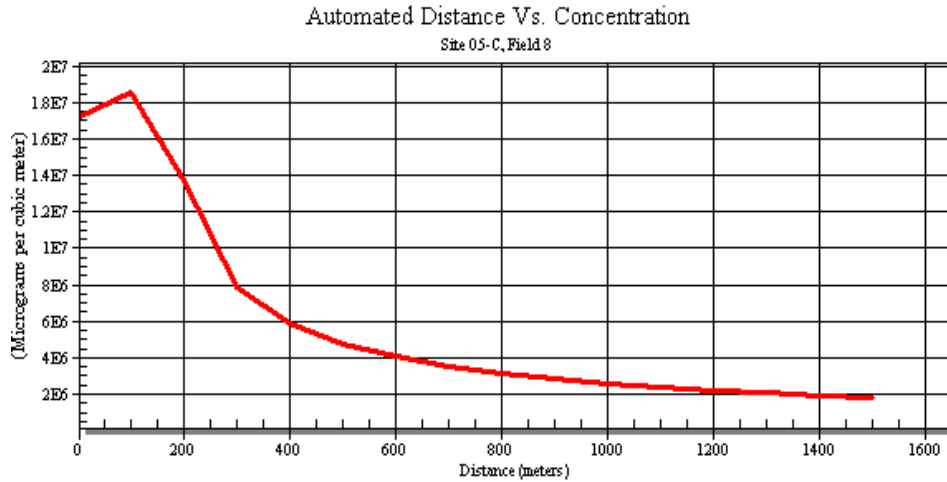


**Figure 5.25: Screen View Output for Site 05-C, Field 8**

**(Emission Case 1 =  $0.153 \text{ OU}/\text{m}^2 - \text{s}$ )**

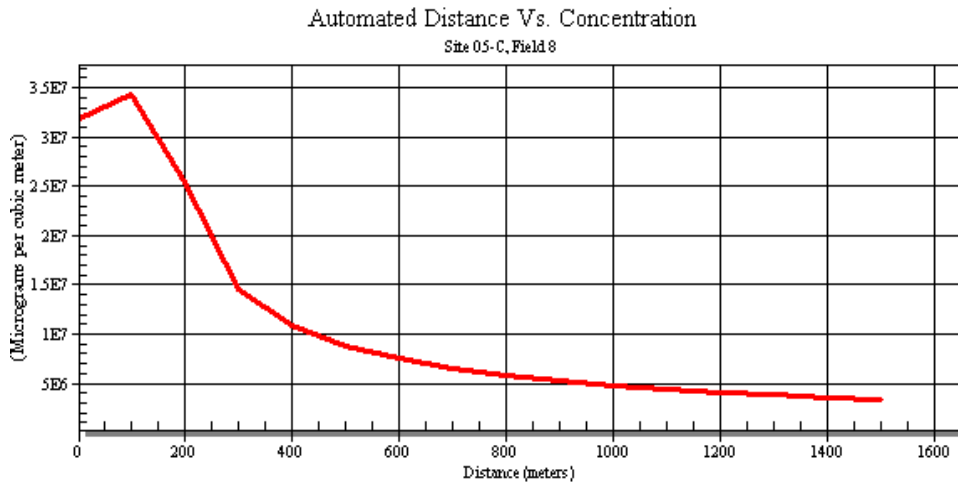


**Figure 5.26: Screen View Output for Site 05-C, Field 8**

**(Emission Case 2 =  $0.283 \text{ OU}/\text{m}^2 - \text{s}$ )**

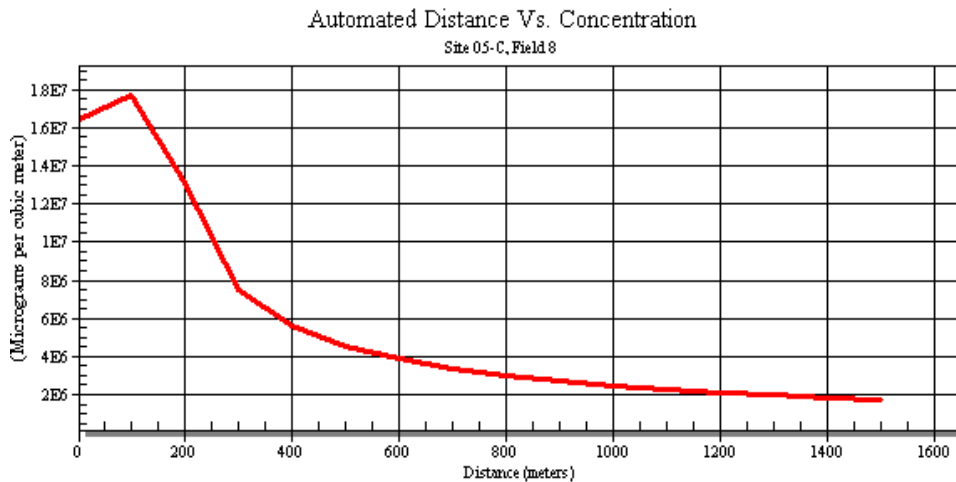


**Figure 5.27: Screen View Output for Site 05-C, Field 8**

**(Estimate Case 3 =  $0.146 \text{ OU}/\text{m}^2 - \text{s}$ )**

### 5.3.3 Validation with Data

The linear relationship of the predicted concentration and the measurement obtained by using the Nasal Ranger field olfactometer were verified by the scatter plots. More specifically, the predicted concentrations were plotted against the best estimate thresholds, 2, 5, and 10 Dilution-to-Thresholds (D/T). Since the measurement locations were not exact, the locations were approximated using subjective judgment along with the MES data and the GIS.

Figures 5.28-5.30 provides the scatter plots for the screening results obtained by using three different emission estimates. Theoretically, the scatter plot should appear as a straight line if a linear relationship exists. Moreover, the scatter plots can tell how well the prediction matches the measurement. For example, in Figure 5.27, for the best estimate threshold 2 D/T and 10 D/T, the predicted concentration values fall in the correct ranges: 2 – 3 D/T for the best estimate threshold 2 D/T and 7 – 14 D/T for the best estimate threshold 10 D/T. However, it varies from 2 D/T to 8 D/T in

case of the best estimate threshold 4 D/T. In Figures 5.28 and 5.29, the predicted concentration values were widely spread over the best estimate thresholds.

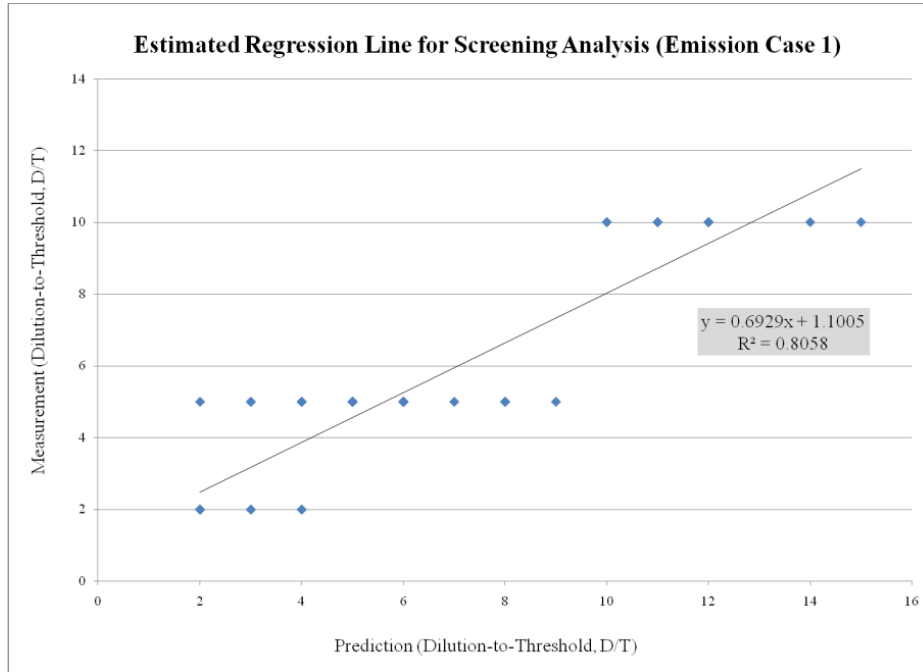


**Figure 5.28 : Scatter Plot for Screening Analysis (Emission Case 1)**

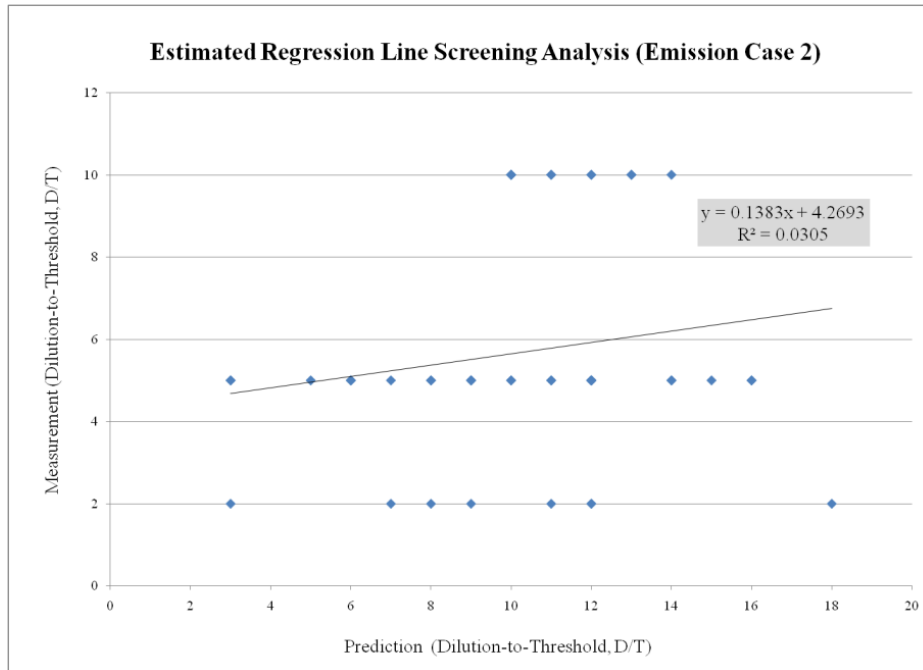


**Figure 5.29 : Scatter Plot for Screening Analysis (Emission Case 2)**

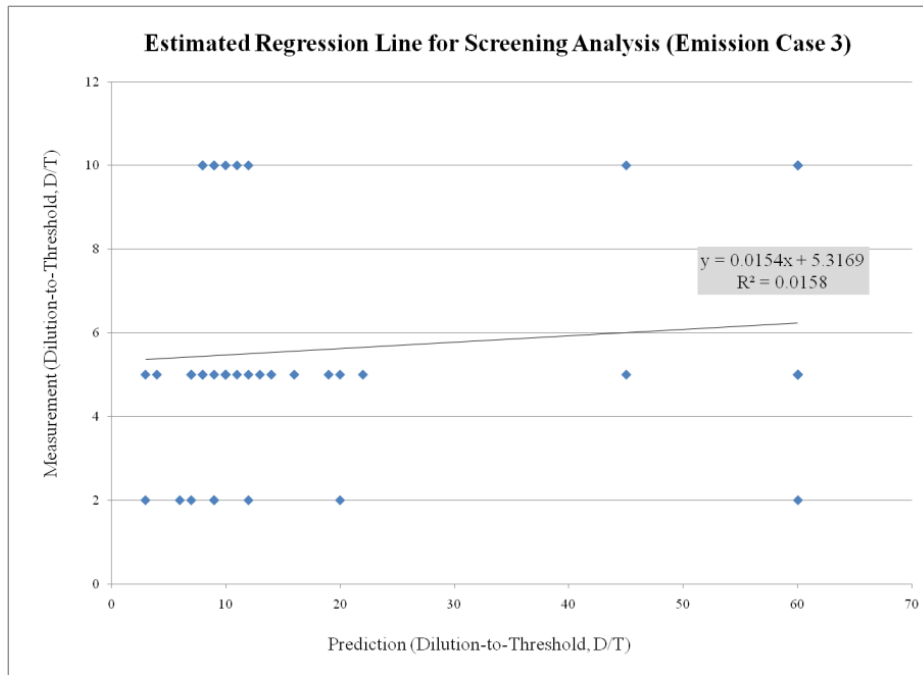


**Figure 5.30 : Scatter Plot for Screening Analysis (Emission Case 3)**

Despite investigating a linear relationship by the scatter plots, the regression analysis was applied to investigate how well the relationship is said to be linear. Tables 5.11 – 5.13 shows the outputs from the regression analysis. With all required parameters, the estimated regression line can be generated from the least squares estimators,  $\hat{\beta}_1$  and  $\hat{\beta}_0$ , as shown in Figures 5.28 – 5.30.

Since the purpose of using linear regression analysis in this study is to validate the results from the screening analysis and the measurement, we focused on the explanatory parameters such as adjusted  $R^2$ , the values close to 1 describe explanatory performance of the model.

The regression analysis output for the screening analysis using the expert opinion for emission estimate (emission case 1) provides the highest adjusted  $R^2$ . In

addition, with the significance level  $\alpha = 0.05$ , the linear relationships for regression coefficients are considered to be statistically significant. In contrast, the regression coefficients for predicted concentration in case 2 and case 3 are not statistically significant at the 95% confident level.

**Table 5.11: Output of Regression Analysis for Screening Analysis (Emission Case 1)**

<i>Summary</i>	Multiple R	R-Square	Adjusted R-Square	StErr of Estimate		
	0.8977	0.8058	0.8013	1.212764163		
<i>ANOVA Table</i>	Degrees of Freedom	Sum of Squares	Mean of Squares	F-Ratio	p-Value	
Explained	1	262.4001771	262.4001771	178.4068	< 0.0001	
Unexplained	43	63.24426736	1.470796915			
<i>Regression Table</i>	Coefficient	Standard Error	t-Value	p-Value	Confidence Interval 95%	
Constant	1.100504147	0.388190036	2.8350	0.0070	0.31764433	1.883363964
Predicted Concentration	0.692876891	0.051874076	13.3569	< 0.0001	0.588262847	0.797490934

**Table 5.12: Output of Regression Analysis for Screening Analysis (Emission Case 2)**

<i>Summary</i>	Multiple R	R-Square	Adjusted R-Square	StErr of Estimate		
	0.1745	0.0305	0.0079	2.709698492		
<i>ANOVA Table</i>	Degrees of Freedom	Sum of Squares	Mean of Squares	F-Ratio	p-Value	
Explained	1	9.918410006	9.918410006	1.3508	0.2515	
Unexplained	43	315.7260344	7.342465917			
<i>Regression Table</i>	Coefficient	Standard Error	t-Value	p-Value	Confidence Interval 95%	
Constant	4.269339501	1.286441823	3.3187	0.0018	1.674982312	6.863696691
Predicted Concentration	0.138267797	0.118965487	1.1623	0.2515	-0.101648972	0.378184567

**Table 5.13: Output of Regression Analysis for Screening Analysis (Emission Case 3)**

<i>Summary</i>	Multiple R	R-Square	Adjusted R-Square	StErr of Estimate		
	0.1257	0.0158	-0.0071	2.730099421		
<i>ANOVA Table</i>	Degrees of Freedom	Sum of Squares	Mean of Squares	F-Ratio	p-Value	
Explained	1	5.146402042	5.146402042	0.6905	0.4106	
Unexplained	43	320.4980424	7.453442847			
<i>Regression Table</i>	Coefficient	Standard Error	t-Value	p-Value	Confidence Interval 95%	
Constant	5.316884588	0.605025447	8.7879	< 0.0001	4.096734488	6.537034688
Predicted Concentration	0.015414543	0.01855057	0.8309	0.4106	-0.021996247	0.052825333

However, since the measurement values were only ranges on the Nasal Ranger field olfactometer scales, the predicted concentrations were associated with the ranges of the measurement scales. For examples, the predicted concentrations of 4, 5, and 6 D/T(s) were associated with the range of 4-6 D/T(s) on the measurement scale, and the predicted concentrations of 7, 8, 9, 10, 11, 12, 13, and 14 were associated with the range of 7-14 D/T(s) on the measurement scale. The regression analysis might not be the appropriate approach to investigate the linear relationship.

A standard error of estimate ( $S_e$ ) in equation 5.12 can be used to measure the accuracy of model predictions. Table 5.14 summarizes the standard error of estimate values for all three cases. Predicted odor concentrations from emission estimate case one provides the least standard error of estimate value, which indicates the best prediction accuracy.

**Table 5.14: Standard Error of Estimates for Screening Model Outputs**

Emission Case	Standard Error of Estimate ( $S_e$ )
1	1.8924
2	6.1832
3	29.1850

#### 5.4 Case Studies: GIS-Based Odor Impact Assessment

##### *5.4.1 Study Areas*

In these case studies, the same land application sites in Albemarle and Orange Counties, as in the case of the screening models (45 land application fields), were investigated by the refined model, AERMOD.

#### 5.4.2 Results

The maximum one-hour predicted concentrations at hypothetical receptor locations with relative dates and times were generated by the AERMOD along with the GIS. The Cartesian grid network was selected to represent evenly spaced hypothetical receptors with a size of square kilometer ( $\text{km} \times \text{km}$ ). However, due to limited availability of meteorological data, only 27 land application fields could be generated from the AERMOD dispersion model.

The results of one-hour concentrations were converted to 3 minute-concentrations, using 0.2 as a power value, accounting for the instantaneous characteristics of odor perception. Using the Geostatistical analyst in the Geographic Information System (GIS), the concentration prediction maps (C-Maps) were created to visualize potential odor impact areas.

Figure 5.31 provides an example of the concentration prediction map (C-Map) for site 06-H, field 3. The map shows the areas of predicted concentrations of 2 and 4 dilution-to-thresholds (D/T). The category 2 D/T can be explained that a receptor can detect the odor from 2 to 3 D/T. Similarly, the 4 D/T represents odor perception of 4 to 6 D/T. The wind direction (WDIR) originates from southwest direction. Another example of a prediction map is provided in Figure 5.32. The map shows the predicted concentration of 2 and 4 D/T. In both cases, the potential odor impacts to neighborhoods can be observed.



**Figure 5.31: Concentration Prediction Map (C-Map) of Field 3, Site 06-H**

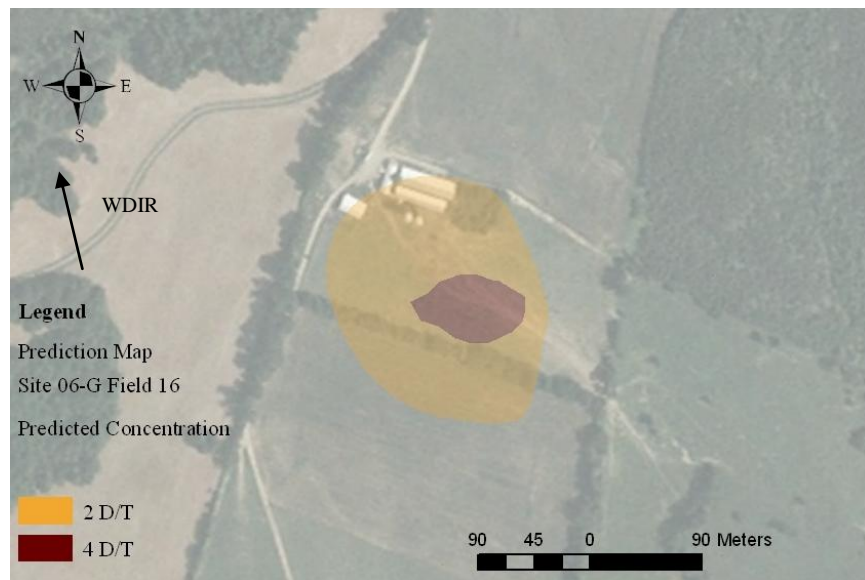


**Figure 5.32: Concentration Prediction Map (C-Map) of Field 16, Site 06-G**

The predicted odor concentration in dilution-to-threshold (D/T) has an advantage that the results from the model can be compared with the dilution scales of the Nasal Ranger field olfactometer also in D/T. However, the predicted concentration areas were focused on the areas that have the field olfactometer reading

greater than 2 D/T since the field olfactometer will interpret a reading of dilution scale of 2 D/T or less as 0 D/T. Therefore, only 13 prediction maps were created.

Unlike the concentration map, the probability map is a map containing probabilities of predicted concentrations exceeding a certain threshold. For example, this study used 7 D/T as the threshold that is defined as the dilution level that may create nuisance condition. Selection of the threshold is subjective and can vary from one practitioner to another. However, selection of lower dilution level is considered a safety factor for sensitive population.

The probability maps of eight land application fields were created. We focused on the areas that predicted odor concentration is 7 D/T or exceeding the category of 4 D/T (4-6 D/T). Figure 5.33 shows an example of the probability map of site 06-G field 16. The map shows three areas where the probabilities are in different ranges. The impact areas associated with the probabilities exceeding 7 D/T can be calculated and used to support a decision for selecting land application fields. The field with smaller areas of impacts with high probabilities is preferred than the larger areas of impacts with the same probabilities.

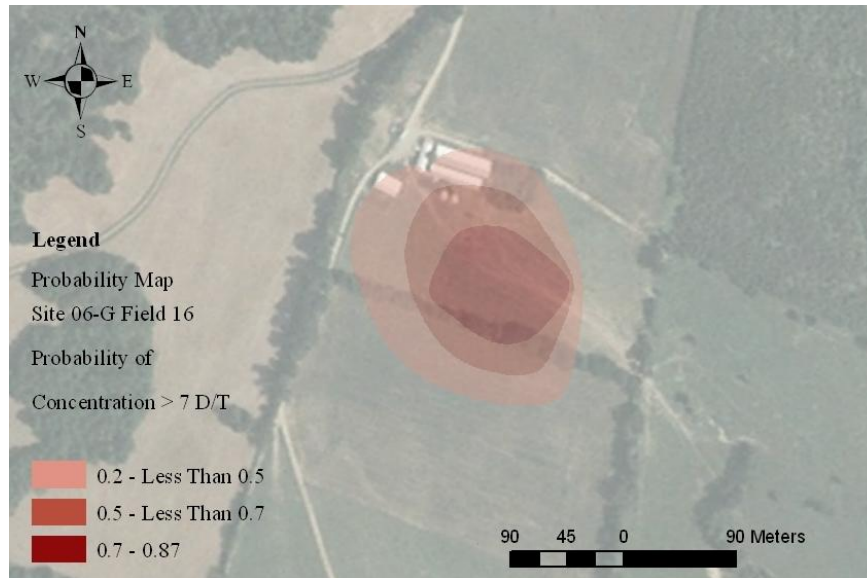


**Figure 5.33: Probability Map (P-Map) of Field 16, Site 06-G**

Intensity maps, as previously mentioned, were created from the power law of sensation. We obtained the data of the constants  $k$  and  $n$  from the DCWASA's Department of Wastewater Treatment (DWT). There were 30 samples with the total sample size of 60. The constants vary from one sample to another. The analysis of variance (ANOVA) was used to confirm that the variations of the constants within sample and among samples exist. Tables 5.15 and 5.16 provide the result of the one-way ANOVA. The null hypothesis ( $H_0$ ) to be tested was whether at least two means are equal at the 0.05 level of significance.

**Table 5.15: ANOVA of Constant  $k$**

<i>OneWay ANOVA Table</i>	Sum of Squares	Degrees of Freedom	Mean Squares	F-Ratio	p-Value
Between Variation	313.98513	29	10.82707	2.66757	0.0047
Within Variation	121.76331	30	4.05878		
Total Variation	435.74844	59			

The grand mean of the  $k$  value is 4.54. The sum of square computations gave treatment sum of squares (SSA) = 313.98513, error sum of squares (SSE) =

121.76331, and total sum of squares (SST) = 435.74844. From the critical values of the F-Distribution, the critical region with  $v_1 = k - 1 = 29$  and  $v_2 = k(n - 1) = 30$  at the significance level = 0.05 gave  $f_{0.05} = 1.84$ .

The decision for this ANOVA results is to reject the null hypothesis and conclude that the  $k$  values do not have the same mean ( $F - Ratio > f_{0.05}$ ).

**Table 5.16: ANOVA of Constant  $n$**

<i>OneWay ANOVA Table</i>	Sum of Squares	Degrees of Freedom	Mean Squares	F-Ratio	p-Value
Between Variation	0.573668	29	0.019782	5.100559	< 0.0001
Within Variation	0.116350	30	0.003878		
Total Variation	0.690018	59			

The grand mean of the  $n$  value is 0.428. The sum of square computations gave SSA = 0.573668, SSE = 0.116350, and SST = 0.690018. From the critical values of the F-Distribution, the critical region with  $v_1 = k - 1 = 29$  and  $v_2 = k(n - 1) = 30$  at the significance level = 0.05 gave  $f_{0.05} = 1.84$ .

The decision for this ANOVA results is to reject the null hypothesis and conclude that the  $n$  values do not have the same mean ( $F - Ratio > f_{0.05}$ ).

In summary, the results of the ANOVA indicated that the values of the constants vary from one sample to another. Using the best estimate of the constants is considered appropriate to create an intensity map. Figure 5.34 shows the power law graph with constants  $k$  and  $n$ . Figure 5.35 shows an example of the intensity map of site 06-G field 16. The map shows odor intensities in referencing scale as n-butanol concentration with their impacted areas. The higher intensities imply higher perception. Even though, the intensity scale is not accounted for personal feeling, analysts can involve the intensity map for odor assessment as the best estimation for human perception.

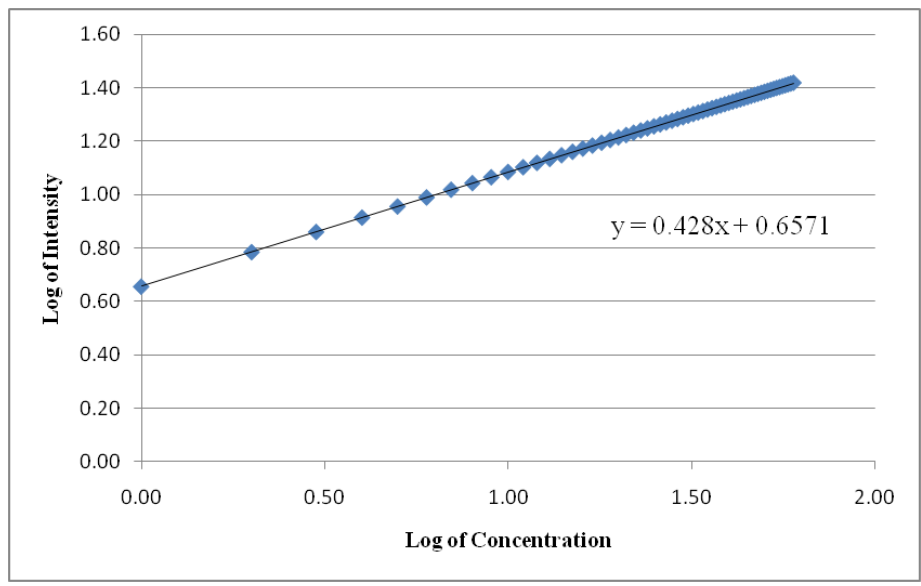


**Figure 5.34: Power Law Graph of Biosolids Odor**

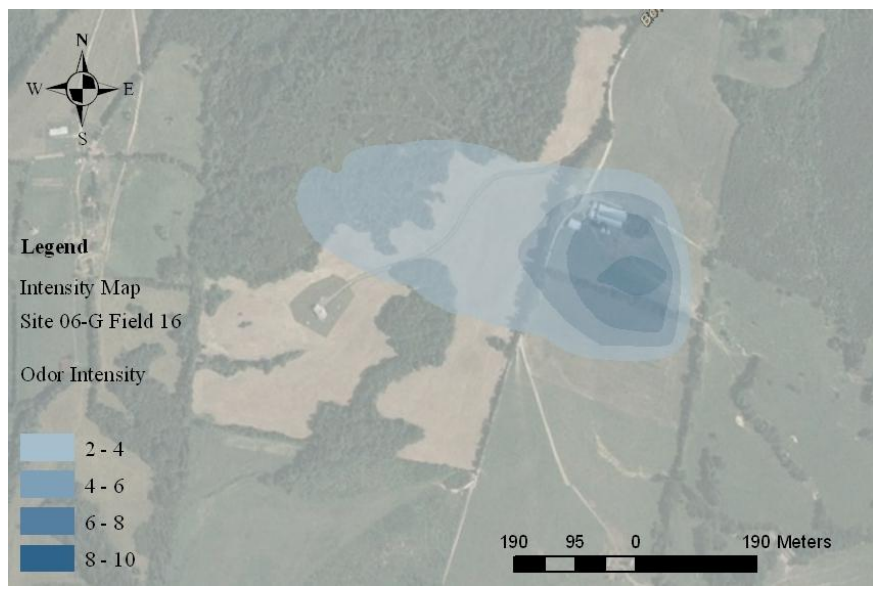


**Figure 5.35: Intensity Map (I-Map) for Field 16, Site 06-G**

The impact areas with expected numbers of population potentially exposed to biosolids odor at land application sites were estimated using the impact area model. The estimated impact area was multiplied by the population density of that particular

county to get expected numbers of population. Table 5.16 shows calculation for the 13 prediction maps. At Site 06-H field 3, for example, the expected numbers of population that could perceive biosolids odor from 2 D/T to 6 D/T are only 1 person.

Note that since the population density was used for the estimation, the expected population, which may be exposed to odor is only the best estimate. The estimates can be improved if population densities for different land-used areas were used. For example, population density for rural area is less than the population density of the county; the expected number of population exposed to odor will be less than the expected number estimated in Table 5.17. However, the expected number of population exposed to odor in Table 5.17 was generated based on the best available information on the population density. Thus, the implementation of this approach requires careful consideration.

**Table 5.17: Expected Number of Population Exposed to Odor**

<i>Site</i>	<i>Field</i>	<i>D/T</i>	<i>Estimated Impact Area (square meters, m<sup>2</sup>)</i>	<i>Population Density (per square miles)</i>	<i>Expected Number of Population</i>
05-C	7	0	969,553.6932	131.5	50
		2	30,400.5304	131.5	2
		8	974,427.3147	131.5	50
06-A	12	2	25,526.9089	131.5	1
		0	958,310.0100	131.5	49
		2	40957.568111	131.5	2
06-E	1	0	914275.429589	131.5	47
		2	70997.769644	131.5	4
		4	13994.378892	131.5	1
06-F	1	0	946,608.6197	131.5	49
		2	27,010.8639	131.5	1
		4	25,648.0945	131.5	1
06-G	15	0	936,128.1861	94	34
		2	32,445.5329	94	1
		4	30,693.8591	94	1

Site	Field	D/T	Estimated Impact Area (square meters, m <sup>2</sup> )	Population Density (per square miles)	Expected Number of Population
06-H	16	0	971,770.2293	94	36
		2	23,920.4065	94	1
		4	3,576.9423	94	0
	17	0	982,032.5253	94	36
		4	17,967.4747	94	1
	3	0	973,584.5387	94	36
		2	21,255.5048	94	1
		4	4,427.5346	94	0
	5	0	980,375.0104	94	36
2		19,304.5550	94	1	
4		4,427.5346	94	0	
06-J	3	0	706,194.1395	94	26
		2	293,805.8405	94	11
06-K	1	0	950,240.8354	131.5	49
		2	49,026.7427	131.5	3
		0	990,323.4801	131.5	51
		2	8,944.0980	131.5	0

#### 5.4.3 Validation with Data

Similar to the screening analysis, the results of predicted concentration for these case studies were validated with the MES odor measurement. The scatter plots of the predicted concentration and the measurement obtained by using the Nasal Ranger field olfactometer were provided in Figures 5.36-5.38. Basically, the maximum 3-minute predicted concentrations were plotted against the best estimate thresholds, 2, 5, and 10 Dilution-to-Thresholds (D/T). As in the case of the screening analysis, the measurement locations were also not exact, and the subjective judgment along with the MES data and the GIS were required to roughly locate the measurement locations.

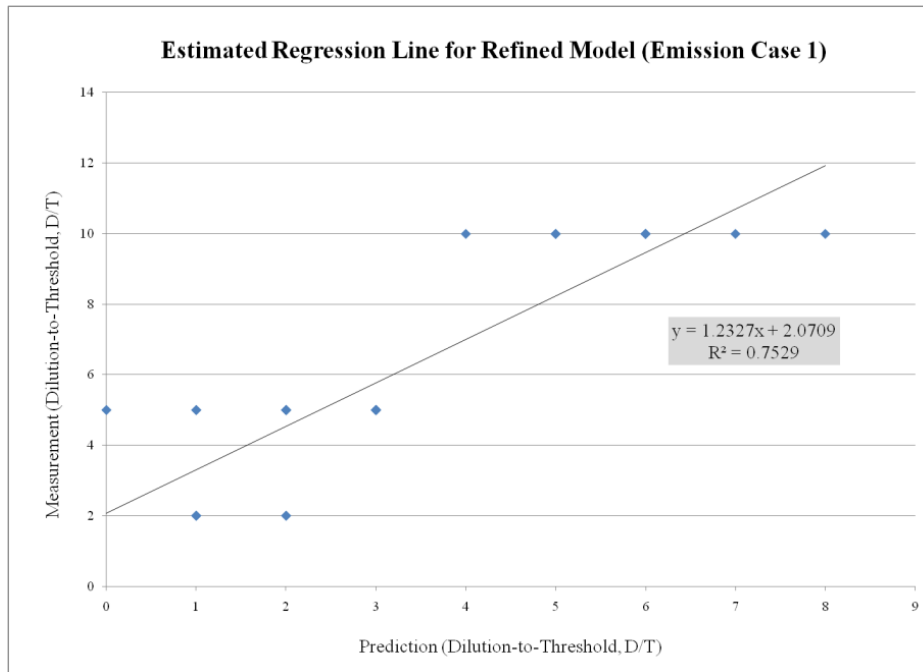


**Figure 5.36: Scatter Plot for Refined Analysis (Emission Case 1)**

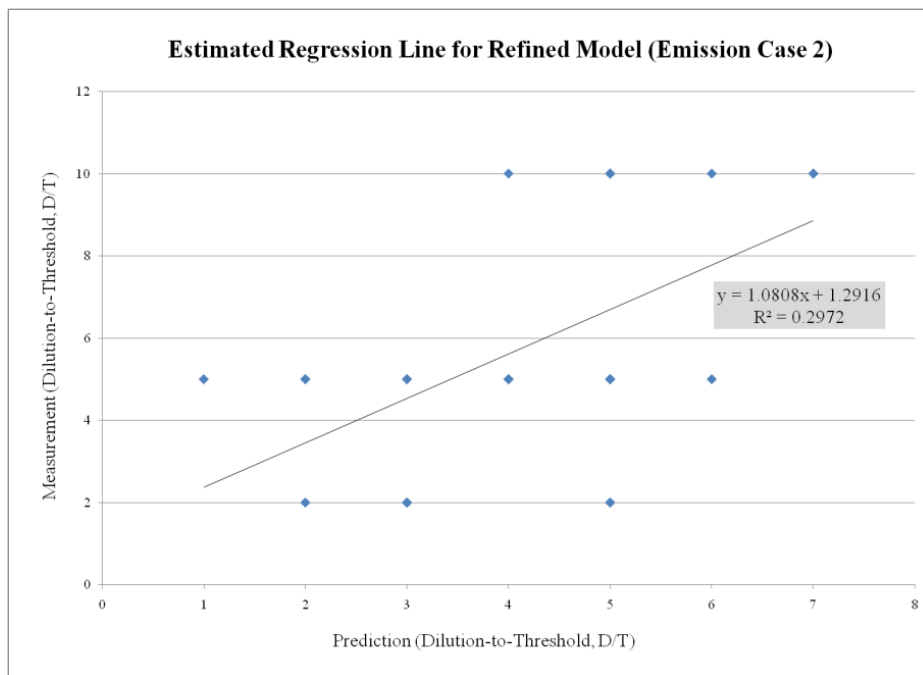


**Figure 5.37: Scatter Plot for Refined Analysis (Emission Case 2)**

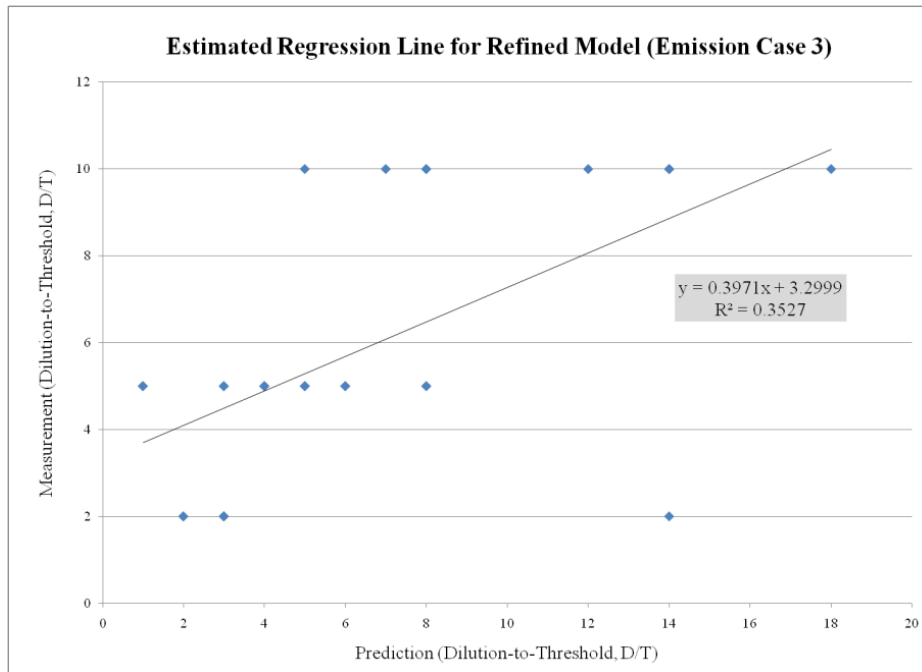


**Figure 5.38: Scatter Plot for Refined Analysis (Emission Case 3)**

Similar to the screening case, the standard error of estimate was used to measure the accuracy of model prediction. Table 5.18 shows standard error of estimate values for the three emission estimates. AERMOD outputs from emission case 2 by using statistical inference provides the best performance for model prediction.

**Table 5.18: Standard Error of Estimates for Refined Model Outputs**

Emission Case	Standard Error of Estimate ( $S_e$ )
1	3.3045
2	3.0854
3	3.7523

### 5.5 Comparing Screening and Refined Models

This study was conducted to investigate how well the screening analysis performed as compared to the refined model. It is a type of model validation technique when there are competing models. The competing models assume alternative hypotheses of the

system of interest (Cullen and Frey, 1999). A screening model simulates concentrations assuming worst-case meteorological conditions, and a refined model requires extensive inputs including full meteorological data and geography for prediction.

Both screening and refined models generate maximum one-hour concentration. However, in this case study, the conversion factor for shorter averaging time prediction was only applied to the refined model, AERMOD. It is because the screening models assume worst-case meteorological conditions; applying the conversion factor to the results from the screening models can lead to overestimation. Therefore, the testing hypothesis is that the results of one-hour concentration from screening models agree with the 3-minute averaging concentration results from refined models.

The regression analysis was performed to investigate how well the results from the Screen View agree with the results from the AERMOD. Figure 5.39 shows the scatter plot of the results from the two models. It can be noticed that the prediction of the Screen View models are overestimated compared with the results from the AERMOD.

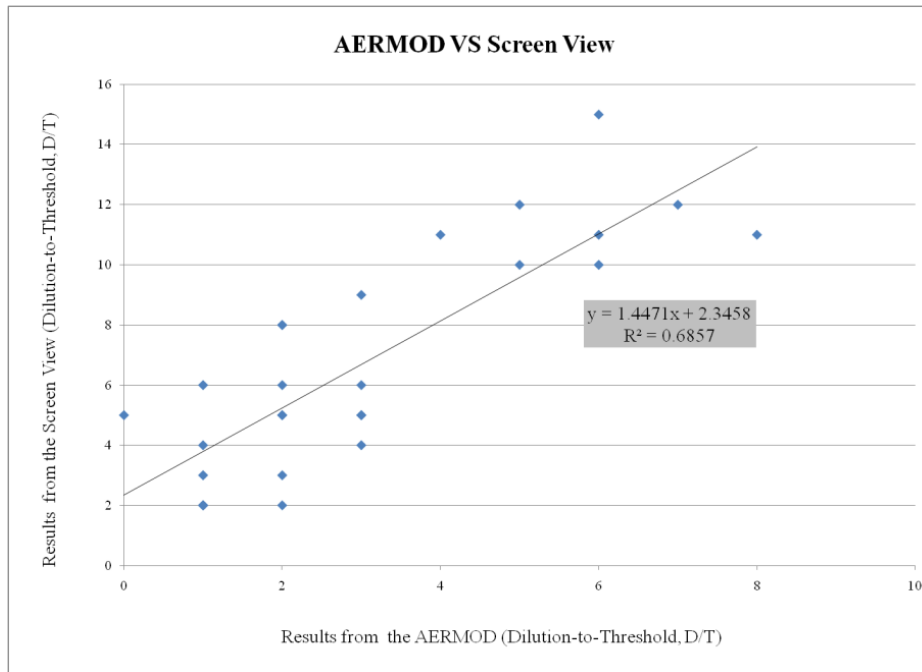


**Figure 5.39: Comparing Results from Screening and Refined Models**

The regression output in Table 5.19 shows that, at the significance level  $\alpha = 0.05$ , the regression coefficients are considered to be statistically significant. Thus, we can conclude that the linear relationship exists. In addition, the adjusted  $R^2$  is almost 0.7 indicating that the model has a 70 percent predictive performance.

**Table 5.19: Output of Regression Analysis for Comparing AERMOD and Screen View**

<i>Summary</i>	Multiple R	R-Square	Adjusted R-Square	StErr of Estimate		
	0.8281	0.6857	0.6732	2.118933616		
<i>ANOVA Table</i>	Degrees of Freedom	Sum of Squares	Mean of Squares	F-Ratio	p-Value	
Explained	1	244.9381934	244.9381934	54.5534	< 0.0001	
Unexplained	25	112.2469918	4.489879671			
<i>Regression Table</i>	Coefficient	Standard Error	t-Value	p-Value	Confidence Interval 95%	
Constant	2.345788474	0.721359625	3.2519	0.0033	0.860120516	3.831456432
Refined Models	1.447118429	0.195926495	7.3860	< 0.0001	1.043600259	1.8506366

## 5.6 Implementation

Wastewater treatment facilities that recycle biosolids through land can apply the approach used in this thesis to support biosolids site selection. Selection of biosolids land application sites is basically a decision problem. In addition, it is repetitive decisions with great uncertainty of outcomes or consequences. Those outcomes, which are downwind odor concentrations, human perception to the odor, and responses, are difficult to predict especially those associated with subjectivity. However, it is a responsibility and necessary for wastewater facilities to assess the possible outcomes from their biosolids recycling programs. However, wastewater treatment plants do not usually have systematic and comprehensive approaches to assess impacts from biosolids odor at land application sites. This research provides an approach called source-transport-perception approach to obtain information on biosolids emissions and potential odor impacts.

From the conceptual model for biosolids site selection shown in Figure 1.1, on a daily operational basis, there are decisions to make for distributing biosolids to land application fields, which can be considered alternatives ( $a_j$ ) for decision makers. The decisions on where we can apply biosolids to on a specific day are subjected to the main criterion( $Cr$ ): reducing adverse effects from biosolids such as negative public responses.

The logic for site selection is to find land application sites that are less likely to cause odor nuisance condition and odor annoyance to neighborhoods. Then one might raise a question such as “How do we know if this site is less likely to cause odor nuisance than others?” With no information of potential impact to population

available, such a question is hard to answer, and the selection of sites relies on subjective judgment.

Using the methodology described previously, we can obtain some information of potential impacts from biosolids odor at land application sites. With historical weather data, the AERMOD simulates one-hour averaging concentrations for biosolids odor in the dilution-to-threshold (D/T) of the following year. The preliminary schedule of biosolids distribution can be created regarding to the relative frequency of occurrence for D/T greater than 7, which is considered as a potential odor nuisance. Figure 5.40 provides an example of a distribution schedule for the whole year that serves as an initial assessment.

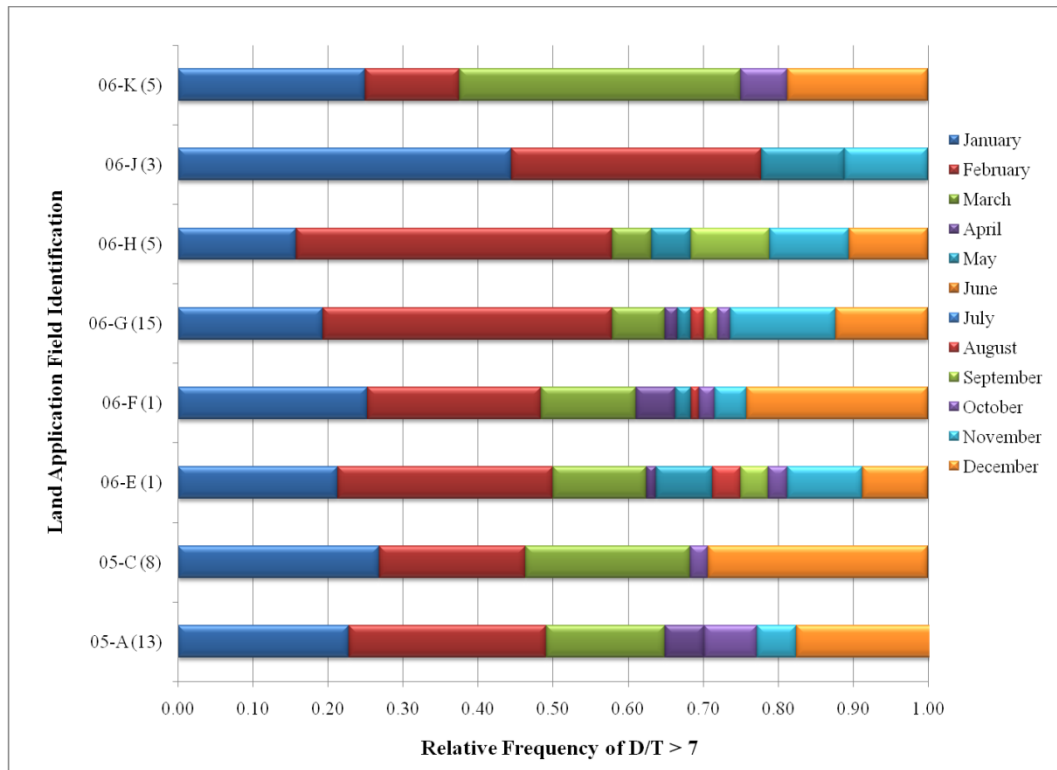


**Figure 5.40: Relative Frequency of D/T Greater Than 7 D/T**

The example assumes that we have eight candidate fields for the following year assuming with state permission and availability of field capacity. The stacked bar graph shows the annual frequencies for each field. In addition, the graph provides information on how often the potential nuisance conditions can occur for particular months. For example, field 06-J (3) has more potential odor nuisance for four months in the year: January, February, May, and November. It also implies that the distribution of biosolids to field 06-J (3) in other months is less likely to cause nuisance conditions, for example when comparing with distribution to field 06-G (15). However, the relative frequency does not mean that, in January, applying biosolids to the field 06-J (3) will promote nuisance condition than field 06-G (15). Further analysis for particular day or period should be conducted to obtain information on potential impacts to the candidate fields.

For example, decision makers might be interested to assess potential impacts for particular period such as from January 12 to 13. Using the historical weather data for this particular period, the predicted odor concentrations for the hypothetical receptors were generated from the AERMOD. The frequencies of D/T for each dilution categories can be obtained as shown in Table 5.20. The information we can extract from Table 5.20 is how often the odor concentrations fall into these dilution categories.

**Table 5.20: Frequency of D/Ts for January 12-13**

D/T	06-E (1)	06-G (15)	06-H (5)	06-J (3)
2	5	4	17	23
4	6	12	20	23
7	48	42	23	12
15	21	9	2	7
30	8	9	4	
60	2			
Total	90	76	66	65

Decision makers can use this information to assess potential odor nuisance if that field will be land-applied. Ranking based on the relative frequency of occurrence of D/T greater than 7 can be performed. The field 06-E (1) is considered to have more potential odor nuisance than other fields in this case, because there is higher frequency ( $79/90 = 0.88$ ) comparing to the others (06-G (15):  $60/76 = 0.79$ , 06-H (5):  $29/66 = 0.45$ , and 06-J (3):  $19/65 = 0.29$ ).

Furthermore, the methodology described in this thesis can also be used to select biosolids land application sites. The assessment of odor impact in term of the frequency of occurrence with a specified period can be performed. Ranking fields regarding to the frequency of occurrence may serve as a supporting tool for decision makers to reduce potential odor impact in the land application fields.

## Chapter 6: Conclusions and Future Works

### 6.1 Conclusions

This dissertation was conducted to study the impact of biosolids odor emissions at land application sites. More specifically, we focused on the three important parameters associated with the odor problem at the land application sites: source, dispersion, and possible odor impact to human. The land application sites from the Blue Plains advanced wastewater treatment plant, managed by the District of Columbia Water and Sewer Authority (DCWASA) were used as case studies.

First we found that emission rates were the crucial variable to assess the impact of the biosolids odor to nearby communities. However, the availability of information on odor emissions was limited. There were only nine emission data available from experiments at the land application sites in 2003 and 77 odor concentrations data as the dilution-to-thresholds (D/T) available from experiments in 2005. The probability distributions were developed to characterize the biosolids odor emissions at the fields and odor concentrations at the plant. Statistically, it can be described by the lognormal distribution.

An analysis of variance (ANOVA) was also employed to investigate the variation of odor emissions from day-to-day operations. The 14 emission samples were collected using the flux chamber method. The results from the ANOVA indicated that there were variations within the same field and from day-to-day operations. This implies that the estimate of emission needs to be updated regularly.

The study applied the U.S. Environmental Protection Agency (EPA)'s dispersion models to investigate odor dispersion in the land application sites. The

screening analysis using the Screen View was first applied to the MES field data in 2005 and 2006. The three different approaches used for estimating biosolids odor emissions at the fields were input into the screening analysis. The first approach was to use the expert opinion on the air flow rate to calculate odor emission rates. The second approach was to use the best estimate from the probability distribution. The simulated-flux chamber method was the other approach to estimate biosolids odor emissions at the field. The predicted odor concentrations for 45 fields were generated from the screening models.

Standard error of estimate ( $S_e$ ) indicated that the emission estimate using the assumed air flow rate provided the best modeling performance in this study by comparing with the MES data. The regression analysis seemed inappropriate to investigate the linear relationship because the prediction concentrations can be associated with ranges of the Nasal Ranger field olfactometer scales.

The refined dispersion model, AERMOD, was also applied to predict the odor concentrations at the hypothetical receptor locations. In addition, the geographic information system (GIS) was used to support visualizing, modeling, and mapping to the AERMOD. Due to limited availability of the meteorological data, only 27 cases were generated. By focusing on the areas that have the odor concentration greater than 2 D/T, the predicted concentration maps (C-Map) for 13 fields were created expressing the areas for odor strength. The probability maps (P-Map) for exceeding certain odor level, 7 dilution-to-thresholds in this case, were also generated. The 7 D/T was used as a criterion for potential odor complaints from neighborhoods.

Similar to the screening analysis, the results generated from the refined models were compared to the measurement. Results from  $S_e$  showed that the predicted concentration with odor emissions estimated by the probability distribution best described the modeling performance.

To assess the impact from biosolids odor, we proposed using two approaches to support the assessment. First, the intensity maps (I-Map), following Steven's power law, were created to estimate the human perception from the stimulus odor concentrations. The other approach was to estimate size of population potentially affected by the odor concentration levels. It was intended to assess the odor impact on the general population and not sensitive individuals. This approach requires calculating areas for each odor strength categories. The population density for the study areas was used as a mean to assess the potential odor impact at land application sites.

In summary, this study is an integration of many subjects including, statistics, environmental engineering, and the geographic information system (GIS) to solve a very complex problem of odor emission, dispersion, and perception at the land application sites.

## 6.2 Future Work

Future work should be first focused on the data that will be used in modeling: emission data, meteorological data, and odor data for model validation.

The emission data, which are considered one of the most important inputs in a dispersion model, should be obtained regularly. More specifically, a comprehensive study for characterizing odor emissions at the Blue Plains treatment facility, during

disposal, and after land application should be conducted to provide decision makers with information on biosolids odor emissions. More specially, the study will provide the information on how much odor is diluted from the Blue Plains to the land-applied biosolids. It will also help support assessment of odor impacts in the fields by providing information on emission rates that can be used in a dispersion model. An extension from Section 4.6 for the study of variation and uncertainty of odor emissions within the field and among fields should also be conducted. DCWASA may consider adding more resources such as people or devices to obtain emission data from various field locations. With information available, DCWASA can improve prediction of biosolids odor emission levels for future application.

DCWASA should consider an alternative if the meteorological data for particular periods are not available. As shown in the case studies in Section 5.4, modeling odor dispersion could not be performed with missing meteorological data. Numerical or simulation methods might be used when there is a lack of the meteorological data.

For validation purposes, information on measurement locations at land application fields should be recorded in coordinates. With more precise measurement location, validation of modeling results can be improved.

Second, with more emission data available, distributions of odor emission data can be developed. The distributions of that data can be incorporated to a dispersion model accounting for variation and uncertainty of emission rates. A stochastic dispersion model can be developed with an appropriate emission distribution.

Last, a Geographic Information System (GIS)-based system for biosolids odor management can be developed. The Maryland Environmental Services (MES) field odor data can be transferred into the GIS database. It will enhance visualization of the field data geographically and improve management of the data. Modeling odor dispersion can also be incorporated into the GIS to reduce modeling and analysis times when assessing odor impacts for candidate fields. With the Geoprocessing tool in the GIS all modeling steps can be automated.

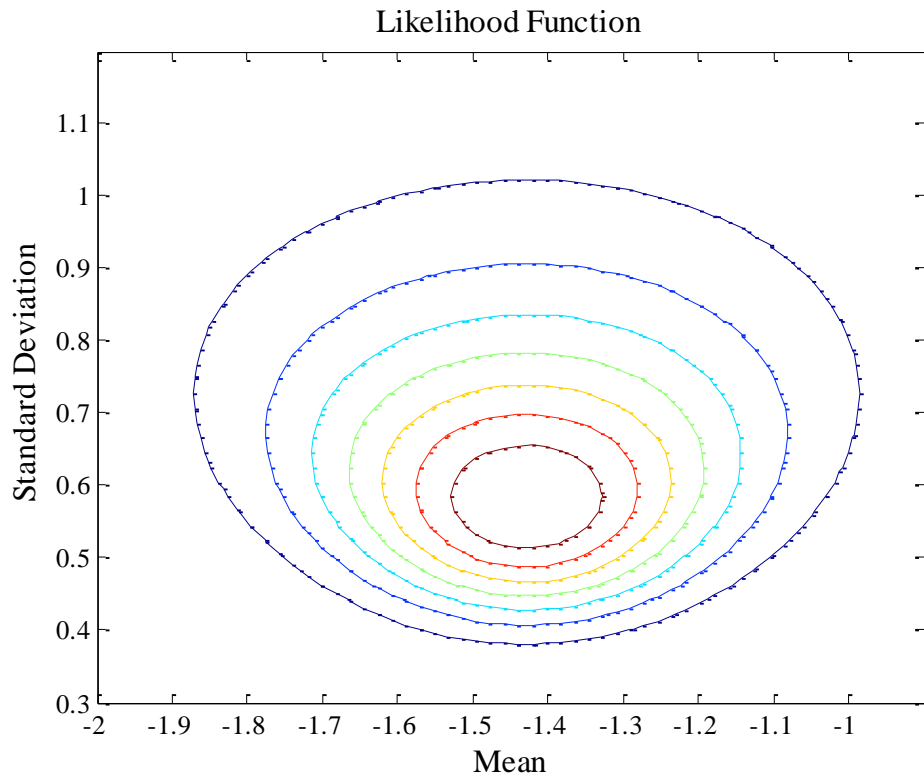
## Appendices

### A-1: Maryland Environmental Services (MES) Field Data

Date Unloaded	County	Site Name	Field Designation	Latitude	Longitude	D/T	Measurement Time
10/17/05	Albemarle	05-A	2	38.19685	-78.59137	4	10:45 AM
10/17/05	Albemarle	05-A	1	38.18975	-78.58676	4	4:45 PM
11/07/05	Albemarle	05-C	11	37.80588	-78.56181	4	9:10 AM
11/07/05	Albemarle	05-C	12	37.80854	-78.56109	4	1:00 PM
11/07/05	Albemarle	05-C	7A	37.81282	-78.55468	4	2:15 PM
11/07/05	Albemarle	05-C	8	37.81065	-78.55485	4	11:30 AM
11/08/05	Albemarle	05-C	14	37.80715	-78.56923	2	1:30 PM
11/08/05	Albemarle	05-C	3	37.81276	-78.55032	2	1:30 PM
11/08/05	Albemarle	05-C	7B	37.81224	-78.55414	2	1:30 PM
11/15/05	Albemarle	05-B	5	37.79162	-78.57089	7	4:00 PM
11/15/05	Albemarle	05-C	5	37.80403	-78.54683	7	1:00 PM
11/15/05	Albemarle	05-C	6	37.80980	-78.54206	7	10:30 AM
11/15/05	Albemarle	05-C	9	37.81463	-78.55995	7	9:00 AM
04/26/06	Orange	06-E	1	38.17723	-78.23468	7	2:00 PM
06/06/06	Orange	06-J	2	38.32127	-77.86198	2	12:00 PM
06/06/06	Orange	06-J	3	38.32100	-77.85588	4	8:45 AM
06/06/06	Albemarle	06-K	1A	37.98684	-78.66082	4	11:00 AM
06/06/06	Albemarle	06-K	5	37.98531	-78.65629	4	9:30 AM
06/06/06	Albemarle	06-K	6	37.98699	-78.66120	4	10:00 AM
06/07/06	Albemarle	06-D	5	38.18676	-78.54874	2	3:00 PM
06/07/06	Albemarle	06-K	1B	37.98684	-78.66082	2	3:00 PM
06/13/06	Albemarle	06-D	1A	38.18222	-78.54522	4	9:00 AM
06/13/06	Albemarle	06-D	1B	38.18200	-78.54579	4	10:00 AM
07/05/06	Albemarle	06-A	12	38.21259	-78.50910	4	3:00 PM
07/05/06	Albemarle	06-A	13	38.21211	-78.51360	4	10:10 AM
07/10/06	Albemarle	06-A	6	38.14063	-78.46726	4	9:00 AM
07/10/06	Albemarle	06-A	7	38.13718	-78.46747	4	10:00 AM
07/11/06	Albemarle	06-A	7	38.13718	-78.46747	4	2:00 PM
07/11/06	Orange	06-B	10	38.19494	-78.11783	4	3:00 PM
07/11/06	Orange	06-B	11	38.19390	-78.11440	4	10:45 AM
07/11/06	Orange	06-B	9	38.19092	-78.11761	4	2:15 PM
07/17/06	Orange	06-B	5	38.19854	-78.11854	2	10:00 AM
07/17/06	Albemarle	06-I	15	37.81288	-78.57368	4	10:00 AM
07/17/06	Albemarle	06-I	16	37.81155	-78.57401	4	12:00 PM

Date Unloaded	County	Site Name	Field Designation	Latitude	Longitude	D/T	Measurement Time
07/18/06	Orange	06-C	3	38.18506	-78.11551	4	3:30 PM
07/18/06	Orange	06-C	4	38.18790	-78.11651	4	10:00 AM
07/18/06	Albemarle	06-F	1	37.79082	-78.57555	7	9:30 AM
07/19/06	Orange	06-H	2	38.18808	-78.12317	2	2:00 PM
07/19/06	Orange	06-H	3	38.18532	-78.11725	7	9:00 AM
07/19/06	Orange	06-H	5	38.19617	-78.12122	7	11:00 AM
07/25/06	Albemarle	06-F	10	37.79664	-78.57384	4	11:00 AM
07/25/06	Albemarle	06-F	13	37.79849	-78.57549	4	10:00 AM
07/25/06	Orange	06-G	15	38.13267	-77.95741	7	2:00 PM
07/25/06	Orange	06-G	16	38.12973	-77.95852	7	11:00 AM
07/25/06	Orange	06-G	17	38.12856	-77.95493	7	9:00 AM

A-2: Verification of Global Maxima for Likelihood Function of Lognormal Distribution



### A-3: AERMOD Model Formulation

#### AERMET

##### a. Derived Parameters in the CBL

$$u_* = \frac{ku_{ref}}{\ln\left(\frac{z_{ref}}{z_0}\right) - \Psi_m\left\{\frac{z_{ref}}{L}\right\} + \Psi_m\left\{\frac{z_0}{L}\right\}}$$

when

$u_*$  - Friction velocity

$k$  - Von Karman constant

$u_{ref}$  - Wind speed at reference height

$z_{ref}$  - Lowest surface layer measurement height for wind

$z_0$  - Roughness length

$\Psi_m$  - Defined by Panofsky and Dutton (1984) for CBL and by Von Ulden and Holtslag (1985) for SBL

$L$  - Monin-Obukhov length

$$L = -\frac{\rho c_p T_{ref} u_*^3}{kgH}$$

when

$\rho$  - Density

$c_p$  - Specific heat at constant pressure

$T_{ref}$  - Ambient temperature in Kelvin that is representative of the surface layer

$H$  - Sensible heat flux

$g$  - the acceleration of gravity

$$w_* = \left( \frac{gH z_{ic}}{\rho c_p T_{ref}} \right)^{1/3}$$

when

$w_*$  - the convective velocity scale

$z_{ic}$  - the convective mixing height

$z_{im}$  - the mechanical mixing height =  $2300u_*^{3/2}$

$z_i$  -  $\max(z_{im}, z_{ic})$

b. Derived parameter in the SBL

$$\theta_* = - \frac{H}{\rho c_p u_*}$$

when

$\theta_*$  - the temperature scale

$$L = \frac{T_{ref}}{kg\theta_*} u_*^2$$

### Vertical Structure of the PBL

a. Wind speed

For  $z < 7z_0$

$$u\{z\} = u\{z = 7z_0\} \left( \frac{z}{7z_0} \right)$$

For  $7z_0 \leq z \leq z_i$

$$u\{z\} = \frac{u_*}{k} \left[ \ln \left( \frac{z}{z_0} \right) - \Psi_m \left\{ \frac{z}{L} \right\} + \Psi_m \left\{ \frac{z_0}{L} \right\} \right]$$

For  $z > z_i$

$$u\{z\} = u\{z = z_i\}$$

$7z_0$  - approximate height of roughness elements

b. Potential temperature gradient

In the convective boundary layer (CBL),  $\frac{\partial \theta}{\partial z} = 0$

In the stable boundary layer (SBL) for the first 100 meters

For  $z \leq 2 \text{ m}$

$$\frac{\partial \theta}{\partial z} = \frac{\theta_*}{k(2)} \left[ 1 + 5 \frac{(z = 2)}{L} \right]$$

For  $2 \text{ m} \leq z \leq 100 \text{ m}$

$$\frac{\partial \theta}{\partial z} = \frac{\theta_*}{kz} \left[ 1 + 5 \frac{(z)}{L} \right]$$

In the stable boundary layer (SBL) above 100 meters

$$\frac{\partial \theta}{\partial z} = \frac{\partial \theta\{z_{mx}\}}{\partial z} \exp \left[ - \frac{(z - z_{mx})}{0.44z_{i\theta}} \right]$$

$z_{mx}$  - 100 meters

$z_{i\theta} = \max(z_{im}, 100 \text{ m})$

c. Vertical turbulence

In the convective boundary layer (CBL),

$$\sigma_{wT}^2 = \sigma_{wc}^2 + \sigma_{wm}^2$$

$\sigma_{wT}^2$  - Total vertical turbulence

$\sigma_{wc}^2$  - the convective portion of the total variance

For  $z \leq 0.1z_{ic}$

$$\sigma_{wc}^2 = 1.6 \left( \frac{z}{z_{ic}} \right)^{2/3} w_*^2$$

For  $0.1z_{ic} < z \leq z_{ic}$

$$\sigma_{wc}^2 = 0.35w_*^2$$

For  $z > z_{ic}$

$$\sigma_{wc}^2 = 0.35w_*^2 \exp \left[ -\frac{6(z-z_{ic})}{z_{ic}} \right]$$

$\sigma_{wm}^2$  – the mechanical turbulence

$$\sigma_{wm}^2 = \sigma_{wml}^2 + \sigma_{wmr}^2$$

$\sigma_{wml}^2$  – the current boundary layer

For  $z < z_i$

$$\sigma_{wml} = 1.3u_* \left( 1 - \frac{z}{z_i} \right)^{1/2}$$

For  $z \geq z_i$

$$\sigma_{wml} = 0$$

$\sigma_{wmr}^2$  - pervious day's boundary layer

At  $z = 0$

$$\sigma_{wmr} = 1.3u_*$$

For  $z > z_i$

$$\sigma_{wmr} = 0.02u\{z_i\}$$

In the stable boundary condition (SBL),  $\sigma_{wT} = \sigma_{wm}$

d. Lateral turbulence

In the convective boundary condition (CBL)

$$\sigma_{vT}^2 = \sigma_{vc}^2 + \sigma_{vm}^2$$

$$\sigma_{vc}^2 = 0.35w_*^2$$

For  $z \leq z_{im}$

$$\sigma_{vm}^2 = \left( \frac{\sigma_{vm}^2 \{z_{im}\} - \sigma_{vo}^2}{z_{im}} \right) z + \sigma_{vo}^2$$

For  $z > z_{im}$

$$\sigma_{vm}^2 = \sigma_{vm}^2 \{z_{im}\}$$

where

$$\sigma_{vm}^2 \{z_{im}\} = \min(\sigma_{vo}^2, 0.25 \frac{m^2}{s^2})$$

$$\sigma_{vo}^2 = 3.6u_*^2$$

In the stable boundary layer (SBL),  $\sigma_{vT}^2 = \sigma_{vm}^2$

### AEMOD Concentration Predictions

$$C_s \{z_r, y_r, z\} = \frac{Q}{\sqrt{2\pi}\tilde{u}\sigma_{zs}} F_y \times \sum_{m=-\infty}^{\infty} \left\langle \exp \left[ -\frac{(z - h_{es} - 2mz_{ieff})^2}{2\sigma_{zs}^2} \right] + \exp \left[ -\frac{(z + h_{es} + 2mz_{ieff})^2}{2\sigma_{zs}^2} \right] \right\rangle$$

$\tilde{u}$  - wind speed

$\sigma_{zs}$  - Total vertical dispersion

$z_{ieff}$  - Effective mechanical mixing height

$h_{es}$  - plume height

$F_y$  - Lateral distribution function

$$F_y = \frac{1}{\sqrt{2\pi}\sigma_y} \exp\left(\frac{-y^2}{2\sigma_y^2}\right)$$
$$\sigma_y = \left(\frac{\tilde{\sigma}_v x}{\tilde{u}}\right) / \left(1 + \frac{x/\tilde{u}}{2T_{Ly}}\right)^p$$

where

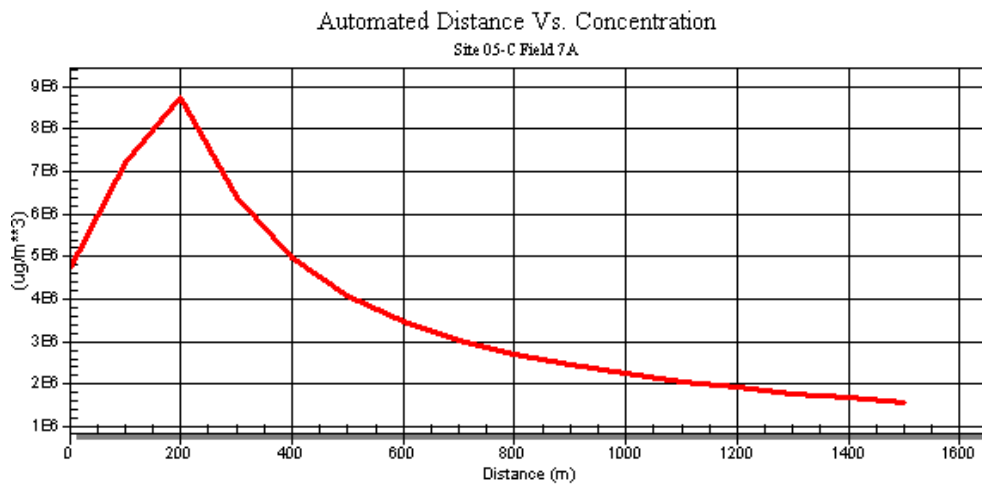
$$p = 0.5$$

$\tilde{u}$  - the wind speed

$\tilde{\sigma}_v$  - Lateral turbulence velocity

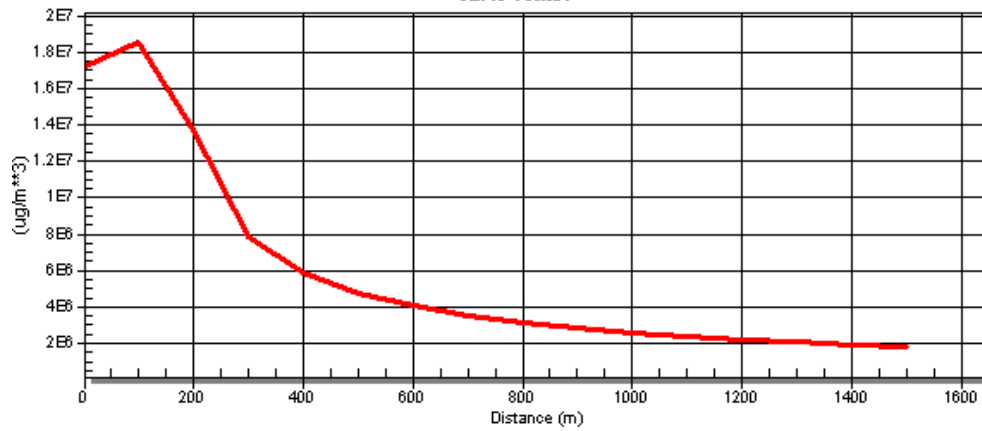
$T_{Ly}$  - Lagrangian integral time scale

### A-5: Screening Model Outputs



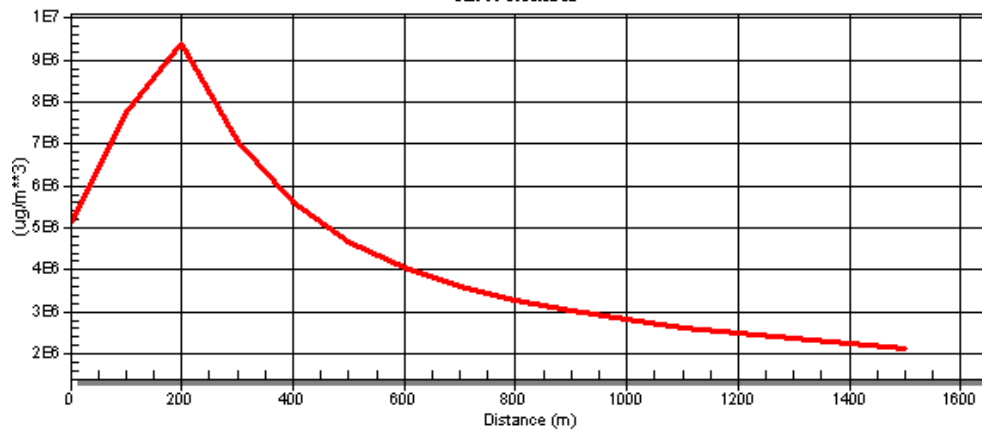
Automated Distance Vs. Concentration

Site 05-C Field 8



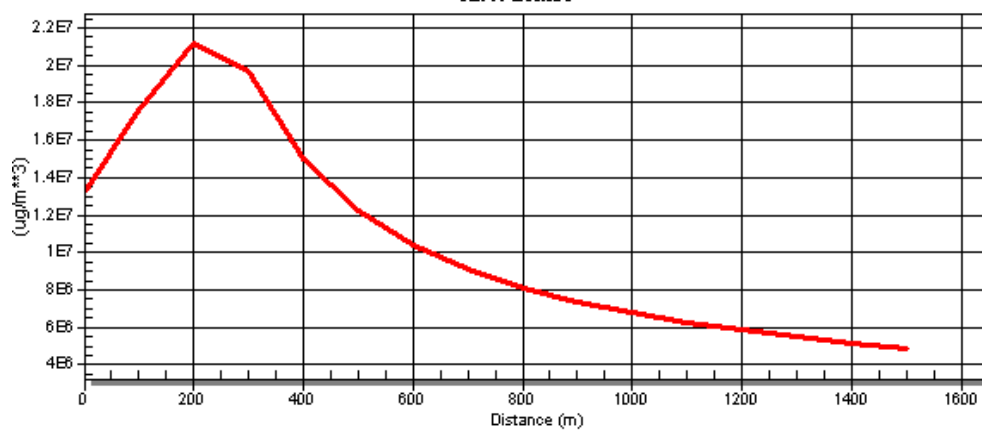
Automated Distance Vs. Concentration

Site 06-A Field 12

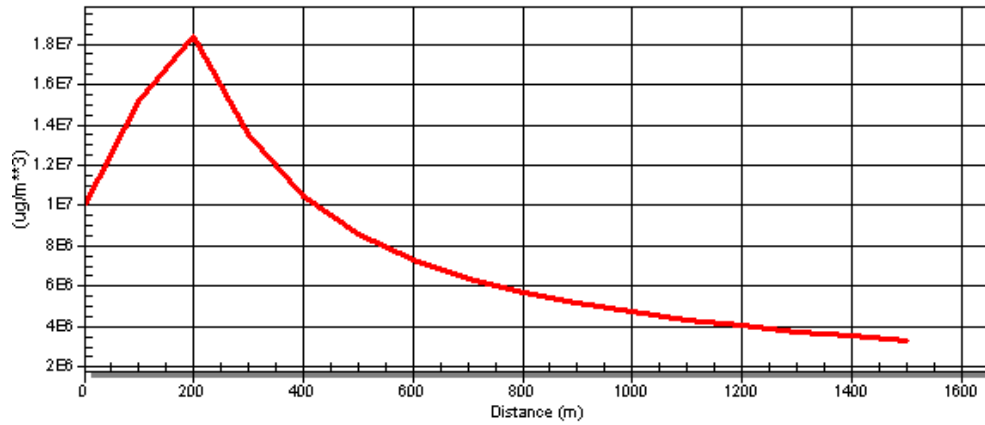


Automated Distance Vs. Concentration

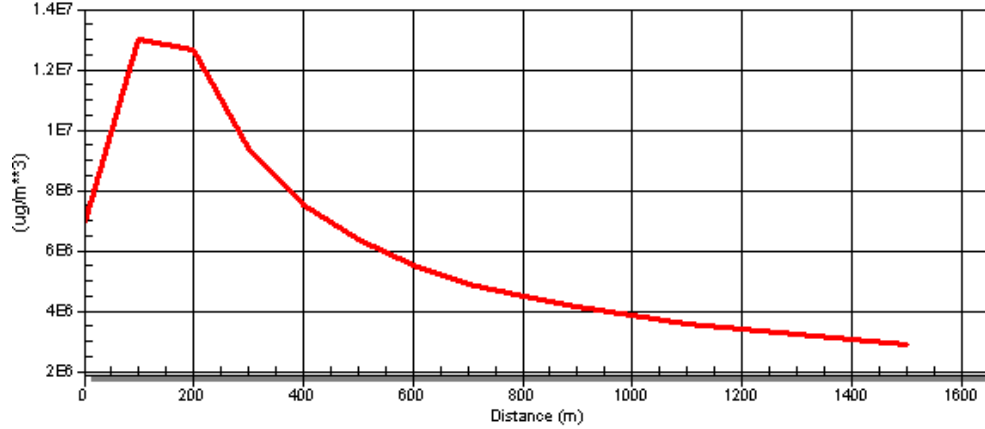
Site 06-E Field 1



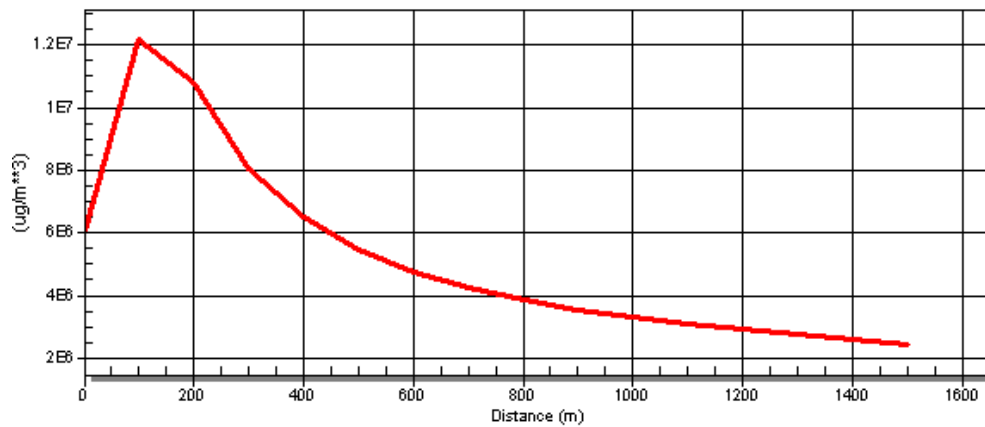
Automated Distance Vs. Concentration  
Site 06-F Field 1



Automated Distance Vs. Concentration  
Site 06-G Field 15

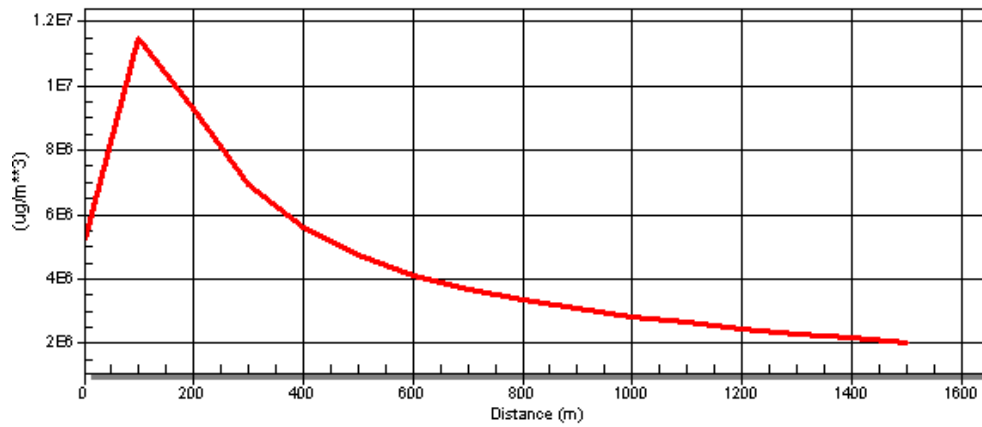


Automated Distance Vs. Concentration  
Site 06-G Field 16



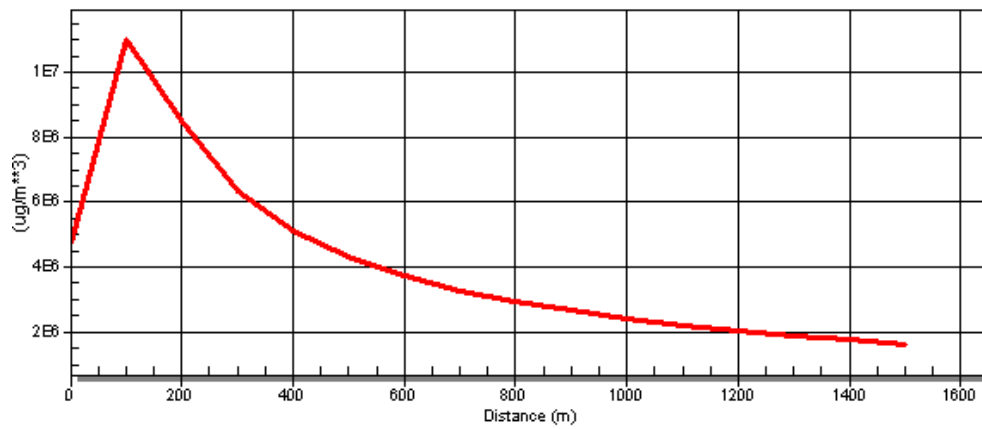
Automated Distance Vs. Concentration

Site 06-G Field 17



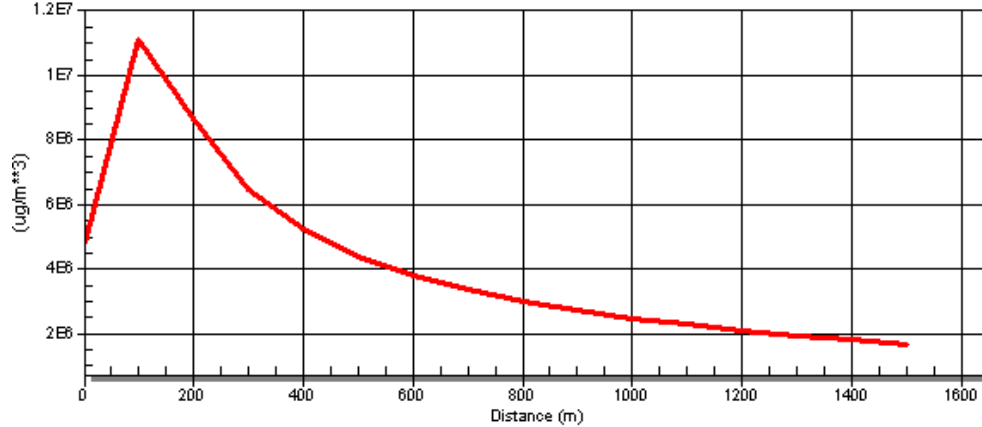
Automated Distance Vs. Concentration

Site 06-H Field 3



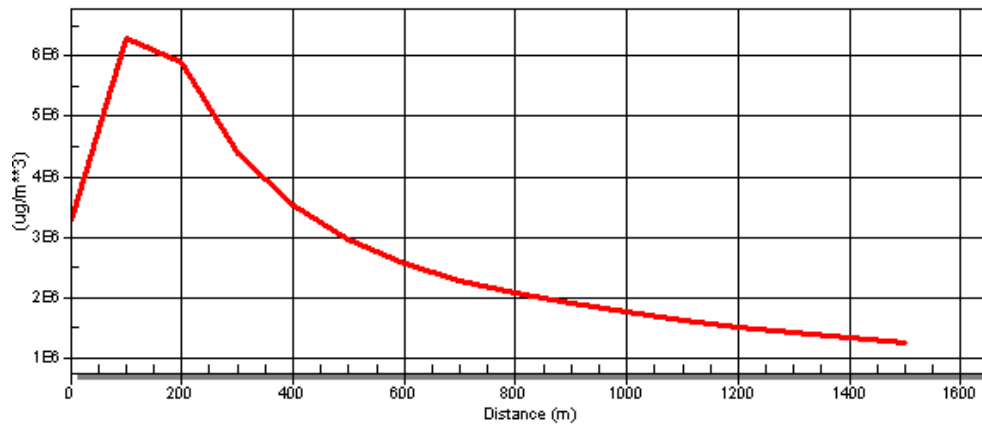
Automated Distance Vs. Concentration

Site 06-H Field 5



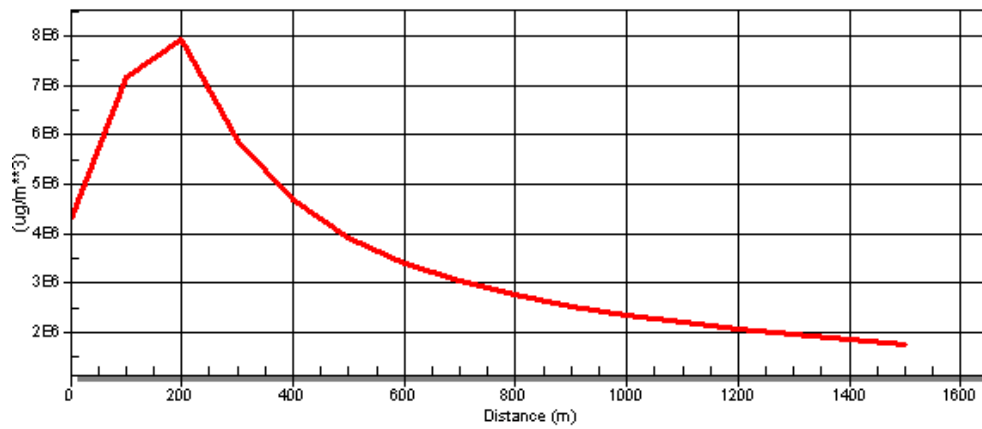
Automated Distance Vs. Concentration

Site 06-J Field 3



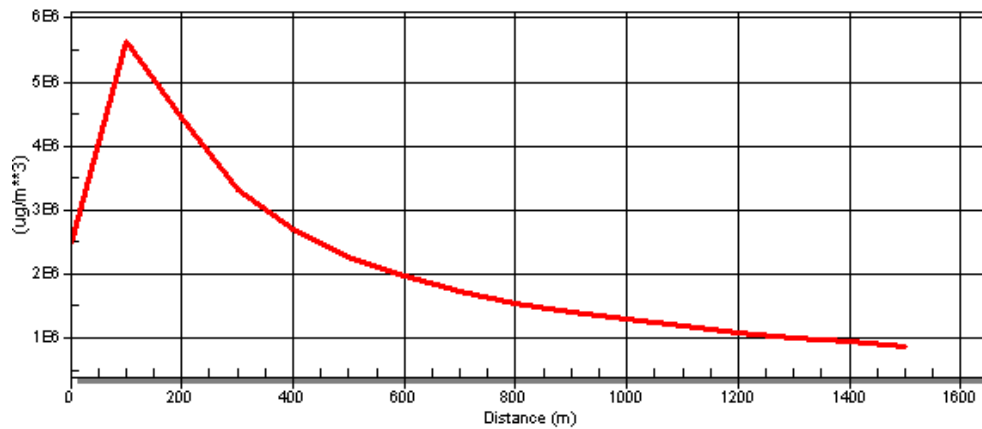
Automated Distance Vs. Concentration

Site 06-K Field 1A

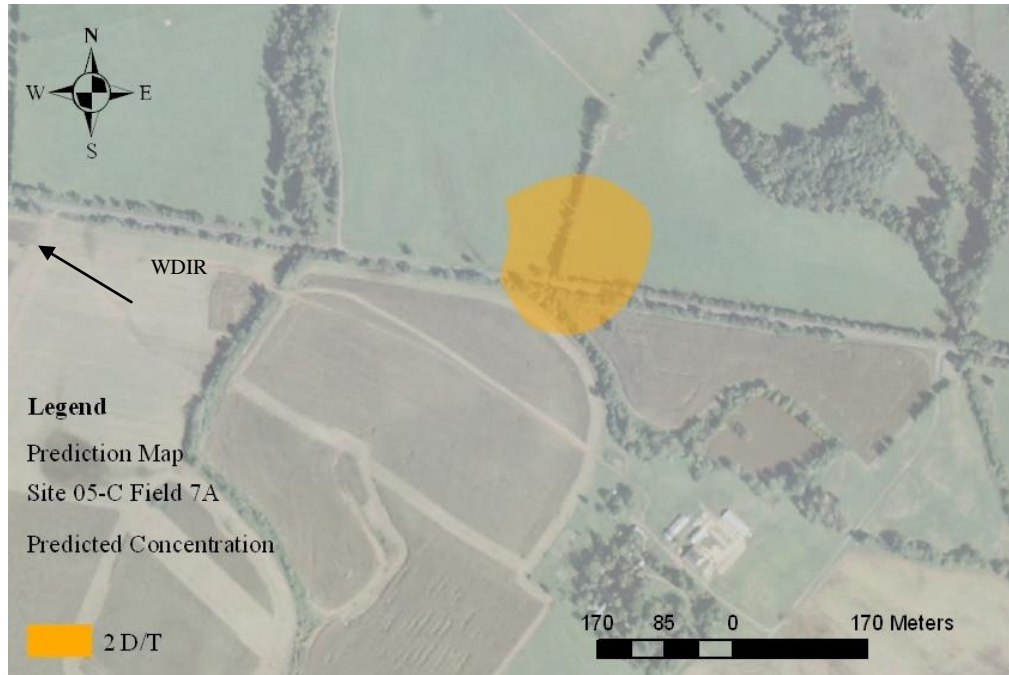


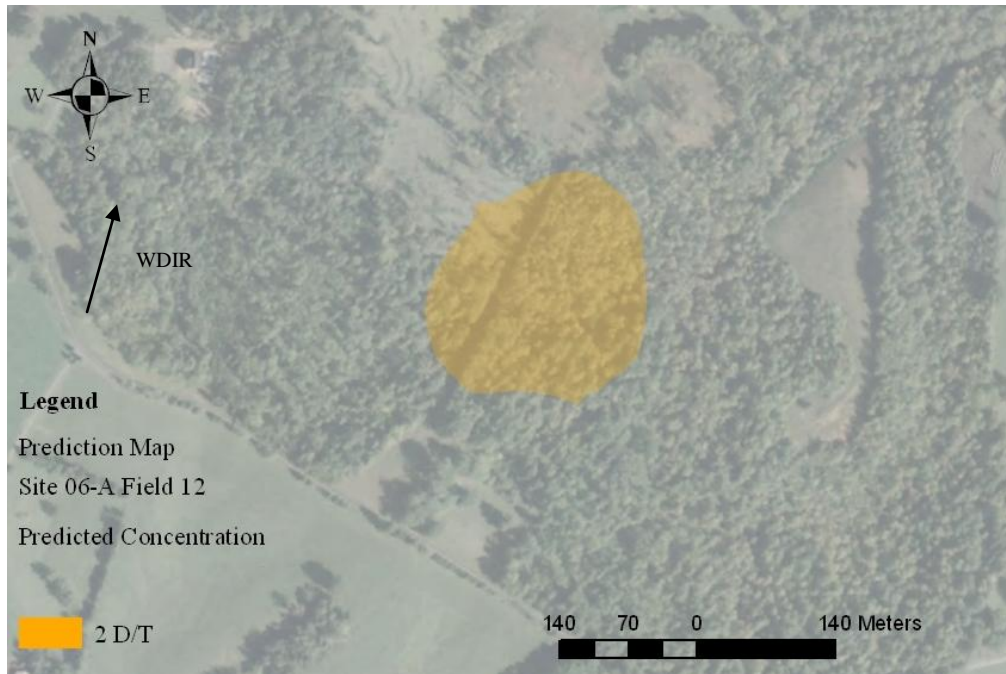
Automated Distance Vs. Concentration

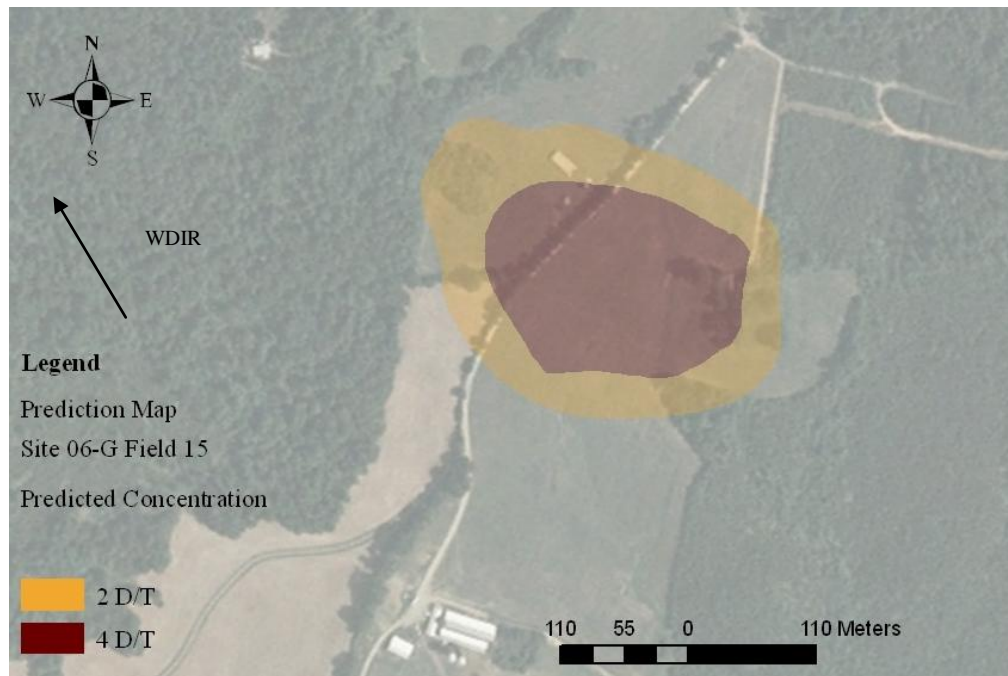
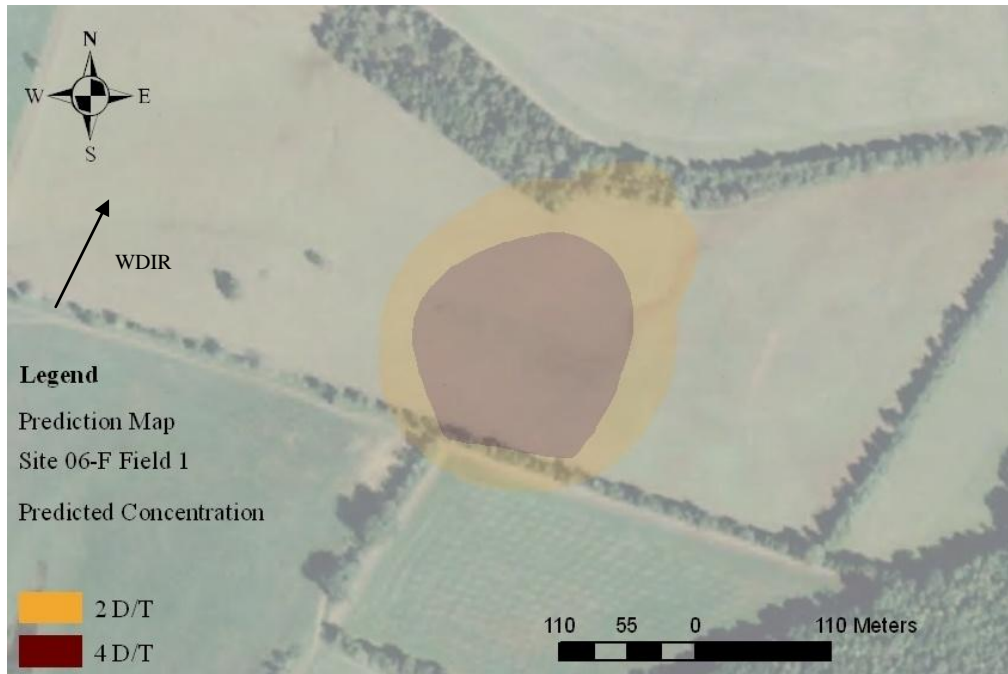
Site 06-K Field 5

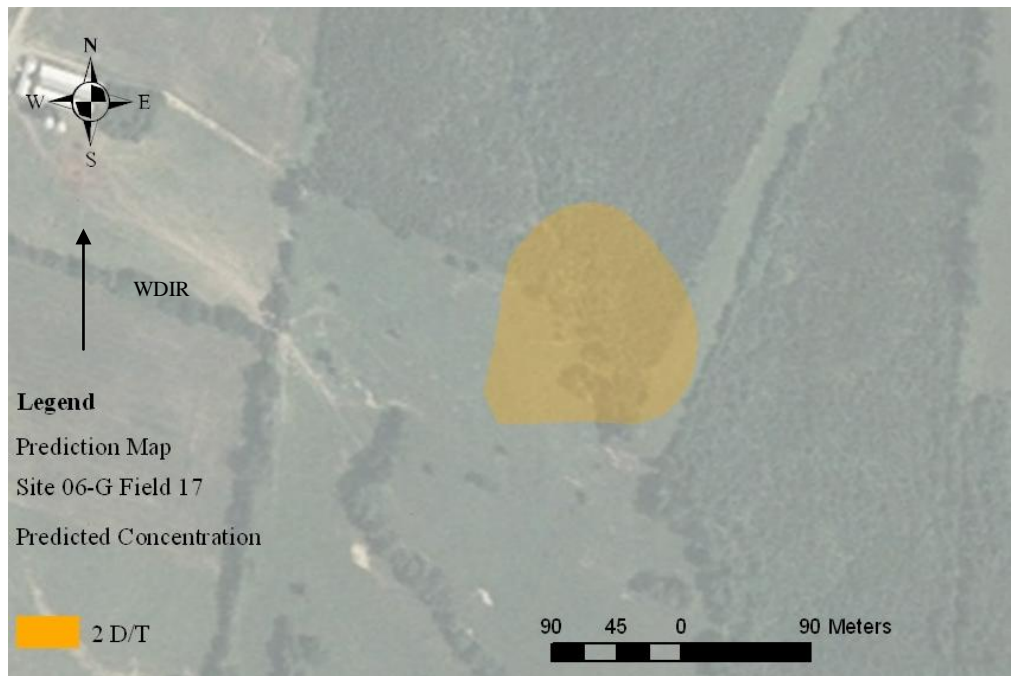
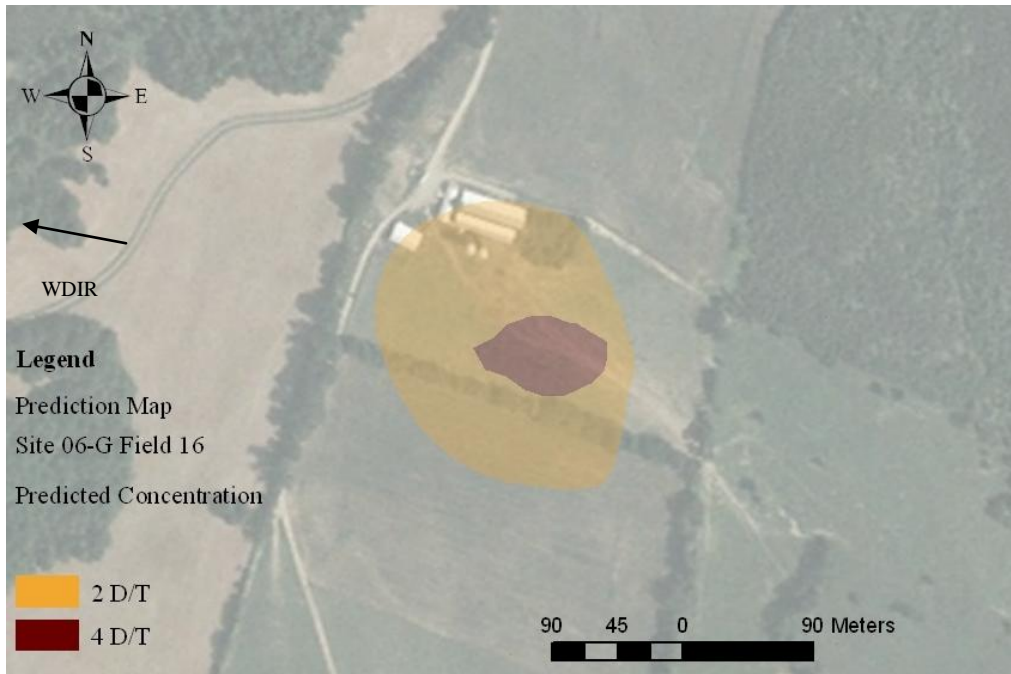


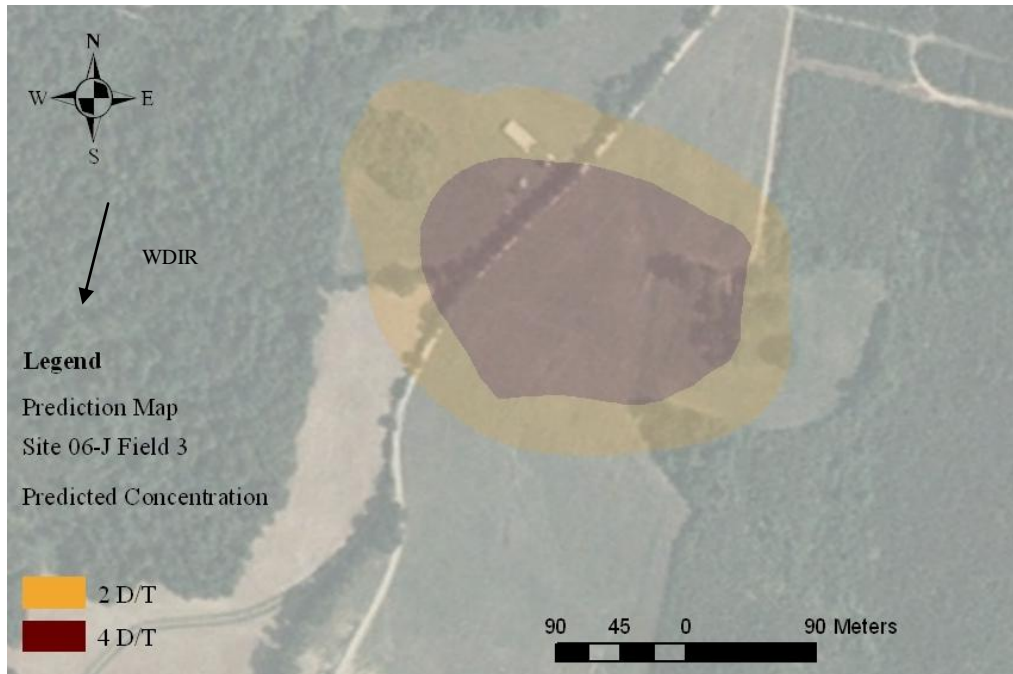
A-6: Concentration Prediction Maps





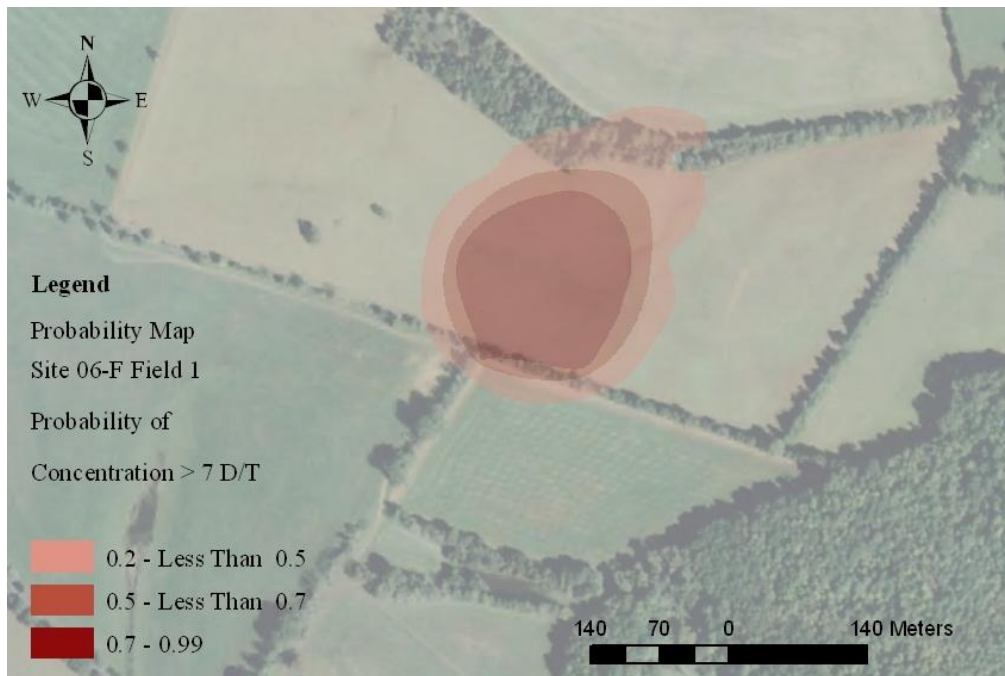
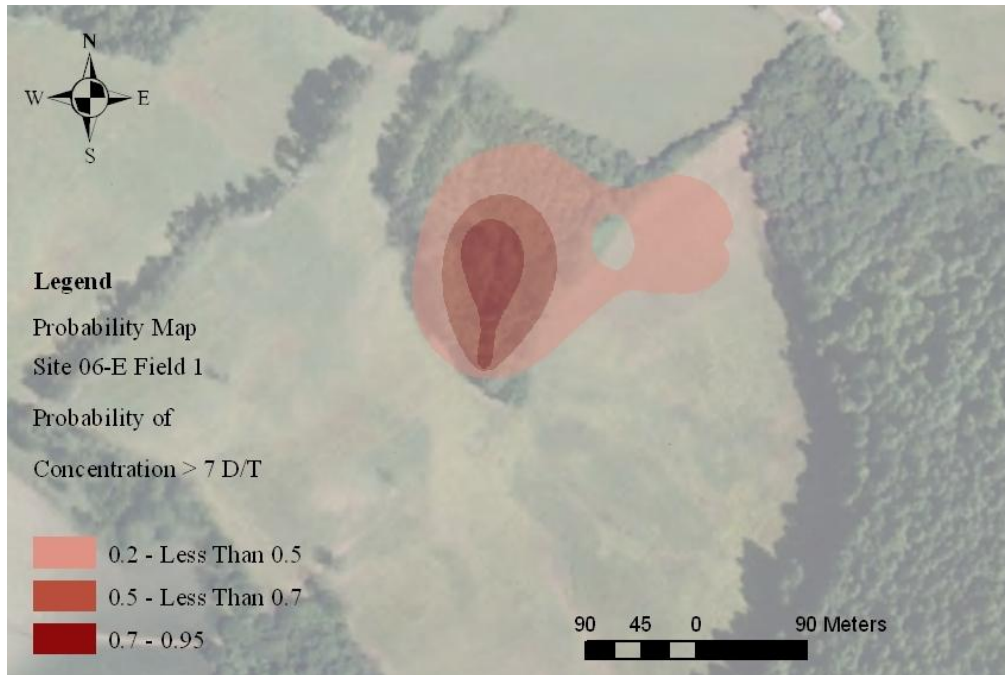


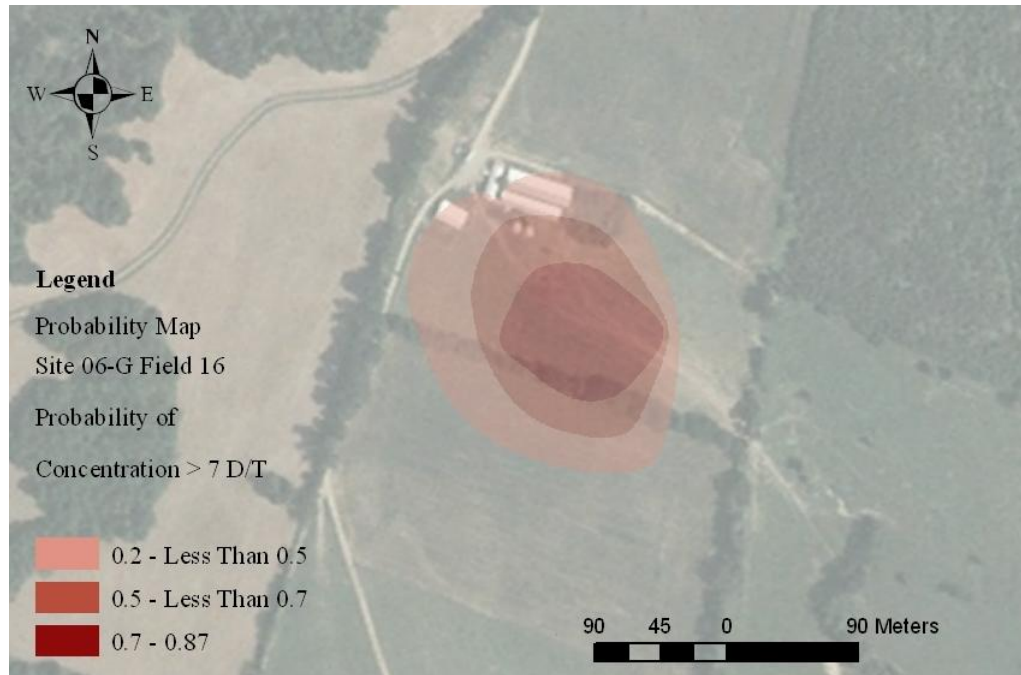
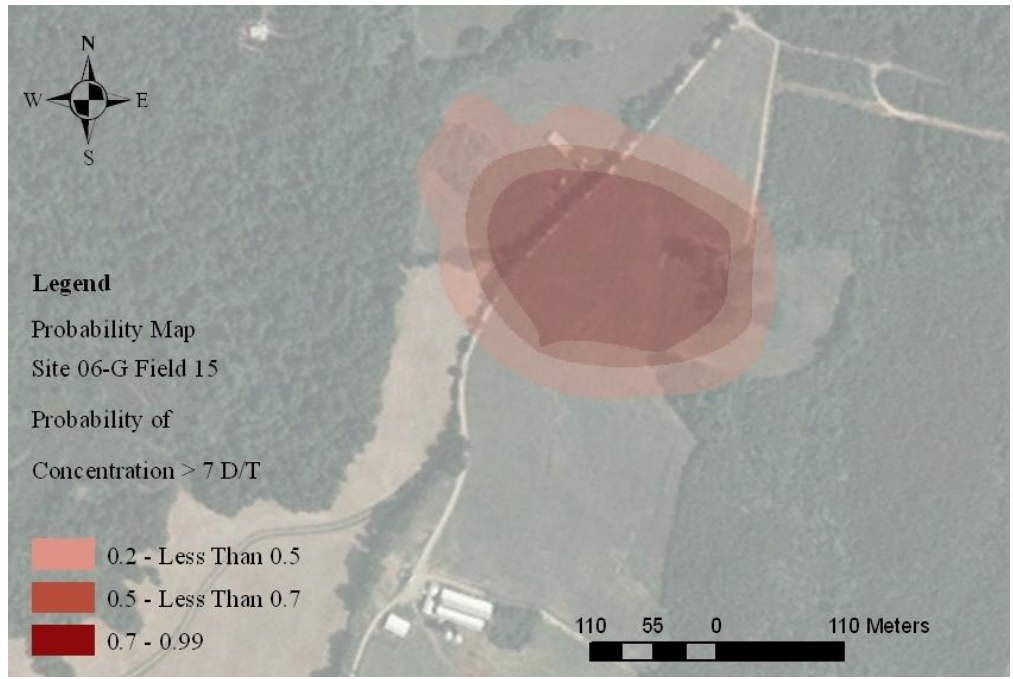


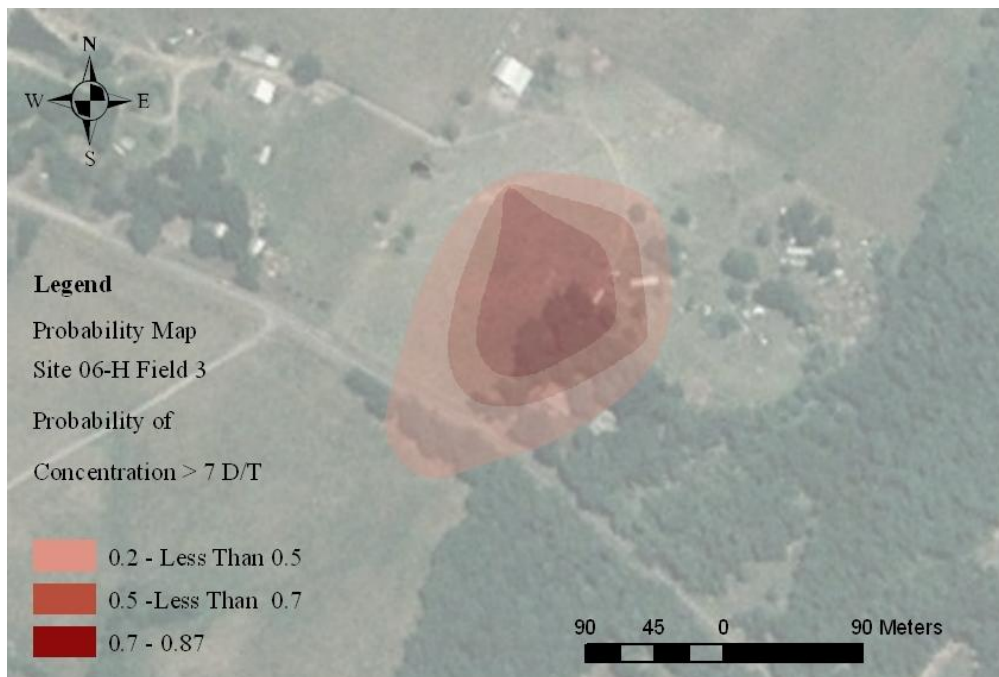
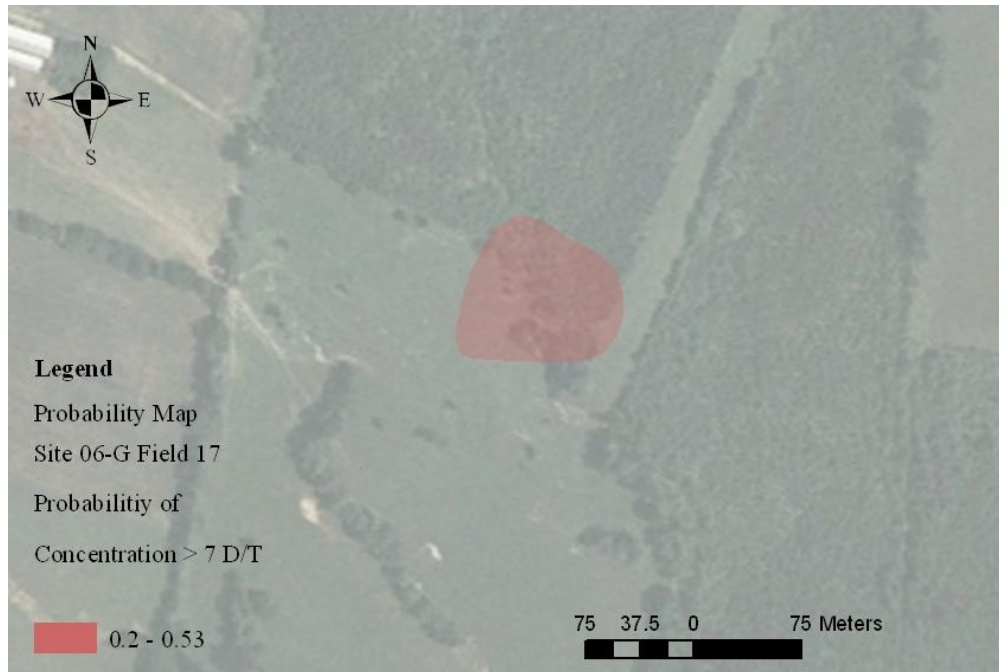


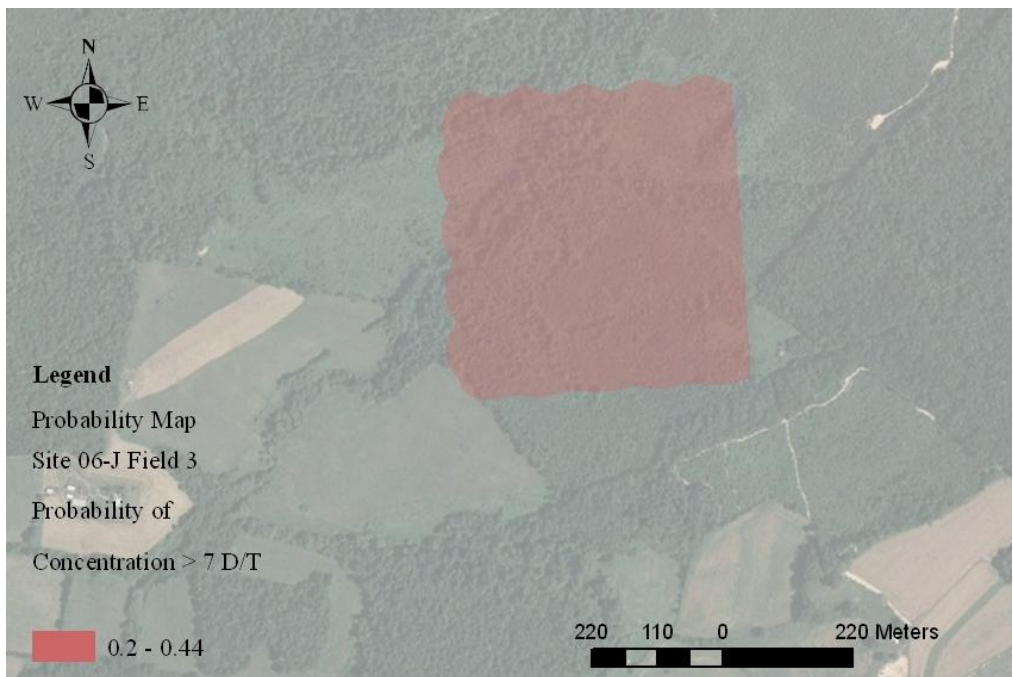
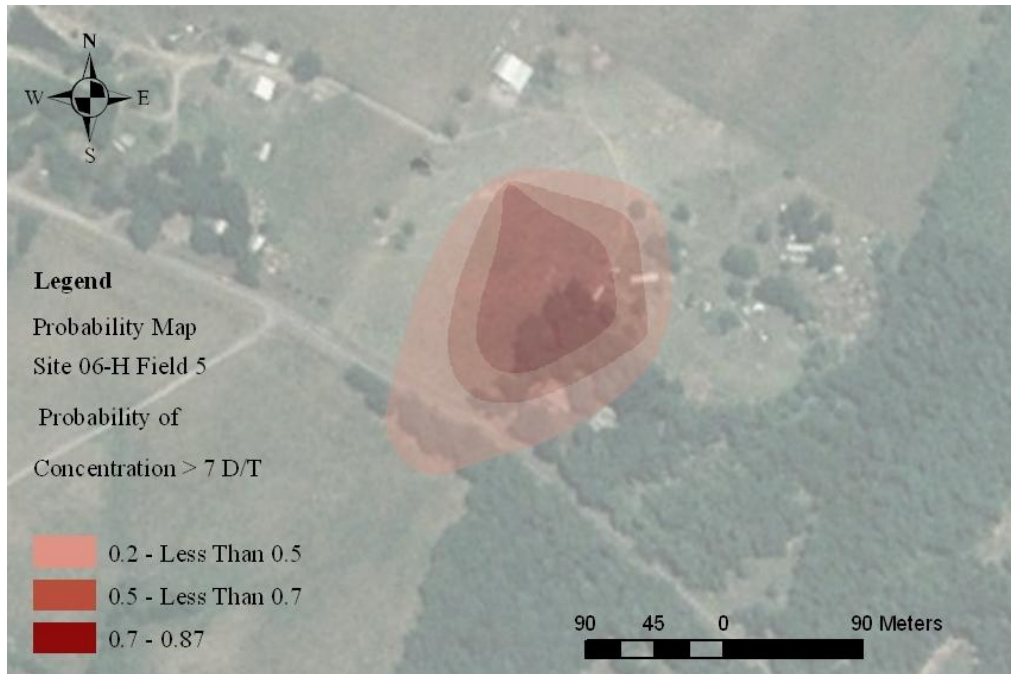


### A-7: Probability Map

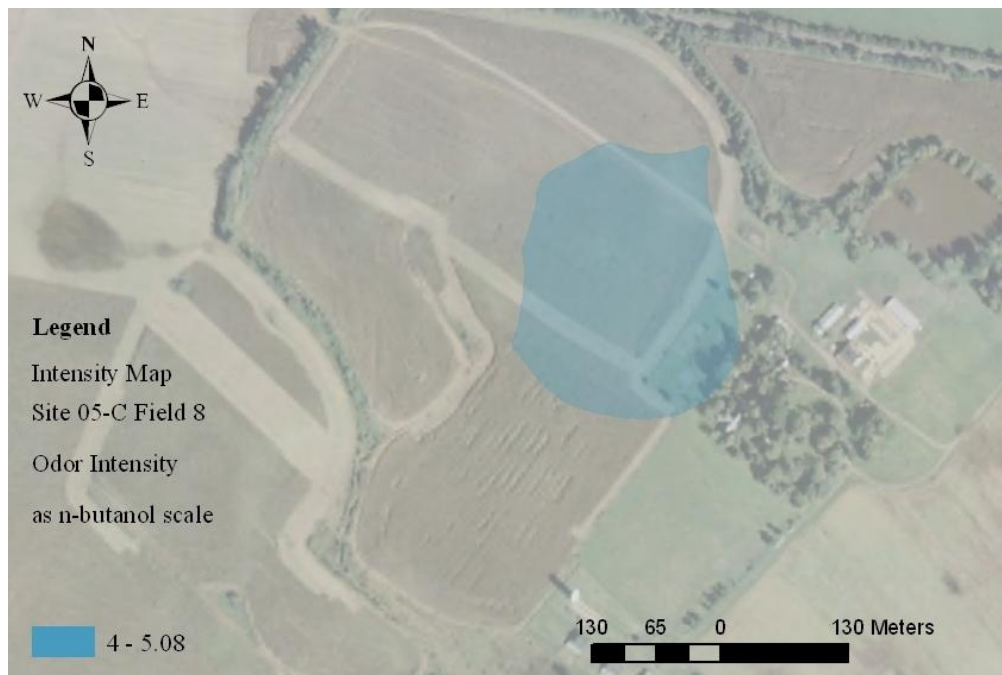
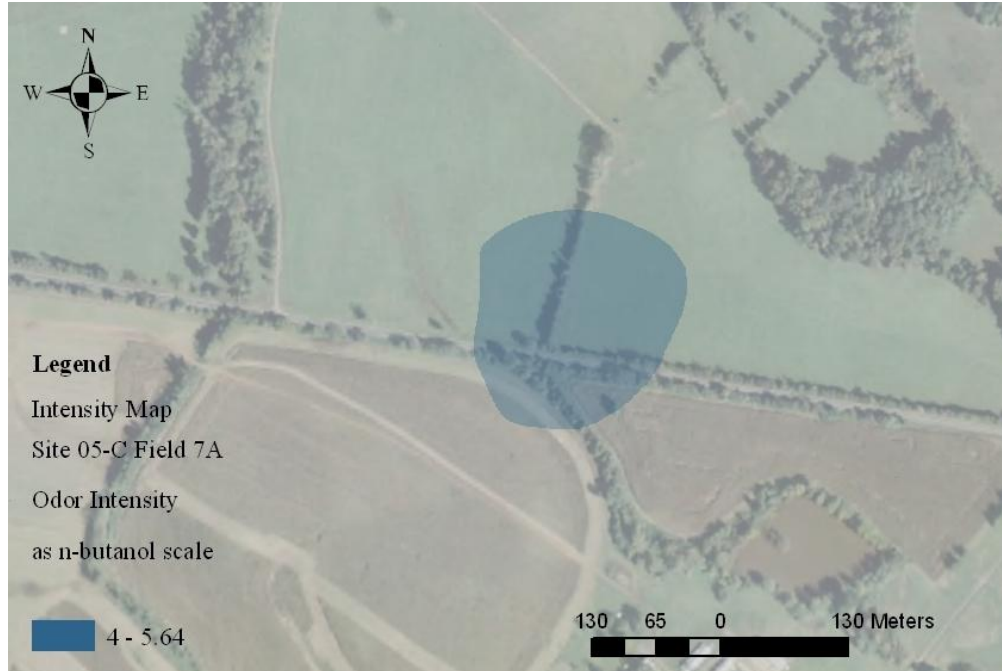


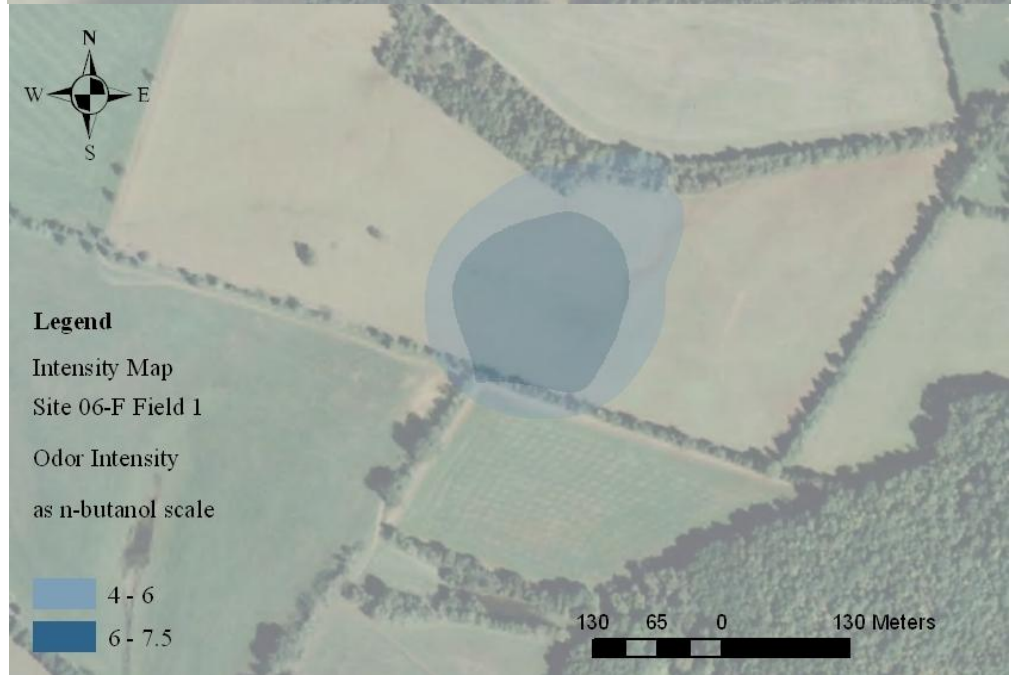
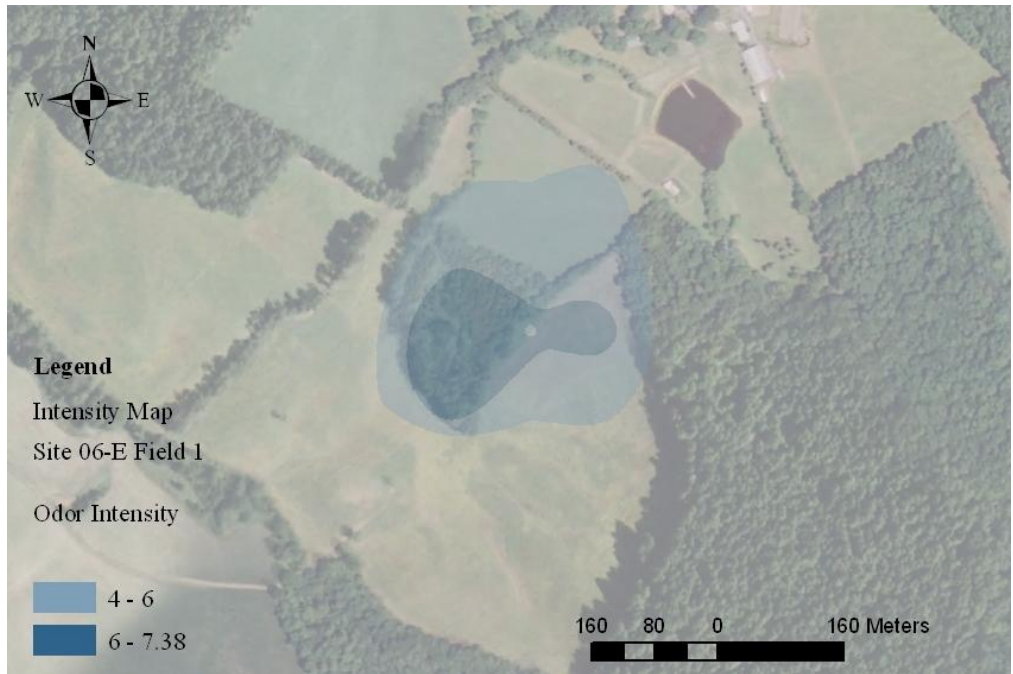


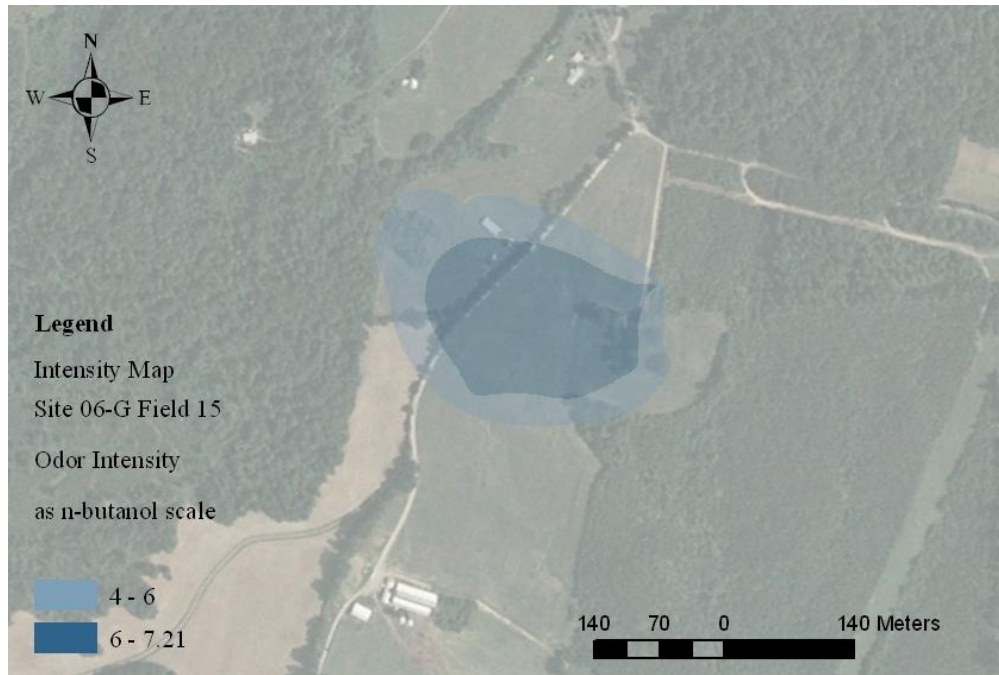


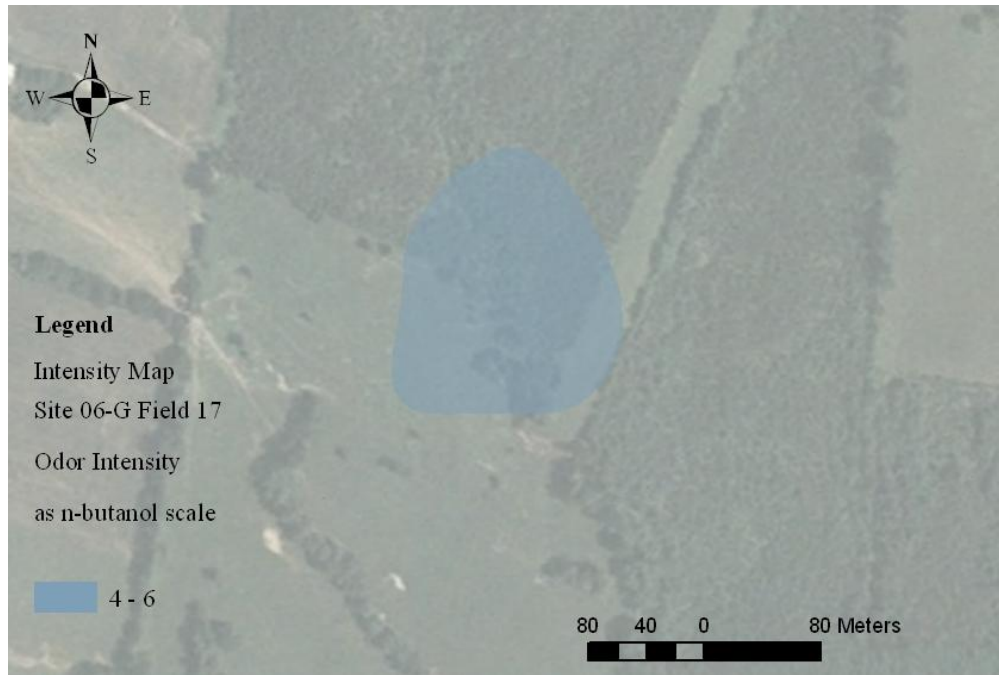


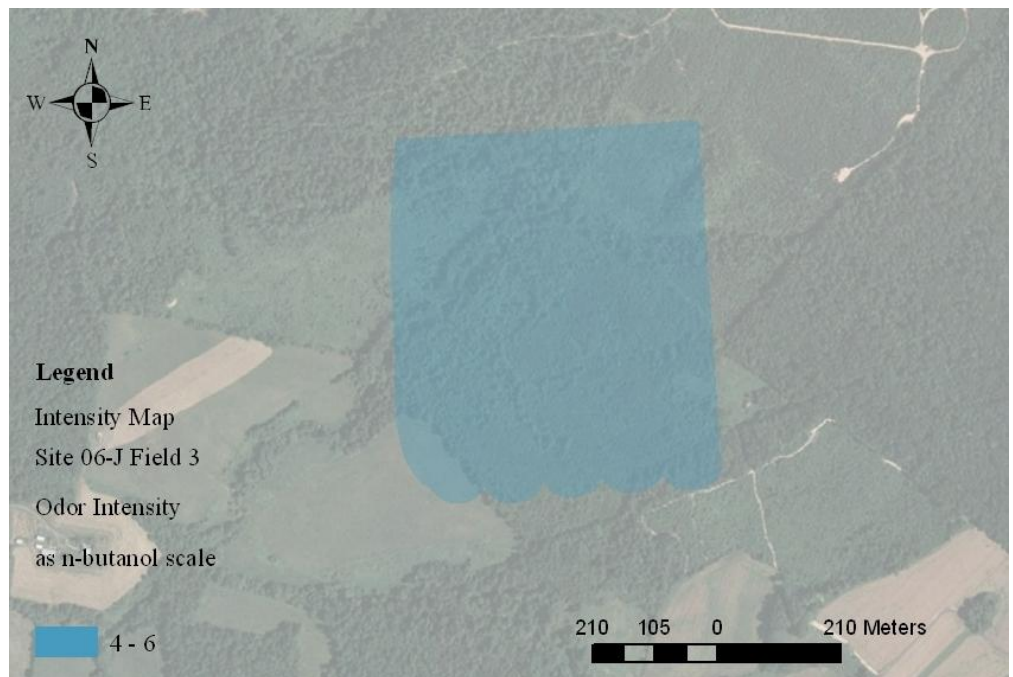
## A-8: Intensity Map

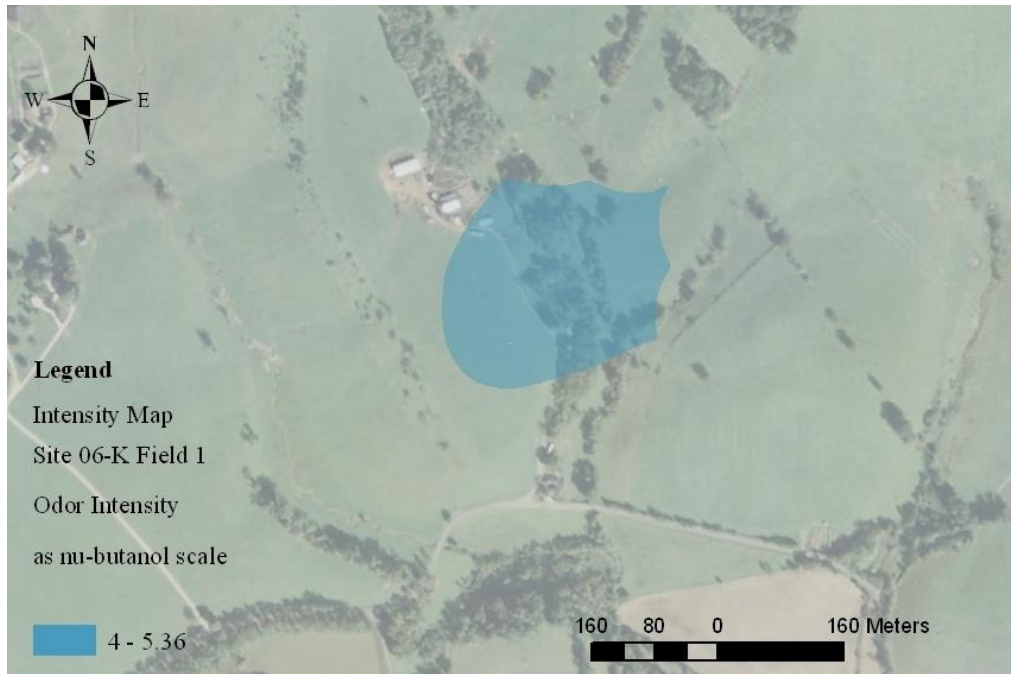












## Bibliography

- ALPERT, J. E. & WU, N. T. (1997) Odor modeling as a tool in site planning.  
*BioCycle*, 38, 75-80.
- BENJAMIN, J. & CORNELL, A. (1970) *Probability, statistics, and decision for civil engineers*, McGraw-Hill, Inc.
- BOX, G. E. P. & TIAO, G. C. (1973) *Bayesian inference in statistical analysis*, Addison-Wesley Publishing Company.
- BREMNER, J. & BANWART, W. (1976) Sorption of Sulfur Gases *Soil Biology Biochemistry*, 8, 79-83.
- CAPODAGLIO, A. G., F. CONTI, L. F. & G. PELOSI, G. U. (2002) Assessing the environmental impact of WWTP expansion: odour nuisance and its minimization. *Water Science and Technology*, 46, 339-346.
- CIMORELLI, A. J., PERRY, S. G., VENKATRAM, A., WEIL, J. C., PAINE, R. J., WILSON, R. B., LEE, R. F., PETERS, W. D. & BRODE, R. W. (2005) AERMOD: A Dispersion Model for Industrial Source Applications. Part I: General Model Formulation and Boundary Layer Characterization. *Journal of Applied Meteorology*, 44, 682-693.
- CLEMEN, R. T. & REILLY, T. (2001) *Making hard decisions with decision tools*, Brooks/Cole.
- CRAWFORD-BROWN, D. J. (2001) *Mathematical methods of environmental risk modeling*, Massachusetts, Kluwer Academic Publishers.
- CULLEN, A. C. & FREY, H. C. (1999) *Probabilistic techniques in exposure assessment*, New York, Plenum press.

- DCWASA (2005a) Biosolids Management Program. Washington, DC, Department of Wastewater Treatment.
- DCWASA (2005b) Blue Plains Advanced Wastewater Treatment Plant. Washington, DC, Department of Wastewater Treatment.
- DIOSEY, P. G. (1997) Atmospheric Dispersion Modeling Techniques for Odor Impact Assessment. *Air & Waste Management Association's 90th Annual Meeting & Exhibition*. Toronto, Ontario, Canada.
- DIOSEY, P. G. (2008) Modeling odors in the age of AERMOD. *WEF/A&WMA Odors and Air Emissions 2008*. Phoenix, AZ, Water Environment Federation.
- EPA, U. S. (1986) Measurement of Gaseous Emission Rates from Land Surfaces Using an Emission Isolation Flux Chamber. Austin Texas.
- EPA, U. S. (1994) A Plain English Guide to the EPA Part 503 Biosolids Rule. Washington DC, Office of Wastewater Management.
- EPA, U. S. (1995a) SCREEN3 Model User's Guide. Research Triangle Park, North Carolina.
- EPA, U. S. (1995b) User's Guide for The Industrial Source Complex (ISC3) Dispersion Models Volume II - Description of Model Algorithms. Research Triangle Park, North Carolina.
- EPA, U. S. (2000a) Guide to Field Storage of Biosolids. Washington, DC, United States Environmental Protection Agency.
- EPA, U. S. (2000b) Land Application of Biosolids. Washington, D.C., Office of Water, U.S. EPA.

- EPA, U. S. (2000c) Odor Control in Biosolids Management. Washington, D.C., Office of Water.
- EPA, U. S. (2004) User's guide for the AERMOD Meteorological Preprocessor (AERMET). Research Triangle Park, NC, Office of Air Quality Planning and Standards.
- EVANYLO, G. K. (2003) Land Application of Biosolids for Agricultural Purposes in Virginia. Department of Crop and Soil Environmental Sciences, Virginia Tech.
- FRANK, S. (2005) Too Hot to Handle. *Biosolids Technical Bulletin*, 10, 1-4.
- FRECHEN, F. B. (2004) Odour emission inventory of German wastewater treatment plants - odour flow rates and odour emission capacity. *Water Science and Technology*, 50, 139-146.
- GABRIEL, S. A., VILALAI, S., PEOT, C. & RAMIREZ, M. (2006) Statistical modeling to forecast odor levels of biosolids applied to reuse sites. *Journal of Environmental Engineering*, 132, 479-488.
- GOLDSTEIN, N. (2007) Biosolids Management Trends in the U.S. *BioCycle*.
- GUILLOT, J.-M., ROUX, J.-C., FANLO, J.-L., ROGNON, C., COSTE, C. & POURTIER, L. (2007) New conception of dynamic flux chambers to follow odor emissions from area sources. *Water practice*, 1, 1-9.
- HAMEL, K. C., P.E. , WALTERS, L. & SULERUD, C. (2004) Land Application Odor Control Case Study. *Residuals and Biosolids Management Conference*. Salt Lake City, UT, Water Environment Federation.

- HAUG, R. T. (1993) *The Practical Handbook of Compost Engineering*, Boca Raton, Florida, Lewis Publishers.
- HENSHAW, P., NICELL, J. & SIKDAR, A. (2006) Parameters for the assessment of odour impacts on communities. *Atmospheric Environment*, 40, 1016-1029.
- HENTZ, L. H. (1998) The Chemical, Biological, and Physical Origins of Biosolids Emissions: A Review. *Biosolids Technical Bulletin*.
- INTARAKOSIT, E. (2006) GIS-based odor dispersion modeling for measuring the effect of DCWASA biosolids in reuse fields. *Civil and Environmental Engineering*. College Park, University of Maryland.
- JANPENGPEN, A., BAECHER, G., KIM, H., PEOT, C. & RAMIREZ, M. (2007) Real Time Monitoring and Forecasting of Odor After Dewatering in Wastewater Treatment. *WEFTEC*. San Diego, CA.
- KAYE, R. & JIANG, K. (2000) Development of odour impact criteria for sewage treatment plants using odour complaint history. *Water Science and Technology*, 41, 57-64.
- KIM, H., MCCONNELL, L., RAMIREZ, M., ABU-ORF, M., CHOI, H. L. & PEOT, C. (2005) Characterization of Odors from Limed Biosolids Treated with Nitrate and Anthraquinone. *Journal of Environmental Science and Health*, A40, 139-149.
- KIM, H., S.MURTHY, L.L.MCCONNELL, C.PEOT, M.RAMIREZ & STRAWN, M. (2002) Characterization of wastewater and solids odors using solid phase microextraction at a large wastewater treatment plant. *Water Science and Technology*, 46, 9-16.

- KIM, H., S.MURTHY, MCCONNELL, L., PEOT, C., RAMIREZ, M. & STRAWN, M. (2003) Examination of Mechanisms for Odor Compound Generation during Lime Stabilization. *Water Environmental Research*, 2003, 121-125.
- LISBOA, H. D. M., GUILLOT, J.-M., FANLO, J.-L. & CLOIREC, P. L. (2006) Dispersion of odorous gases in the atmosphere - Part I: Modeling approaches to the phenomenon. *Science of the Total Environment*, 361, 220-228.
- MCGINLEY, C. & MCGINLEY, M. (2002) Odor Testing Biosolids for Decision Making. *Water Environment Federation Specialty Conference: Residuals and Biosolids Management Conference*. Austin, TX.
- MCGINLEY, C. M., MAHIN, T. D. & POPE, R. J. (2000) Elements of Successful Odor/Odour Laws. *WEF Odor / VOC 2000 Specialty Conference*. Cincinnati, OH.
- MCGINLEY, M. & MCGINLEY, C. (2004) Comparison of Field Olfactometers in a Controlled Chamber Using Hydrogen Sulfide as the Test Odorant. *Water Science and Technology*, 50, 75-82.
- MCGINLEY, M. & MCGINLEY, C. (2005) Measuring Composting Odors for Decision Making. *U.S. Composting Council 2005 Annual Conference*. San Antonio, TX.
- MCINTYRE, A. (2000) Application of dispersion modelling to odour assessment: a practical tool or a complex trap? *Water Science and Technology*, 41, 81-88.
- NICELL, J. & HENSHAW, P. (2007) Odor impact assessments based on dose-response relationships and spatial analyses of population response. *Water practice*, 1, 1-14.

- NICELL, J. A. (2003) Expressions to relate population responses to odor concentration. *Atmospheric Environment*, 4955-4964.
- OLESZKIEWICZ, J. A., MAVINIC, D.S. (2002) Wastewater biosolids: an overview of processing, treatment, and management. *Journal of Engineering Science*, 1, 75-88.
- P.GOSTELOW, PARSONS, S. A. & LOVELL, M. (2004) Integrated Odour Modelling for Sewage Treatment Works. *Water Science and Technology*, 5, 169-176.
- PERRY, S. G., CIMORELLI, A. J., PAINE, R. J., BRODE, R. W., WEIL, J. C., VENKATRAM, A., WILSON, R. B., LEE, R. F. & PETERS, W. D. (2005) AERMOD: A Dispersion Model for Industrial Source Applications. Part II: Model Performance against 17 Field Study Databases. *Journal of Applied Meteorology*, 44, 694-708.
- POOSTCHI, E. B. B. (1985) Development of a strategy for quantifying the impact of odorous emissions from stationary sources on the surrounding communities. *Chemical Engineering*. Ontario, University of Windsor.
- PORTER, R. C. & ELEENTER, D. (2008) Dispersion Model Parameters that Affect the Impacts from Area Sources Using AERMOD. Pheonix, AZ, Water Environment Federation.
- RAFSON, H. J. (1998) *Odor and VOC Control Handbook*, McGraw-Hill.
- RAZIK, A. (2005) Standard Procedure for Odor Monitoring for DCWASA and WSSC Land Application Inspection Projects Maryland Environmental Services.

- ROSENFELD, P. E. & SUFFET, I. H. (2004) Understanding odorants associated with compost, biomass facilities, and the land application of biosolids. *Water Science and Technology*, 49, 193-199.
- RYNK, R. & GOLDSTEIN, N. (2003) Reducing odor impacts at land application sites. *BioCycle*.
- SCHNELLE, K. & DEY, P. (2000) *Atmospheric Dispersion Modeling Compliance Guide*, McGraw-Hill.
- SEKYIAMAHA, K. H. (2004) Identification of Seasonal Variations in Volatile Sulfur Compound Production and Release in the Secondary Treatment System of a Wastewater Treatment Plant. *Civil and Environmental Engineering*. College Park, University of Maryland.
- SIMMS, K. L., S.WILKINSON & S.BETHAN (2000) Odour nuisance and dispersion modelling: an objective approach to a very subjective problem. *Water Science and Technology*, 41, 89-96.
- SINGH, A. K., SINGH, A. & ENGELHARDT, M. (1997) The Lognormal Distribution in Environmental Applications. Washington, DC, U.S. EPA.
- SMITH, R. J. (1995) A Gaussian Model for Estimating Odour Emissions from Area Sources. *Mathematical Computing and Modelling*, 21, 23-29.
- STEVENS, S. S. (1960) The psychophysics of sensory function. *American Scientist*, 48, 226-253.
- STEVENS, S. S. (1962) The Surprising Simplicity of Sensory Metrics. *American Psychologist*, 17, 29-39.

- SUFFET, I. H., BURLINGAME, G. A., ROSENFELD, P. E. & BRUCHET, A. (2004) The value of an odor-quality-whell classification scheme for wastewater treatment plants. *Water Science and Technology*.
- TODD WILLIAMS & SERVO, S. (2005) Odor Modeling at a Biosolids Composting Facility. *BioCycle*, 46, 25-28.
- TURK, A., JOHNSTON, J. & MOULTON, D. (1974) *Human Responses to Environmental Odors*, New York, Academic Press, INC.
- VILALAI, S. (2008) Statistical odor prediction models for supporting biosolids odor management. *Civil and Environmental Engineering*. College Park, University of Maryland.
- VOELZ, L. D., THOMPSON, J. K., GAUDES, R. J., ABI-SAMRA, S., SCHIRRIPA, R., TORRES, E. M., DILLON, C. D., AHN, T. & RAINE, T. J. (2006) Odor Modeling for Overall Odor Control Planning. *WEF/AWWA Odors and Air Emissions*. Water Environment Federation.
- WALPOLE, R. E., MYERS, R. H., MYERS, S. L. & YE, K. (2002) *Probability and statistics for engineers and scientists*, Upper Saddle River, New Jersey, Prentice-Hall, Inc.
- WEBSTER, R. & OLIVER, M. A. (2007) *Geostatistics for environmental scientists*, Padstow, Cornwall, John Wiley & Sons, Ltd.
- WU, N. (2000) Odor Modeling As First Line of Defense. *BioCycle*.
- YANG, G. & HOBSON, J. (2000) Odour nuisance - advantages and disadvantages of a quantitative approach. *Water Science and Technology*, 41, 97-106.

